

REPORT NO.  
UCB/EERC-87/19  
NOVEMBER 1987

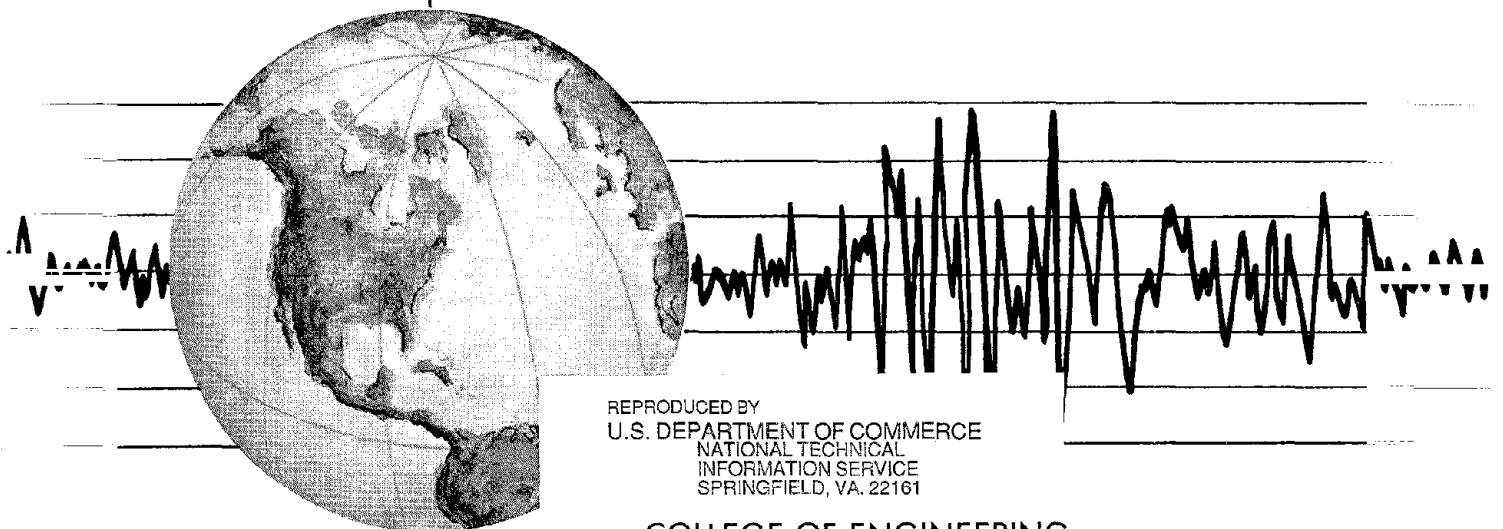
EARTHQUAKE ENGINEERING RESEARCH CENTER

# ANALYTICAL MODELS FOR PREDICTING THE LATERAL RESPONSE OF R C SHEAR WALLS: EVALUATION OF THEIR RELIABILITY

by

ALFONSO VULCANO  
VITELMO V. BERTERO

Report to the National Science Foundation



REPRODUCED BY  
U.S. DEPARTMENT OF COMMERCE  
NATIONAL TECHNICAL  
INFORMATION SERVICE  
SPRINGFIELD, VA. 22161

COLLEGE OF ENGINEERING  
UNIVERSITY OF CALIFORNIA AT BERKELEY

For sale by the National Technical Information Service, U.S. Department of Commerce, Springfield, Virginia 22161.

See back of report for up to date listing of EERC reports.

DISCLAIMER

Any opinions, findings, and conclusions or recommendations expressed in this publication are those of the authors and do not necessarily reflect the views of the National Science Foundation or the Earthquake Engineering Research Center, University of California, Berkeley

<b>REPORT DOCUMENTATION PAGE</b>	<b>1. REPORT NO.</b> NSF/ENG-87042	<b>2.</b>	<b>3. Recipient's Accession No.</b> PB88-178983
<b>4. Title and Subtitle</b> Analytical Models for predicting the Lateral Response of R C Shear Walls: Evaluation of their Reliability		<b>5. Report Date</b> November 1987	
<b>7. Author(s)</b> Alfonso Vulcano and Vitelmo V. Bertero		<b>8. Performing Organization Rept. No.</b> UCB/EERC-87/19	
<b>9. Performing Organization Name and Address</b> Earthquake Engineering Research Center University of California 1301 South 46th Street Richmond, California 94804		<b>10. Project/Task/Work Unit No.</b>  <b>11. Contract(C) or Grant(G) No.</b> (C) (G) CEE 80-09478	
<b>12. Sponsoring Organization Name and Address</b> National Science Foundation 1800 G. Street, N.W. Washington, D.C. 20550		<b>13. Type of Report &amp; Period Covered</b>  <b>14.</b>	
<b>15. Supplementary Notes</b>			
<b>16. Abstract (Limit: 200 words)</b>  Attention is focused on a wall model recently proposed by Japanese researchers. This model, based on a macroscopic approach, idealizes the generic wall member as three vertical line elements with infinitely rigid beams at the top and bottom floor levels. The two outside elements are truss elements to represent the axial stiffness of the boundary columns; the central element is a one-component model constituted by horizontal, vertical and rotational springs to represent, respectively, the shear stiffness of the wall, the vertical axial stiffness and the flexural stiffness of the central panel. Modifications of this wall model are developed in the studies reported. The main modification is aimed at improving the simulation of the hysteretic behavior of the axial elements adopted by the Japanese. These axial elements are replaced by new elements which simulate more closely the hysteretic behavior of a R C column member under axial load reversals. In order to check the effectiveness and reliability of the modified wall model a numerical investigation is carried out by calibrating the results against measured behavior of a series of R C structural walls that have been tested at the University of California at Berkeley. The modified wall model proves to be effective and suitable for incorporation in a practical nonlinear analysis of R C multistory structural systems.			
<b>17. Document Analysis</b> <ul style="list-style-type: none"> <li>a. Descriptors</li> <li>b. Identifiers/Open-Ended Terms</li> <li>c. COSATI Field/Group</li> </ul>			
<b>18. Availability Statement:</b>  Release unlimited		<b>19. Security Class (This Report)</b> Unclassified	<b>21. No. of Pages</b> 91
		<b>20. Security Class (This Page)</b> Unclassified	<b>22. Price</b> AD5 14.95



**ANALYTICAL MODELS FOR PREDICTING  
THE LATERAL RESPONSE OF R C SHEAR WALLS :  
EVALUATION OF THEIR RELIABILITY**

by

**Alfonso Vulcano**

Associate Professor  
Dipartimento di Strutture - Università della Calabria  
Arcavacata di Rende (Cosenza) - Italy

and

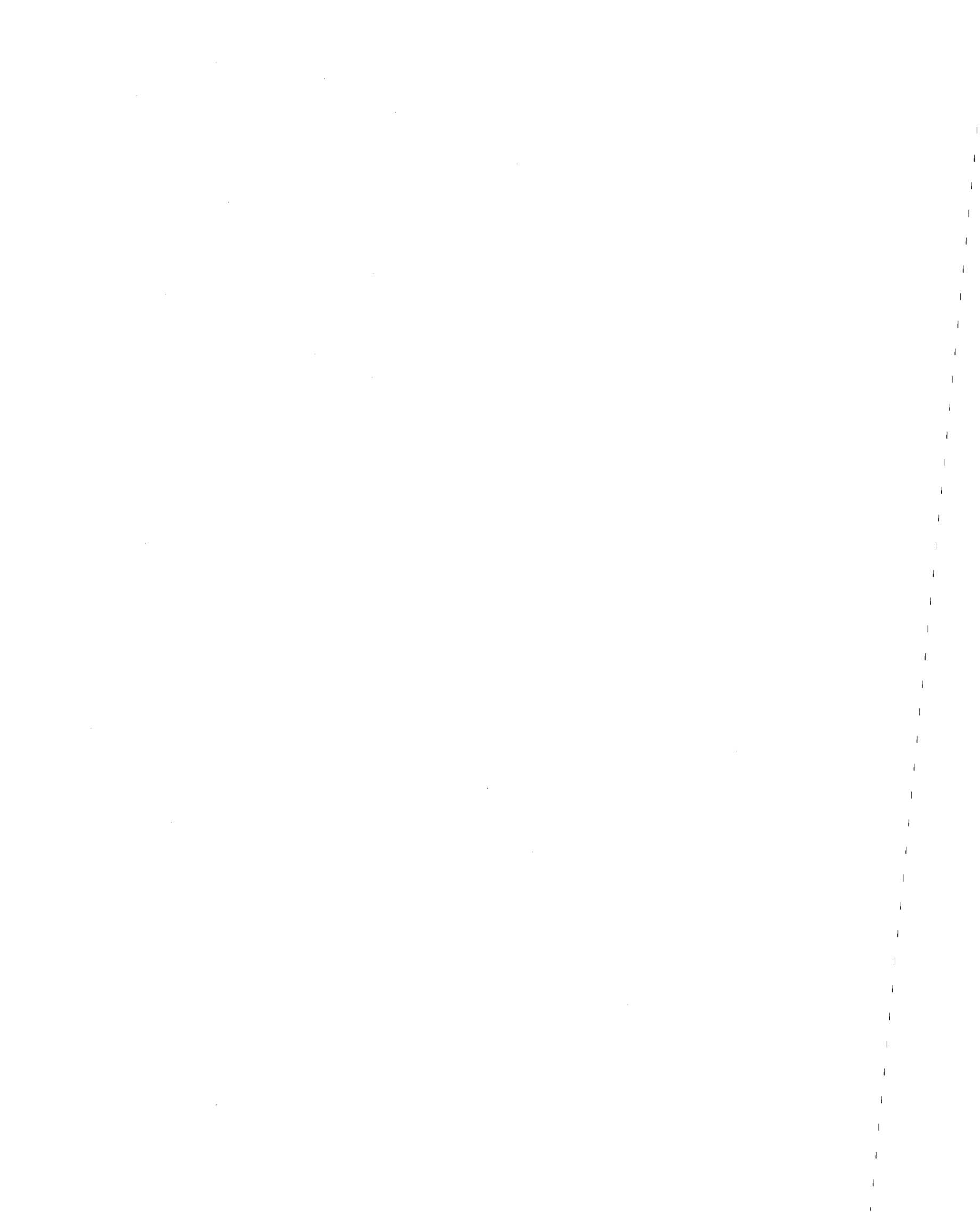
**Vitelmo V. Bertero**

Professor of Civil Engineering  
University of California - Berkeley

**A Report to Sponsor:  
National Science Foundation**

**Report No. UCB/EERC - 87/19  
Earthquake Engineering Research Center  
College of Engineering  
University of California  
Berkeley, California**

**November 1987**



## ABSTRACT

Relative simplicity with reasonable reliability is emphasized as the prerequisite of a R C shear wall model to be incorporated in a practical nonlinear analysis of a R C multistory structural system containing shear walls. Attention is focused on a wall model recently proposed by Japanese researchers. This model, based on a macroscopic approach, idealizes the generic wall member as three vertical line elements with infinitely rigid beams at the top and bottom floor levels. The two outside elements are truss elements to represent the axial stiffness of the boundary columns; the central element is a one-component model constituted by horizontal, vertical and rotational springs to represent, respectively, the shear stiffness of the wall, the vertical axial stiffness and the flexural stiffness of the central panel.

Modifications of the above wall model are proposed and developed in the studies reported herein. The main modification is aimed to improve the simulation of the hysteretic behavior of the axial elements adopted by the Japanese researchers. These axial elements are replaced by new elements which simulate more closely the hysteretic behavior of a R C column member under axial load reversals.

In order to check the effectiveness and reliability of the modified wall model a numerical investigation is carried out by calibrating the results against measured behaviour of a series of R C structural walls that have been tested at the University of California at Berkeley.

The modified wall model proves to be effective and suitable to be incorporated in a practical nonlinear analysis of R C multistory structural systems. Even though an apparently satisfactory correlation of the measured and analytical responses is found, under high shear stresses the correct prediction of the flexural and shear displacement components of the total displacement is very difficult and very sensitive to the choice of many of the parameters involved in the modified wall model.

Some recommendations are advanced in order to improve further the analytical wall model.



## ACKNOWLEDGEMENTS

The research reported herein was supported, in part, by the National Science Foundation Grant Number CEE 80-09478. The research started as a part of a cooperative research program between Italy and the U.S.A., sponsored by the Italian Research Council.

This part of the research was completed during the stay of Professor Alfonso Vulcano at the University of California at Berkeley as a Visiting Scholar. Professor Vulcano gratefully acknowledges the financial support of the Training and Studies Center of Southern Italy.

Finally, the authors wish to acknowledge the assistance of Dr. Beverley Bolt for the editing of this report.



# TABLE OF CONTENTS

<b>CHAPTER 1 - INTRODUCTION</b>	1
1.1 General	1
1.2 Objectives and Scope of the Report	2
<b>CHAPTER 2 - GENERAL REVIEW OF R C WALL MODELS</b>	4
2.1 Introduction	4
2.2 Models Derived from a Macroscopic Approach	6
2.2.1 Equivalent Beam Model	6
2.2.2 Equivalent Truss Model	7
2.2.3 Three-Vertical-Line-Element Model	8
<b>CHAPTER 3 - SELECTED WALL MODEL :</b>	
<b>THREE-VERTICAL-LINE-ELEMENT MODEL</b>	9
3.1 General Description of the Model	9
3.2 Hysteresis Model	10
3.2.1 Axial-Stiffness Hysteresis Model	10
3.2.2 Origin-Oriented Hysteresis Model	12

<b>3.3 Stiffness Properties of the Model Elements</b>	13
3.3.1 Truss Elements	13
3.3.2 Central Element Springs	13
(a) Vertical Spring	13
(b) Horizontal Spring	13
(c) Rotational Spring	15
<b>3.4 Proposed Axial-Stiffness Hysteresis Model</b>	17
<b>CHAPTER 4 - METHOD OF ANALYSIS</b>	20
<b>4.1 Wall Discretization and Elastic Stiffness Matrix</b>	20
<b>4.2 Equilibrium Equations and Iterative Solution Process</b>	21
<b>CHAPTER 5 - NUMERICAL STUDIES</b>	23
<b>5.1 General</b>	23
<b>5.2 Description of the Test Structures</b>	23
<b>5.3 Modeling of the Test Structures</b>	24
<b>5.4 Comparison of Experimental and Analytical Curves</b>	25
5.4.1 Monotonic Loading (Specimens 3 and 5)	25
5.4.2 Cyclic Loading (Specimens 4 and 6)	26
<b>5.5 Parametric Studies</b>	28

<b>CHAPTER 6 - SUMMARY, CONCLUSIONS AND RECOMMENDATIONS</b>	<b>34</b>
<b>6.1 Summary</b>	<b>34</b>
<b>6.2 Conclusions</b>	<b>36</b>
<b>6.3 Recommendations for Future Research</b>	<b>37</b>
<b>REFERENCES</b>	<b>39</b>
<b>APPENDIX A</b>	<b>45</b>
<b>APPENDIX B</b>	<b>49</b>
<b>TABLES</b>	<b>53</b>
<b>FIGURES</b>	<b>57</b>



# CHAPTER 1

## INTRODUCTION

### 1.1 General

The use of Reinforced Concrete (R C) shear walls in multistory buildings is very effective in providing resistance and stiffness against lateral loads induced by wind and/or earthquake. Well-designed R C coupled walls and frame-wall structural systems are particularly effective during severe earthquake ground motions when a considerable amount of the energy input has to be dissipated by reversed inelastic deformations.

Extensive research, both analytical and experimental [1-39], has been carried out in order to clarify, and then to simulate, the hysteretic behavior of isolated and coupled R C walls, as well as of R C frame-wall structural systems. Recent research has improved the understanding of the inelastic behavior of such structures significantly. These advances have provided helpful information for the development of suitable analytical models.

An analytical model should be capable of closely describing both the hysteretic behavior of each structural member and the interaction of connected members. Nevertheless, the analytical model should be relatively simple so that the analysis can be performed with reasonable computational effort. This last requirement is particularly important when multistory structural systems have to be analyzed. In these cases, models derived from a macroscopic approach prove to be more effective than detailed mechanical models. In fact, the former models require relatively limited storage and, most important, significantly lower computational effort.

Although suitable analytical models have been proposed for realistic and practical prediction of the hysteretic behavior of R C beam members, many uncertainties about the formulation of a reliable model for the practical analysis of R C structural walls persist. Therefore, while there has been a marked improvement in the analysis of R C frame structures in the last two decades, the analysis of R C frame-wall structural systems has not comparably improved.

Many important features of the hysteretic behavior observed during experiments on a full-scale seven-story building have been incorporated in the Three-Vertical-Line-Element Model, recently proposed by Kabeyasawa et al. [27] to simulate the inelastic response of R C structural walls. Even though there is good correlation between the observed and computed responses for the overall structure, further improvements in the wall model are believed possible.

In this report attention is focused on the modeling of R C structural walls and, in particular, on the aforementioned model which is shown to be reasonably reliable and suitable for incorporation in a practical nonlinear analysis of multistory structural systems.

## **1.2 Objectives and Scope of the Report**

The main objectives of the work described in this report are as follows:

- (1) to discuss features and limitations of previously proposed R C shear wall models and to select a relatively simple and reasonably reliable wall model, that can be efficiently incorporated in a practical nonlinear analysis of R C multistory structural systems that use R C shear walls;
- (2) to check the effectiveness and reliability of the selected wall model in light of the measured behavior of isolated R C structural walls;

- (3) to evaluate the sensitivity of the response of the selected wall model to the characteristic parameters involved in the analysis;
- (4) to make suggestions that would improve the reliability of the selected wall model.

In Chapter 2 a general review of R C wall models available in the literature is given, discussing their features and limitations.

In Chapter 3 attention is focused on the Three-Vertical-Line-Element Model. An analytical model idealizing the hysteretic behavior of a R C column member under axial load reversals is proposed and incorporated in the aforesaid wall model.

In Chapter 4 the features of the nonlinear analysis adopted and the computer program coded on the basis of this method are discussed.

Results of a numerical investigation and a parametric study, referring to a group of isolated R C structural walls tested by Vallenias et al. [4] at the University of California at Berkeley, are presented and discussed in Chapter 5.

Lastly, in Chapter 6 the conclusions of the present work and recommendations for future research are given.

## CHAPTER 2

### GENERAL REVIEW OF R C WALL MODELS

#### 2.1 Introduction

Many analytical models have been proposed to predict the nonlinear response of R C structural walls. However, they can be classified into two broad groups :

- (1) detailed models derived using mechanics of solids (microscopic approach);
- (2) simplified models to predict a specific overall behavior (macroscopic approach).

Models derived from a microscopic approach are based on a detailed interpretation of the local behavior. Even though the microscopic approach is desirable, its implementation involves many difficulties due both to the lack of completely reliable basic models and the complexities involved in a detailed solution. Although, the Finite Element Method offers a powerful analytical tool to perform the numerical analysis [40], the computation is generally very time-consuming and requires a large storage: thus, in practice the microscopic approach is restricted to the analysis of structural systems less complex than multistory frame-wall structural systems, such as a single wall or an assemblage of two coupled walls.

On the other hand, models based on a macroscopic approach attempt to describe the overall behavior by means of a simplified idealization. The main advantages of these models consist in the relatively limited storage and, above all, in the significantly less computational effort than that required by detailed analytical models. However,

models deriving from a macroscopic approach have several limitations, the main one being that usually the analytical results are valid only for the conditions on which the derivation of the model is based.

An alternative to the two above-mentioned approaches would be their combination. For instance, simplified models could be used to idealize structural members whose inelastic deformations are expected to be predominant; or, a preliminary analysis by a microscopic approach could provide helpful information about the structural idealization to be adopted in selecting a suitable simplified model.

In any case the model which is adopted, regardless of the approach from which it has been derived, should describe and predict the different components of inelastic deformation: flexural and shear deformations, as well as fixed end rotation caused by bond slippage of the tensile reinforcement embedded in the foundation. Moreover, the model should be capable of simulating the observed deformation patterns due to different failure modes: flexural, sliding shear or splitting-crushing of the web at the base of the wall.

It should be noted that to have an efficient wall system the web splitting-crushing mode of failure should be avoided or delayed sufficiently so that it will not control the behavior of the system. Although this mode of failure can be simulated when a microscopic approach is followed, its simulation becomes very difficult by models based on a macroscopic approach. In spite of this limitation, in the following emphasis will be placed on simplified models derived from a macroscopic approach, because they are relatively simple and, therefore, suitable for efficient incorporation in a nonlinear analysis of multistory structural systems in which splitting-crushing of the web is avoided or delayed enough not to be the controlling mode of failure.

## 2.2 Models Derived from a Macroscopic Approach

### 2.2.1 Equivalent Beam Model (EBM)

One current modeling technique for a frame-wall system considers the generic shear wall member replaced at its centroidal axis by a line element and connected by rigid links to the frame beams; the fixed-end rotation at any connection interface with the frame beams can be taken into account by introducing a nonlinear rotational spring whose mechanical properties can be defined on the basis of bar slippage due to bond deterioration.

Computer programs based on a one-component model are generally used [41-42]. This model consists of a flexural elastic member with a nonlinear rotational spring at each end. The inelastic moment-rotation relationship of each spring is determined by assuming a given location of the contraflexure point, e.g. that one based on the initial elastic stage. This is an advantage, because the inelastic end rotation depends only on the bending moment at the end and any moment-rotation hysteresis model can be adopted for the spring. However, this feature of the model is also a weakness, because the actual moment distribution and the propagation of inelasticity along the beam are disregarded.

In order to account for the variation of location of the contraflexure point, Otani [43] introduced some modifications to the model. But when the contraflexure point moves suddenly a numerical problem arises because of the sign change of the member end moments. To overcome this difficulty and to simulate the propagation of inelasticity adequately, the wall element can be discretized into a suitable number of short segments [36-39]; or different models [44-45], more sophisticated than a one-component model, can be adopted in order to account for the spread of the inelastic deformations in the critical regions . These models, however, and in particular the

further subdivision when a one-component model is adopted require such large storage and computational effort as to make the analysis of multistory structural systems unfeasible.

To account for the inelastic shear deformation effects in a coupled wall system, Takayanagi et al. [37] introduced additional plastic hinges at the ends of each line element representing a wall member. Although the computed and measured responses matched very well, it is important to observe that the sliding deformation mode of the wall cannot be represented.

The main limitation of modeling R C structural walls by adopting any equivalent beam model lies in the assumption that rotations occur around points belonging to the centroidal axis of the wall. With this assumption important features of the behavior of R C frame-wall structural systems (i.e., migration of the neutral axis of the wall cross-section, rocking of the wall, etc.) are disregarded and their consequent effects (i.e., outriggering interaction with the frame surrounding the wall, etc.) are not accounted for adequately.

### 2.2.2 Equivalent Truss Model (ETM)

Another modeling technique represents the wall as an equivalent truss system. Unlike the beam model, this model accounts for the stress redistribution caused by the diagonal cracks. However, difficulties arise in defining both the geometry and the mechanical properties of the equivalent truss system. For example, on the basis of experimental test results, Hiraishi [29] introduced a non-prismatic truss member whose cross-sectional area was determined taking into account the stress along the height of the boundary column under tension.

Further difficulties are due to changes in the structural topology which depends on crack propagation during the loading history. Helpful information in regards to this can be provided by a preliminary finite element solution, but the analysis is then much more time-consuming [4].

### 2.2.3 Three-Vertical-Line-Element Model (TVLEM)

Recently, after experiments on a full-scale model of a seven-story R C building, Kabeyasawa et al. developed a mathematical model for R C structural walls [27]. A good correlation of the observed and computed responses was found. The wall model, although relatively simple, incorporates the main features of the experimentally observed behavior (i.e., migration of the neutral axis of the wall cross-section, rocking of the wall, etc.), which the equivalent beam model fails to describe, as mentioned in Section 2.2.1.

For this reason the TVLEM can be considered to be one of the most suitable models among the R C wall models available in the literature for incorporation in a practical nonlinear analysis of multistory structural systems. In the next Chapters attention will be focused on this type of model and some proposals made for improving the original model.

It is worth mentioning that the TVLEM can be generalized as a Multi-Vertical-Line-Element Model. An approach of this kind was followed by Charney [22], who adopted a multi-axial-spring-in-parallel model (LINKS Model) to describe the flexural inelastic behavior of the base of a structural R C wall, part of a 1/5-scale test frame-wall structure.

## CHAPTER 3

### SELECTED WALL MODEL : THREE-VERTICAL-LINE-ELEMENT MODEL

#### 3.1 General Description of the Model

The model shown in Fig. 3.1a was formulated by Kabeyasawa et al. [27] to idealize a generic wall member as three vertical line elements with infinitely rigid beams at the top and bottom floor levels: two outside truss elements represented the axial stiffness of the boundary columns, while the central element was a one-component model with vertical, horizontal and rotational springs concentrated at the base. However, a finite rigid element of length  $ch$  could be placed between the spring assembly and the lower rigid beam. \* The wall model was intended to simulate the deformation of the wall member under a uniform distribution of curvature.

-----  
\* The value of the dimensionless parameter  $c$  could be chosen in such a way that  $ch$  represents the height of the center of relative rotation between top and bottom levels (Fig. 3.1b). With a suitable choice of the  $c$  value it is possible to define an effective relationship between the relative flexural displacement  $\Delta v_{\text{flexural}}$  and the relative rotation  $\Delta\phi$  ( $\Delta v_{\text{flexural}} = (c-1) h \Delta\phi$ ). A suitable value of  $c$  can be selected as based on the expected curvature distribution along the inter-story height  $h$  ( $0 \leq c < 1$ , if the curvature sign does not change along the inter-story height).

The model is capable of describing flexural and shear deformations, while the deformation due to the fixed end rotation is not accounted for. Flexural and sliding shear modes of failure can be described, while, as already mentioned in Section 2.1 for all the models based on a macroscopic approach, the web splitting-crushing mode of failure is not simulated.

The hysteresis models and stiffness properties (illustrated in Sections 3.2 and 3.3, respectively) adopted by Kabeyasawa et al. to simulate the hysteretic behavior of the model elements were based on the experience coming from experimental tests. Many of the assumptions contained in Sections 3.2 and 3.3 are empirical and sometimes even seem arbitrary. Nonetheless many of these assumptions, unless differently specified, are kept in the studies reported herein in order to check the reliability of the model. A parametric study is presented in Chapter 5 to emphasize the sensitivity of the wall model to different values of the characteristic parameters affecting the model response.

## **3.2 Hysteresis Models**

### **3.2.1 Axial-Stiffness Hysteresis Model (ASHM)**

The behavior of a R C column under axial load reversals is very complex. The simplified model shown in Fig. 3.2 was proposed in Reference 27 and tentatively used to describe the axial force-deformation relationship of the three vertical line elements of Fig. 3.1a.

The skeleton curve was defined by assuming the axial stiffness as constant in compression. When the net axial load changed its sign from compression to tension, the stiffness was reduced to 90% of the initial compressive elastic stiffness in order to account for some stiffness degradation due to cracking and bond deterioration. After

tensile yielding - supposed to occur when longitudinal reinforcement yielded under the net tensile load - the stiffness was reduced to 0.1% of the initial elastic stiffness in order to represent some strain hardening.

Before reaching the point  $Y = (D_{yt}, F_y)$  corresponding to tensile yielding, the response point followed the usual bilinear hysteresis rules between the two points  $Y$  and  $Y' = (D_{ye}, -F_y)$ .

Once tensile yielding occurred, then the response point followed the bilinear hysteresis rules between  $Y'$  and the point  $M = (D_m, F_m)$  corresponding to the maximum tensile strength  $F_m$  previously attained. The unloading stiffness  $K_r$  was assumed to be

$$K_r = K_c (D_{yt} / D_m)^\alpha \quad (3.1)$$

in which

$D_{yt}$  = tensile yielding point deformation;

$D_m$  = maximum deformation amplitude greater than  $D_{yt}$ ;

$\alpha$  = unloading stiffness degradation parameter, which was assumed equal to 0.9. \*

-----  
 \* It should be noted that the choice of the  $\alpha$  value is very important in order to obtain a realistic unloading path. In fact, the greater is the tensile ductility factor  $\mu_t = D_m / D_{yt}$ , the smaller is the unloading stiffness  $K_r$ , which, according to Eq. (3.1), could attain the limit value  $K_{lim} = K_{lim}(\mu, \alpha)$  indicated in Fig. 3.3a. In other words, for each value of  $\mu_t$  a limit value  $\alpha_{lim}$  can be defined for the parameter  $\alpha$  such that, if  $\alpha > \alpha_{lim}$  ( $\alpha < \alpha_{lim}$ ) then  $K_r < K_{lim}$  ( $K_r > K_{lim}$ ). However, the unloading path defined by the condition  $K_r < K_{lim}$ , that is  $K_r < K_r'$ , is unrealistic because during an unloading phase subsequent to a tensile yielding the response of the R C column strongly depends on the steel behavior, which does not match a path of this type.

It can be shown that

$$\alpha_{lim} = \log \{ [2K_t / K_c + (\mu_t - 1)K_h / K_c] / [K_t / K_c + \mu_t] \} / \log \mu_t^{-1}, \quad \mu_t > 1$$

Some curves representing  $\alpha_{lim}$  versus  $\mu_t$  for different values of the ratio  $K_t / K_c$  are plotted in Fig. 3.3b. All these curves, which prove to be practically insensitive to the value of the ratio  $K_h / K_c$ , refer to the value 0.001 assumed for this ratio in Reference 27. It is worth noting that, by referring to the curve corresponding to the values assumed in Reference 27 for  $\alpha$ ,  $K_t / K_c$  and  $K_h / K_c$  (0.90, 0.90 and 0.001, respectively), the unloading stiffness  $K_r$  attains the limit value for  $\mu_t \cong 1.165$ ; in order to have  $K_r > K_{lim}$  for any realistic choice of the  $\mu_t$  value, then  $\alpha < 0.687$ .

Furthermore, additional rules were applied between Y' and M. During a loading phase in tension, when the response point reached the point M, then the response point moved on the branch of the skeleton curve in tension corresponding to the tensile hardening stiffness  $K_h$ , in this way renewing the point M. Moreover, during an unloading phase from M the response point reached the point  $(D_x, F_m - F_y)$  and then moved toward the compressive characteristic point Y'; however, the point Y' was not reached because the response point moved toward the point  $Y'' = (2D_{yc}, -2F_y)$  from the stiffness hardening point  $P = (D_p, F_p)$  corresponding to the deformation

$$D_p = D_{yc} + \beta (D_x - D_{yc}) \quad (3.2)$$

in which

$D_x$  = deformation at the point corresponding to the change of the unloading stiffness;

$\beta$  = parameter for stiffness hardening point, which was assumed equal to 0.2.

### 3.2.2 Origin-Oriented Hysteresis Model (OOHM)

An Origin-Oriented Hysteresis Model, which dissipates small hysteresis energy, was used for both the rotational and horizontal springs at the base of the central vertical element (Fig. 3.4). A trilinear skeleton curve was used for both these springs. The response point moved along a line connecting the origin and the previous maximum response point in each direction. Once the response point reached the previous maximum point, the response point followed the skeleton curve renewing the maximum response point.

It should be noted that, because of the choice of the OOHM, the shear stiffness degradation was taken without accounting for the cracking effects due to the presence of both the actual axial force and the bending moment. As pointed out later in the discussion of the numerical investigation (Chapter 5), there are discrepancies between the measured and predicted shear behaviors for the test walls considered in this work, whereas in Reference 27 the predicted response of the overall structure correlated very

well with the observed one. These different results arise because in the latter case the inelastic behavior of the tested structure was essentially flexural, while the shear stiffness remained practically elastic.

Although in the studies reported herein attention is focused on the ASHM, the above-mentioned discrepancies require that the use of the OOHM to represent the stiffness properties of the horizontal spring be revised.

### **3.3 Stiffness Properties of the Model Elements**

#### **3.3.1 Truss Elements**

The axial stiffness properties of the two outside truss elements (represented by the stiffnesses  $K_1$  and  $K_2$  in Fig. 3.1a) were defined as for an independent column by referring to the area of the boundary columns. As previously said, the hysteretic behavior was simulated by using the ASHM.

#### **3.3.2 Central Element Springs**

##### **(a) Vertical Spring**

The axial stiffness properties of the central element (represented by the stiffness  $K_v$  in Fig. 3.1a) were determined by referring to the area of the central panel bounded by the inner faces of the two boundary columns. The same rules adopted for the truss elements were used to describe the hysteretic behavior of the vertical spring belonging to the central element.

##### **(b) Horizontal Spring**

The shear resistance of the wall was provided by the horizontal spring in the central element.

The value of the stiffness of the horizontal spring ( $K_h$  in Fig. 3.1a) in the initial elastic range represents the shear stiffness of the wall in this range, which was defined as

$$K_s = G A_w / \chi h \quad (3.3a)$$

in which

$G$  = elastic shear modulus;

$A_w$  = area of the shear wall section (Fig. 3.5);

$\chi$  = shape factor for shear deformation;

$h$  = inter-story height.

The shape factor  $\chi$  was calculated by the following formula proposed by Tomii and Osaki [24]:

$$\chi = 3(1+u)[1-u^2(1-v)] / 4[1-u^3(1-v)] \quad (3.3b)$$

in which  $u$  and  $v$  are the geometrical parameters shown in Fig. 3.5.

The shear cracking was assumed to occur at a shear force

$$V_c = 0.438 f_c'^{1/2} A_w \quad (f_c' \text{ in MPa}) \quad (3.4)$$

The ultimate shear resisting capacity was calculated by the empirical formula proposed by Hirose [25]:

$$V_u = [ 0.0679 \rho_t^{0.23} (f_c' + 17.6) / (M / V L + 0.12)^{1/2} + 0.845 (f_{wh} \rho_{wh})^{1/2} + 0.1 \sigma_0 ] b_e j \quad (f_c' \text{ and } f_{wh} \text{ in MPa}) \quad (3.5)$$

where

$\rho_t$  = effective tensile reinforcement ratio as a percentage =  $100 A_s / b_e (L - a/2)$ ;

$A_s$  = area of longitudinal reinforcement in tension-side boundary column;

$M / V L$  = shear-span-to-depth ratio;

$\rho_{wh}$  = effective horizontal wall reinforcement ratio =  $A_{ws} / b_e s$ ;

$b_e$  = average width of wall section;

$s$  = spacing of horizontal wall reinforcement;

$\sigma_0$  = average stress over entire wall cross-section area;

$j = (7/8)(L - a/2)$ ;

L, a = geometrical parameters (Fig. 3.5).

In Reference 27 the ratio  $\alpha_s$  of the stiffness after shear cracking to the initial elastic stiffness  $K_s$  was determined by the empirical formula:

$$\alpha_s = 0.14 + 0.46 \rho_{wh} f_{wh} / f_c' \quad (3.6)$$

The stiffness after shear yielding was taken to be 0.1% of the initial elastic stiffness  $K_s$  in order to account for some strain hardening.

### (c) Rotational Spring

The stiffness properties of the rotational spring (represented by the stiffness  $K_r$  in Fig. 3.1a) were defined by referring to the wall area bounded by the inner faces of the two boundary columns. Even though it is not completely clear how these properties were defined, it seems that the displacement compatibility of the central panel with the boundary columns was disregarded.

For the purpose of computing the wall rotation, the bending moment was assumed to distribute uniformly along the story height with an amplitude equal to the moment at the critical section of the wall.

Cracking would occur when the extreme fiber strain under the gravity load and overturning moment became zero in its way to be a tensile strain. The yielding moment was calculated as the moment about the centroid of the wall section caused by the yielding of all vertical reinforcement, including also the gravity loading effect. The stiffness after yielding was taken to be 0.1% of the initial elastic stiffness, assuming in this way some strain hardening.

It should be noted that the assumption of these stiffness properties regardless of the displacement compatibility results in a wrong evaluation of the flexural and axial contributions of the central panel to the response of the entire wall. This is emphasized in Figs. 3.6a and 3.6b, in which, respectively, the flexural moment around the central

axis and the axial force, both versus curvature, are shown for the entire wall and its parts (boundary columns and central panel). All the curves refer to the section of a framed wall tested by Vallenias et al. [4] (Specimen 3), which was subjected to a constant axial force  $N_r = 868$  kN.

The analytical curves were obtained using the computer program UNCOLA [46]. In Fig. 3.6a the curve obtained for the central panel assumed isolated is shown together with the curve corresponding to the entire wall as well as the curves obtained for the boundary columns and the same central panel by satisfying the condition of displacement compatibility. These last two curves were obtained on the basis of the same strain profile associated with each of the values of the curvature that were considered by analyzing the entire wall cross-section. The same procedure was used to calculate the contributions of axial force which correspond to the boundary columns ( $N_b$ ) and central panel ( $N_p$ ) according to the condition of displacement compatibility (Fig. 3.6b).

As shown in Fig. 3.6a, the flexural contribution of the central panel results in a more marked softening effect when the condition of displacement compatibility is satisfied. Under this last condition a decompression effect is observed for the central panel, whereas it is subjected to a constant compression force if supposed isolated, that is if the displacement compatibility with the boundary columns is disregarded (Fig. 3.6b).

In view of these results, the assumptions made by Kabeyasawa et al. about the stiffness properties of the rotational spring seem questionable. In fact, in Reference 27 the OOHM described in Section 3.2.2 was adopted also for the rotational spring, thus accounting for some strain hardening, and the axial force in the central panel was assumed constant.

In order to overcome the above-mentioned limitations, in the following all the properties of the rotational spring, unless differently specified, will be defined by a moment-curvature analysis based on the displacement compatibility. The moment-curvature relationship ( $M-\psi$ ) so derived is idealized as a trilinear curve. As a consequence,

the skeleton curve of the rotational spring is also idealized as trilinear and the moment-rotation ( $M-\phi$ ) relationship under cyclic loading is simulated by the OOHM already presented in Section 3.2.2. As an example, in Fig. 3.7 the idealization of the moment-curvature relationship is shown with reference to the central panel of Specimen 3, whose flexural response based on the condition of displacement compatibility has been previously shown in Fig. 3.6a (see also APPENDIX A).

### **3.4 Proposed Axial-Stiffness Hysteresis Model**

The behavior of a R C column under axial load reversals is not clearly understood. Kabeyasawa et al. developed and tentatively used the ASHM described in Section 3.2.1, the properties of which were defined by empirical laws and some assumptions based on results from experimental tests.

In order to have a better understanding of the hysteretic behavior of the column and reduce the empirical assumptions, the model shown in Fig. 3.8a is proposed and incorporated in the selected wall model. The column member is idealized as two axial elements in series: one element (i.e., element 1) is a one-component model to represent as a whole the axial stiffness of the column segments in which the bond is still active, while the other element (i.e., element 2) is a two-component model to represent the axial stiffness of the remaining segments of steel and cracked concrete (i.e., components (S) and (C), respectively) for which the bond has almost completely deteriorated.

The proposed model is capable of idealizing the main features of the actual hysteretic behavior of the materials and their interaction: yielding, hardening and the Bauschinger effect for the steel, cracking of the concrete and onset of contact stresses during the closure of cracks, degradation of the bond between concrete and steel and so on. Adequate constitutive laws should be used to idealize the actual behavior of the steel and concrete, particularly the variation of the contact stress during the closure of cracks. Moreover, a suitable law should be used for the dimensionless bond-degradation

parameter  $\lambda$ , which also defines the lengths of the two elements constituting the model in order to simulate the tension-stiffening effect. Even though refined results can generally be attained by very sophisticated assumptions, above all it is desirable to simplify the mathematical model to limit the cost of the numerical analysis.

To carry out a first check of the accuracy that can be achieved by the proposed ASHM, very simple assumptions are made here which preserve, however, the essential features of the above-mentioned observed phenomena. In particular, the constitutive laws for the model components shown in Fig. 3.8a are simply taken to be as follows: linearly elastic for the overall element 1; bilinear with the hardening slope depending on the value  $r$  assumed for the steel-hardening ratio, and linearly elastic in compression neglecting the tensile strength capacity of the concrete, respectively, for the components S and C constituting the element 2.

According to the simplified assumptions just mentioned, the axial force-deformation relationship for the column member is of the kind shown in Fig. 3.8b, in which typical states of the model (i.e., steel yielding in tension and compression, as well as closure of the cracks) can be easily recognized on the basis of the idealized constitutive laws. The stiffnesses in compression  $K_c$ , in tension  $K_t$  and after tensile yielding  $K_h$  can be expressed by the following equations, respectively:

$$K_c = (E_c A_c + E_s A_s) / h \quad (3.7a)$$

$$K_t = 1 / \{ (1-\lambda)h / (E_c A_c + E_s A_s) + \lambda h / (E_s A_s) \} \quad (3.7b)$$

$$K_h = 1 / \{ (1-\lambda)h / (E_c A_c + E_s A_s) + \lambda h / (r E_s A_s) \} \quad (3.7c)$$

in which  $r$  is the steel hardening ratio and the same value  $E_c$  has been assumed for the concrete modulus in compression and in tension.

From Eqs. (3.7), once the value of the model stiffness in compression  $K_c$  is fixed, the values of both the stiffness in tension  $K_t$  and the stiffness after tensile yielding  $K_h$  can be adjusted by assuming for  $\lambda$  and  $r$  suitable values to simulate the observed

hysteretic behavior. In the following, even though this is questionable, the values of  $K_t$  and  $K_h$  will be selected according to the corresponding values adopted by Kabeyasawa et al. ( $K_t = 0.90 K_c$  ;  $K_h = 0.001 K_c$ ) in order to check the reliability of the wall model. However, in order to check the sensitivity of the response of the wall model to different choices of these parameters a parametric study was conducted and the results are presented in Chapter 5.

It is important to note that, even though the primary skeleton curve is the same for both axial-stiffness hysteresis models shown in Figs. 3.2 and 3.8b, the hysteretic behavior under cyclic loading is generally different. The ASHM in Fig. 3.2 contains more rules than the simplified hysteresis model in Fig. 3.8b. Notwithstanding, the model proposed here, besides being easily recognizable, is capable of many improvements (i.e., more-refined constitutive laws for the model components based on the observed hysteretic behavior of the materials, suitable laws to idealize the contact effects due to the closure of cracks, calibration of the bond-degradation parameter  $\lambda$  according to experimentally observed tension-stiffening effects on the basis of a suitable law for describing the degradation of the steel-concrete bond, etc.).

# CHAPTER 4

## METHOD OF ANALYSIS

### 4.1 Wall Discretization and Elastic Stiffness Matrix

The wall is discretized as a set of wall members, one for each story. The generic wall member is idealized by the wall model described in Chapter 3, modified by the inclusion of the proposed ASHM.

The elastic stiffness matrix  $\mathbf{K}_e$  [6x6] of the generic wall member is formulated with reference to the six displacement/load components at the center of the top and bottom rigid beams (Fig. 3.1a). By assuming in general a finite rigid element of length  $ch$  placed between the spring assembly of the central element and the lower rigid beam (Fig. 3.1b), the matrix  $\mathbf{K}_e$  is defined by the following equation in terms of elastic energy:

$$\begin{aligned} 1/2 \mathbf{u}_e^T \mathbf{K}_e \mathbf{u}_e = 1/2 \{ & (K_1 + K_2 + K_v) (w_m - w_{m-1})^2 + [K_\phi + (K_1 + K_2) \ell^2 / 4] (\phi_m - \phi_{m-1})^2 + \\ & + \ell (K_2 - K_1) (w_m - w_{m-1}) (\phi_m - \phi_{m-1}) + K_H [v_m - v_{m-1} + (1-c)h\phi_m + ch\phi_{m-1}]^2 \} \end{aligned} \quad (4.1)$$

where  $\mathbf{u}_e = \{v_m, w_m, \phi_m, v_{m-1}, w_{m-1}, \phi_{m-1}\}^T$  is the displacement vector of the generic wall member (Fig. 3.1a). The matrix  $\mathbf{K}_e$  so formulated is shown in Fig. 4.1.

The elastic stiffness matrix  $\mathbf{K}_E$  [3n x 3n] of the wall is hence obtained as an assemblage of the stiffness contributions of the  $n$  wall members in which the wall has been discretized.

## 4.2 Equilibrium Equations and Iterative Solution Process

The analytical response of the wall is evaluated by an incremental step-by-step procedure. At each step of the analysis, once the initial conditions and the increment of the load vector  $\mathbf{p}$  [ $3n \times 1$ ] are known, the state of strain and stress at the step end is obtained by the initial stress-like iterative procedure shown in Fig. 4.2.

On the basis of a trial displacement vector  $\mathbf{u}_1^{(\omega)}$  [ $3n \times 1$ ] for the discretized wall at the end of the step, the stress state in the generic spring constituting the wall element can be calculated. This can be accomplished in an explicit way for the horizontal and rotational springs, while an iterative procedure is generally needed for the truss elements and central vertical spring, for which the hysteretic behavior is described by the proposed two-element-in series model described in Section 3.4.

This iterative procedure is needed in order to satisfy the following incremental equations, which express displacement compatibility and equilibrium, respectively:

$$\Delta D = \Delta D_1 + \Delta D_2 \quad (4.2a)$$

$$\Delta F_1(\Delta D_1) = \Delta F_2(\Delta D_2) = \Delta F \quad (4.2b)$$

where the subscripts 1 and 2 refer, respectively, to the two elements in series constituting the axial model. However, the iterative procedure, which is described in detail in Fig. 4.3, is not necessary before cracking occurs ( $\lambda=0$ ) or if the stiffening effect is negligible ( $\lambda=1$ ).

Finally, once the stress state of each spring is known, the vector  $\mathbf{s}[\mathbf{u}_1^{(\omega)}]$  [ $3n \times 1$ ], which represents the structural reaction corresponding to the trial displacement vector at the end of the step, can be calculated. In order to find the displacement vector  $\mathbf{u}_1$  such that the corresponding vector  $\mathbf{s}[\mathbf{u}_1]$  satisfies the equilibrium equations, the following iterative scheme is used:

$$\mathbf{r}^{(k)} = \mathbf{s}[\mathbf{u}_1^{(k)}] - \mathbf{p}_1 \quad (4.3a)$$

$$\mathbf{u}_1^{(k+1)} = \mathbf{u}_1^{(k)} - \mathbf{H} \mathbf{r}^{(k)} \quad (4.3b)$$

where the index  $k$  refers to the generic iteration loop and  $\mathbf{H}$  is a suitable iteration matrix. The iterative process is stopped when an appropriate measure of the residual vector  $\mathbf{r}^{(k)}$  becomes less than a prefixed tolerance.

As shown in Reference 47, the convergence of the iterative process (4.3) is ensured under very broad hypotheses on the mechanical behavior of the structure if the iteration matrix is taken as

$$\mathbf{H} = \{ (1-\zeta) \mathbf{K}_M + \zeta \mathbf{K}_T \}^{-1} \quad , \quad 0 \leq \zeta < 0.5 \quad (4.3)$$

where  $\mathbf{K}_M$  is a maximizing stiffness matrix (e.g., the elastic stiffness matrix  $\mathbf{K}_E$  if the behavior is elastic-perfectly plastic) and  $\mathbf{K}_T$  a generic tangent stiffness matrix of the discretized structure.

The procedure just described has been coded as a computer program for the nonlinear analysis of R C structural walls. The flow chart of this computer program, which is organized by subroutines (INPUT, LOADS, ASSEM, SOLVE , STRUCT, OUTPUT) to perform different operations, is shown in Fig. 4.4.

## CHAPTER 5

### NUMERICAL STUDIES

#### 5.1 General

In order to check the effectiveness and the reliability of the R C wall model obtained by incorporating in the wall model presented in Reference 27 the ASHM proposed in this report (Section 3.4), a numerical investigation was carried out using the computer program presented in Section 4.2. Parametric studies were also performed to evaluate the sensitivity of the response of such a wall model to the characteristic parameters involved in the analysis. For these purposes isolated R C structural walls previously tested at the Earthquake Engineering Research Center of the University of California at Berkeley provided the experimental results and are referred to as the test structures.

After a description of these test structures and their modeling, the analytical results obtained for the wall model will be compared with the experimental ones. Lastly, the results of the parametric study will be presented.

#### 5.2 Description of the Test Structures

The four 1/3-scale test specimens, previously tested at the University of California at Berkeley by Vallenias et al. [4], were intended to idealize the three lower stories of both a framed wall (Specimens 3 and 4, Fig. 5.1a) and rectangular wall (Specimens 5

and 6, Fig. 5.1b) designed, respectively, for the ten-story and seven-story prototype buildings shown in Figs. 5.2a and 5.2b, respectively. These buildings were designed in such a way that earthquake ground motions could induce high shear stresses of the same magnitude in both kinds of wall.

Detailed wall cross-sections and loading patterns of the specimens are shown in Figs. 5.3 and 5.4, respectively. As it can be observed in Fig. 5.4, the axial force and moment-to-shear ratio ( $M/V$ ) were assumed constant for each of the specimens. Specimens 3 and 5 were subjected to a monotonic loading, while Specimens 4 and 6 were subjected to a cyclic loading.

### **5.3 Modeling of the Test Structures**

The test walls were modeled by idealizing each wall story as the wall member model in Fig. 3.1a. The structural models so obtained are shown in Fig. 5.5a for Specimens 3 and 4, and in Fig. 5.5b for Specimens 5 and 6. The stiffness properties of the model elements were based on the mechanical properties of the materials reported for the test walls at the time of testing in Reference 4 and are summarized in Table 5.1 and Table 5.2, respectively, for Specimen 3 (4) and Specimen 5 (6). Typical constitutive curves of the steel and concrete (unconfined and confined) are shown in Fig. 5.6a and Fig. 5.6b, respectively. Details of the stiffness properties of the model elements are shown in APPENDIX A for Specimen 3 (4) and in APPENDIX B for Specimen 5 (6).

## 5.4 Comparison of Experimental and Analytical Curves

### 5.4.1 Monotonic Loading (Specimens 3 and 5)

Experimental and computed responses are shown in Figs. 5.7 and 5.8, respectively, for the framed wall (Specimen 3) and rectangular wall (Specimen 5) subjected to monotonic loading.

With reference to Figs. 5.7a and 5.8a, it should be noted that the analytical model does not account for the fixed end deformation caused by slippage of the longitudinal reinforcement along its embedment in the foundation. Even though this kind of deformation ( $\delta_{3 \text{ fixed end}}$ ) contributed only a minor portion to the total displacement  $\delta_3$  at the third floor (as reported in Reference 4), it has been subtracted from the total displacement ( $\delta_3' = \delta_3 - \delta_{3 \text{ fixed end}} = \delta_{3 \text{ flexural}} + \delta_{3 \text{ shear}}$ ) to make the experimental and analytical curves shown in Figs 5.7a and 5.8a comparable.

The correlation of experimental and analytical curves is apparently good for plots of base shear  $V$  versus the net top displacement  $\delta_3'$  (Figs. 5.7a and 5.8a) as well as versus the flexural displacement  $\delta_{3 \text{ flexural}}$  (Figs. 5.7b and 5.8b) or the shear displacement  $\delta_{3 \text{ shear}}$  (Figs. 5.7c and 5.8c) at the third floor. However, it must be noted that, because of the flattening of these curves near the maximum strength, it is very difficult to correlate the flexural and shear displacement components of the analytical model and the corresponding measured ones. A parametric study, the results of which are presented in Section 5.5, pointed out that the values of these displacement components given by the analytical model proved to be very sensitive to the choice of several parameters (e.g., bond degradation parameter  $\lambda$ , steel hardening ratio  $r$ , yield shear  $V_y$  assumed for the horizontal spring, etc.). Therefore, caution is recommended in assuming the computed displacement components as a correct prediction of the measured displacement components, particularly when high shear stresses are expected, as was the case for the test walls considered in these studies.

#### 5.4.2 Cyclic Loading (Specimens 4 and 6)

In Fig. 5.9 analytical and experimental results for both the flexural and shear displacement components of the framed wall under cyclic loading (Specimen 4) are separately shown. The analytical results have been obtained as follows: for any value of the measured net top displacement ( $\delta_3' = \delta_{3 \text{ flexural}} + \delta_{3 \text{ shear}}$ ) drawn in the characteristic cycles of the loading program adopted for Specimen 4 (i.e., LP 0, 46,48, 58, 60, 70, 72, 82, 84), it is assumed that the analytical model will give the same value of this displacement and therefore the base shear required to produce this value is computed.

Analogous results for the rectangular wall under cyclic loading (Specimen 6 ; LP 0, 149, 180, 255, 280, 372, 392, 532, 560) are shown in Fig. 5.10.

While for Specimen 4 (Fig. 5.9) the analytical model underestimates the shear deformations (and overestimates the flexural ones) in comparison with the measured ones, a better prediction of the two displacement components is observed in Fig. 5.10 for Specimen 6. However, as already said, such prediction depends on the choice of several parameters. For instance, for Specimen 4, a good prediction of both the shear and flexural displacement components is obtained by simply assuming for  $K_h$  a suitable value greater than the adopted value (0.001  $K_c$ ).

In particular, the results shown in Fig. 5.10, besides showing the inadequacy of the OOHM to idealize the measured hysteretic shear behavior accurately, show a satisfactory correlation for the measured and analytical responses due to flexural deformations. It should be noted that the flexural response idealized by the wall model essentially depends on the assumptions adopted for the proposed ASHM.

In order to have an idea of the kind of response obtained by adopting the proposed ASHM, the responses of the two outside truss elements and the central vertical spring, all corresponding to the first story of the model of Specimen 6 in Fig. 5.5b, are shown in Fig. 5.11. It is interesting to observe that, with reference to the generic cycle of loading in Fig. 5.10 (for example, the loading cycle 1-2-1), while the response of both the outside truss elements describes one loading cycle (for example, the loading cycle 1-2-1

in Figs. 5.11a, b), the response point of the central vertical spring moves twice in each of the directions of loading (as, for example, in the loading process 1, 1', 2, 2', 1 in Fig. 5.11c). Furthermore, the initial deformation of the central vertical spring, corresponding to a shortening, is no longer attained during the loading cycles following the tensile yielding of the same spring. Indeed, the minimum displacement progressively attained during these loading cycles corresponds to a growing elongation of the centroidal axis of the wall.

In spite of the simplified assumptions adopted in these studies for the proposed ASHM (which, as mentioned in Section 3.4, is certainly capable of improvement), the flexural response idealized by the wall model compares satisfactorily with that obtained by the use of more sophisticated models.

To emphasize this last assertion, in Fig. 5.12 the flexural response obtained for Specimen 4 by adopting the wall model considered in these studies is compared with the two curves reported in Reference 4, which were obtained experimentally and by using the ANSR-I computer program, both with reference to a loading cycle corresponding to the range  $\pm 20$  mm of the flexural displacement at the third level.

Even though the simplified wall model considered in these studies provides a description of the measured flexural response slightly less accurate than that obtained by the detailed finite element solution (ANSR-I) reported in Reference 4, the advantages arising from the use of the former model are obvious, particularly in terms of computational effort. However, it should be noted that neither of the analytical models accounts for the resistance degradation that Specimen 4 suffered because of previous loading cycles.

## 5.5 Parametric Studies

As mentioned in the previous section, for a given value of the net top displacement as well as of the flexural or shear displacement component, there is a good correlation between the experimental and analytical values of the shear strength. On the other hand, for a given value of shear strength close to the maximum shear strength of the wall, the prediction by the wall model of the measured flexural and shear displacement components has been very difficult, because of the flattening of the experimental and analytical curves (Figs. 5.7 and 5.8).

In order to check the sensitivity of these two analytical displacement components to different parameters involved in the analysis, a parametric study was carried out with reference to Specimen 3.

Measured and analytical displacement components are compared in Figs. 5.13a and 5.13b, which refer, respectively, to the third and first floor levels. The analytical displacement components have been obtained by assuming different values of the parameters  $c$  and  $V_y$ . It can be observed that the analytical displacement components corresponding to the same data on which the results discussed in Section 5.4 are based (in particular,  $c = 0$  and  $V_y = 1101$  kN for all the stories) provide, in comparison with the measured displacement components, an overestimation of the flexural displacement and an underestimation of the shear displacement.

As shown in Fig. 5.13b, a good correlation of experimental and analytical curves referring to the first level is obtained by simply assuming for  $c$  and  $V$  suitable values ( $c = 0.20$  and  $V_y = 1101$  kN for all the stories). However, for these same values of  $c$  and  $V_y$  the correlation of the curves corresponding to the third floor level is not satisfactory (Fig. 5.13a).

As shown in Fig. 5.13a, a satisfactory correlation of the displacement components at the third floor level is obtained by assuming  $c = 0.20$  and different values of  $V_y$  for each story, depending on the corresponding value of the ratio  $M / V L$  (see APPENDIX A). However, for these new values of  $V_y$  the analytical wall model overestimates the net

displacement ( $\delta_1' = \delta_{1 \text{ shear}} + \delta_{1 \text{ flexural}}$ ) and, particularly, the shear displacement component at the first floor level (Fig. 5.13b). This last effect is produced by a concentration of post-yielding shear deformations at the first story, because of the fact that the external shear is constant along the story height (Fig. 5.4a), while the minimum value of the yielding shear is just that corresponding to the first story ( $V_y = 1101 \text{ kN}$ ). On the other hand, if the  $V_y$  value is assumed the same for all the stories, as in the two cases previously discussed, the shear deformations are uniformly distributed among the three stories.

The results in Fig. 5.13 discussed above give some idea of the difficulty of predicting by the adopted wall model the shear and flexural displacement components at each floor for a given value of the shear, when this value is close to the maximum shear strength. At the same time they show the need for carrying out an extensive parametric study in order to check the sensitivity of the displacement components to different parameters.

As can be observed in Fig. 5.14, the displacement components at the first floor are very sensitive to the choice of the parameter  $c$ . Subsequent to the yielding of the truss element in tension, depending on the choice of  $c$ , the occurrence of yielding in the central vertical spring (when  $c = 0$  and  $c = 0.20$ ) and in the horizontal spring (when  $c = 0.30$  and  $c = 0.50$ ) gives rise to a sudden increase of the flexural or shear displacement component, respectively. For example, for  $c = 0$  the flexural displacement is overestimated and the shear displacement underestimated, while the opposite happens for  $c = 0.5$ . This last value of  $c$ , because of the trapezoidal curvature distribution along the height of the first story of Specimen 3, can be considered an upper bound for  $c$ .

As previously shown in Fig. 3.7, if the condition of displacement compatibility between boundary columns and central panel is satisfied, the flexural response of the central panel results in a softening effect for large deformations, while in Reference 27 a hardening effect is simulated by the OOHM after yielding of the rotational spring. On

the basis of a trilinear idealization of the skeleton curve of the rotational spring, the sensitivity of the displacement components to different choices of the softening ratio  $p_\phi$  were studied. As shown in Fig. 5.15, the softening deformations of the rotational spring can considerably affect the displacement components, in spite of the fact that the flexural contribution of the central panel is relatively small in comparison with that provided by the boundary columns (Fig. 3.6a): the larger the absolute value of  $p_\phi$ , the larger the flexural deformations (the smaller the shear deformations). It should be noted that, when a negative value of  $p_\phi$  is selected, a problem arises with the convergence of the iterative procedure described in Section 4.2 if the corresponding tangent stiffness matrix is not positive definite (see Reference 47). In order to avoid this problem, the (positive) value of  $r$  selected for the axial-stiffness elements of the wall model should be large enough to compensate the effect of the negative value of  $p_\phi$ . For this reason all the analytical results shown in Fig. 5.15 have been obtained by assuming the value  $r = 0.001$ , greater than the values specified in APPENDIX A for the outside truss elements and the central vertical spring.

The sensitivity to the bond-degradation parameter  $\lambda$  and the steel hardening ratio  $r$ , which affect the stiffness of the two outside truss elements and the central vertical spring was also studied.

The results obtained by assuming different values of  $\lambda$  for the two outside truss elements are shown in Figs. 5.16 and 5.17, which correspond, respectively, to the values  $p_\phi = 0$  and  $p_\phi = -0.03$  of the softening ratio. All the curves have been obtained by assuming the value  $r = 0.001$  for the steel hardening ratio.

A comparison of the curves in Figs. 5.16 and 5.17 shows that, while for  $p_\phi = 0$  the sensitivity to the  $\lambda$  value selected for the two outside truss elements is less evident, for  $p_\phi = -0.03$  the displacement components are very sensitive even to small variations of  $\lambda$ . Analogous results, which are omitted for the sake of brevity, have been obtained by assuming different values of  $\lambda$  only for the central vertical spring.

As shown in Fig. 5.18 for the case of  $p_q = -0.03$ , the displacement components are very sensitive to the choice of the  $r$  value selected for the outside truss elements and the central vertical spring. It is interesting to note that, the greater the  $r$  value, the smaller the flexural displacement at both the third floor (Fig. 5.18a) and first floor (Fig. 5.18b), but the greater the net displacement at the first floor ( $\delta_1' = \delta_{1\text{ shear}} + \delta_{1\text{ flexural}}$ , Fig. 5.18b).

This last effect is due to the fact that the results shown in Fig. 5.18 have been obtained by assuming different values of  $V_y$  at each story (see APPENDIX A). As said above with reference to Figs. 5.13, the assumption of the minimum value of  $V_y$  for the first story of the wall model causes a concentration of post-yielding deformations at this story. Thus, for greater values of  $r$ , while the first-floor flexural deformation decreases, the first-floor shear deformation increases because of the greater value of the shear which has to be developed in order to obtain by the wall model the same value of the net top displacement at the third floor  $\delta_3'$  attained for smaller values of  $r$ . The same effect is observed in Figs. 5.15b, 5.16b and 5.17b, which show results based on the same assumption about the  $V_y$  value.

All the above results show the difficulty of controlling the flexural and shear displacement components by the wall model. Further difficulties arise in selecting suitable values of the parameters in order to obtain an accurate description of the flexural and shear response. Because of the inadequacy of the OOHM to simulate the shear behavior under high shear stresses, as pointed out in Section 5.4, attention is focused on the flexural response.

The results shown in Fig. 5.19b refer to the flexural response of a wall member of unit height under a uniform distribution of flexural moment. The results obtained from the UNCOLA analysis, previously shown in Fig. 3.6a, by referring to the response of the boundary columns and central panel under displacement compatibility, are compared with those obtained for the truss elements and rotational spring of the modified wall model, whose stiffness properties were based on the data reported in APPENDIX A, except  $r = 0.001$ . In order to compare the results corresponding to the UNCOLA

analysis with those obtained by the modified wall model for  $c = 0$ , the wall model results have been plotted assuming an abscissa scale which is twice the abscissa scale corresponding to the UNCOLA results. In this manner the results of the UNCOLA analysis and those obtained by the modified wall model give the same horizontal displacement for the wall member under consideration (Fig. 5.19a).

The sensitivity of the flexural response of the wall model to the choice of the  $\lambda$  value assumed for the two outside truss elements is now studied. As shown in Fig. 5.19a, the flexural response of the central panel based on the UNCOLA analysis is well described by adopting the trilinear idealization for the skeleton curve of the rotational spring, whose response does not depend on the value of  $\lambda$ . The flexural contribution of the two outside truss elements of the wall model is almost unaffected by different choices of  $\lambda$  in the range of wall model rotations less than the rotation corresponding to the yielding point of the central vertical spring. While this yielding point is practically the same for all the curves corresponding to different values of  $\lambda$ , the slope of these curves after the yielding of the central vertical spring depends on the value assumed for  $\lambda$ .

All the curves representing the flexural response of the two outside truss elements of the wall model give, before yielding of the truss element in tension, a good description of the curve obtained by the UNCOLA analysis for the flexural response of the boundary columns, although the former curves provide an overestimation of the curve obtained by the UNCOLA analysis for larger deformations. This result can be explained if we observe that the UNCOLA analysis is based on a fiber model of the wall cross-section, which gives a refined description of the progressive steel yielding in the central panel, whereas the flexural response of the two outside truss elements exhibits sudden changes of stiffness due to the yielding of the truss element in tension and then to the yielding of the central vertical spring. The presence of this last spring produces strengthening and stiffening effects which are particularly important before its yielding.

In order to reduce these strengthening and stiffening effects and obtain a better correlation between the results obtained by the UNCOLA analysis and the wall model, the yielding strength of the central vertical spring was adjusted in a fictitious way (it was reduced to the value  $F_y = 475$  kN, against the actual value  $F_y = 803.088$  kN calculated in APPENDIX A). Nonetheless, this fictitious choice of  $F_y$  for the central vertical spring results in a better correlation of the results obtained by the UNCOLA analysis (based on displacement compatibility) and the adopted wall model also in terms of axial forces in the boundary columns and the central panel (Fig. 5.19c).

The results shown in Fig. 5.19 suggest that, in order to improve the description of the flexural response by the wall model, it is desirable to modify this model in order to have a more gradual description of the progressive steel yielding in the central panel. For instance, the LINK Model proposed in Reference 22 pursues this objective, at least with reference to the base of the wall.

## CHAPTER 6

### SUMMARY, CONCLUSIONS, AND RECOMMENDATIONS

#### 6.1 Summary

The primary objective of the studies reported herein was to select among different models available in literature a relatively simple and reasonably accurate wall model, suitable for incorporation in a practical nonlinear analysis of R C multistory structural systems that use shear walls.

For this purpose models based on a macroscopic approach are more suitable than models based on a microscopic approach, which require a larger storage and are very time-consuming. In Chapter 2, after discussing features and limitations of the models available in the literature, attention is focused on the Three-Vertical-Line-Element Model recently proposed by Kabeyasawa et al. [27]. This model was selected because, although relatively simple, it incorporates the main features of the experimentally observed behavior of R C structural walls (i.e., migration of the neutral axis of the wall cross-section, rocking of the wall, etc.). The model describes flexural and shear deformations of the wall, while the deformation produced by the fixed end rotation due to the slippage of the longitudinal reinforcement embedded in the foundation is not accounted for. The model can simulate flexural as well as sliding shear modes of failure, but cannot simulate web crushing-splitting mode of failure, as is the case for all the models based on a macroscopic approach.

Chapter 3 gives details about the original wall model proposed by Kabeyasawa et al. as well as about how the hysteresis models and stiffness properties of the elements constituting this model were modified in the studies reported herein.

The axial hysteretic behavior of the elements constituting the modified wall model is described by a two-element-in-series model, which is proposed in this report to idealize the hysteretic behavior of a R C column member under axial load reversals. The proposed Axial-Stiffness-Hysteresis Model takes advantage of the fact that its mechanical properties are conceptually based on the actual hysteretic behavior of the materials and their interaction, in such a way that the actual tension-stiffening effect can be described. In defining the mechanical properties of the two elements in series constituting this proposed model some simplifying assumptions are made.

Regarding the rotational and horizontal springs, which respectively describe the flexural behavior of the central panel and the shear behavior of the wall, the force-deformation relationship is based on an Origin-Oriented Hysteresis Model which is the same as adopted in Reference 27.

In order to check the effectiveness and the reliability of the wall model so derived a numerical investigation was carried out by assuming as test walls a group of R C structural walls previously tested by Vallenias et al. [4]. For this purpose a computer program, based on the numerical procedure described in Chapter 4, was developed.

In Chapter 5, after the description of the test walls and their modeling, the results of the numerical investigation are presented and discussed.

Under monotonic loading the modified wall model predicts the measured shear satisfactorily if the analytical and experimental results are compared for the same value of the flexural or the shear displacement. If the same kind of comparison is made under cyclic loading, the measured flexural response is still predicted with satisfactory accuracy by the modified wall model. On the contrary, the measured shear response is

not adequately described by the modified wall model under cyclic loading because of the inadequacy of the Origin-Oriented Hysteresis Model to simulate the shear hysteretic behavior under high shear stresses.

Furthermore, as a parametric study showed, under high shear stresses the description of the measured flexural and shear displacement components by the modified wall model is very difficult and very sensitive to the choice of many parameters.

## 6.2 Conclusions

The studies conducted herein allow the following conclusions to be drawn.

- (1) The Three-Vertical-Line-Element Model proposed in Reference 27 is relatively simple and, therefore, it can be efficiently incorporated in the analysis of complex multistory R C structural systems that use shear walls.
- (2) The Three-Vertical-Line-Element Model is capable of simulating many important features of the experimental measured behavior (i.e., migration of the neutral axis of the wall cross-section , rocking effect, flexural and shear modes of failure, etc.). However, as in the case of all the models based on a macroscopic approach, the web splitting-crushing mode of failure is not simulated.
- (3) The two-element-in-series model proposed in this report in order to simulate the hysteretic behavior of a R C column member under axial load reversals allows a physical interpretation of this behavior, based on the actual mechanical properties of the materials and their interaction.
- (4) Under monotonic loading the modified Three-Vertical-Line-Element Model, obtained after incorporating the proposed two-element-in-series model to simulate the axial hysteretic behavior of the line elements constituting the wall model, provides a satisfactory prediction of the measured shear if the same value of the measured

flexural or shear deformation is assumed for this wall model. On the other hand, for a given value of shear force near the maximum shear strength, it becomes very difficult to predict the measured displacement accurately, because of the flattening of the curves representing the relationship between the shear and the flexural deformation as well as between the shear and the shear deformation.

- (5) Under cyclic loading the modified Three-Vertical-Line -Element Model provides a satisfactory simulation of the flexural hysteretic behavior if the same value of the flexural displacement is assumed to compare analytical and experimental results. The measured shear response, however, is not adequately described by the modified wall model, because of the inadequacy of the Origin-Oriented-Hysteresis Model to describe the shear hysteretic behavior for high shear stresses, as was the case for the test walls considered in these studies.

### **6.3 Recommendations for Future Research**

Even though the Three-Vertical-Line-Element Model proved to be effective and reasonably accurate in simulating the hysteretic flexural behavior of the wall, further improvements could be introduced by pursuing the following studies.

- (1) A more refined description of the flexural behavior of the wall could be obtained from one or both the following approaches:
- (a) More refined (yet relatively simple) laws, based on the actual behavior of the materials and their interaction, should be used to describe the response of the two elements in series constituting the proposed Axial-Stiffness Hysteresis Model.
  - (b) The geometry of the wall model should be modified on the basis of a multi-axial-spring-in-parallel model (like the LINKS model adopted in Reference 22) in order to gradually account for the progressive yielding of the steel in the central panel.

- (2) Hysteresis models, more refined than the Origin-Oriented Hysteresis Model, should be used to simulate the shear behavior of the wall when high shear stresses are expected.
- (3) Particularly under high shear stresses, the flexural and shear displacement components of the wall should be evaluated by relating in some way the flexural and shear responses of the wall model, which at present are independently described by the wall model - apart from satisfying the equilibrium condition. The wall model should also be capable of accounting for variation of shear stiffness due to changes of the axial and/or flexural strengths.
- (4) Deformations produced by the fixed end rotation due to slippage of the longitudinal reinforcement embedded in the foundation should be incorporated in the wall model.
- (5) Further efforts should be devoted to developing models based in part on a microscopic approach, which would be capable of simulating the web splitting-crushing mode of failure, but would, at the same time, be relatively simple in order to carry out the analysis in reasonable computational time. This could be achieved by using more detailed models for those regions of the wall for which the above mode of failure is expected (i.e., the regions at the base of R C structural walls, which are part of multistory frame-wall structural systems).
- (6) A better calibration of the parameters affecting the response of the wall model is needed in order to improve the prediction of the measured hysteretic behavior.

## REFERENCES

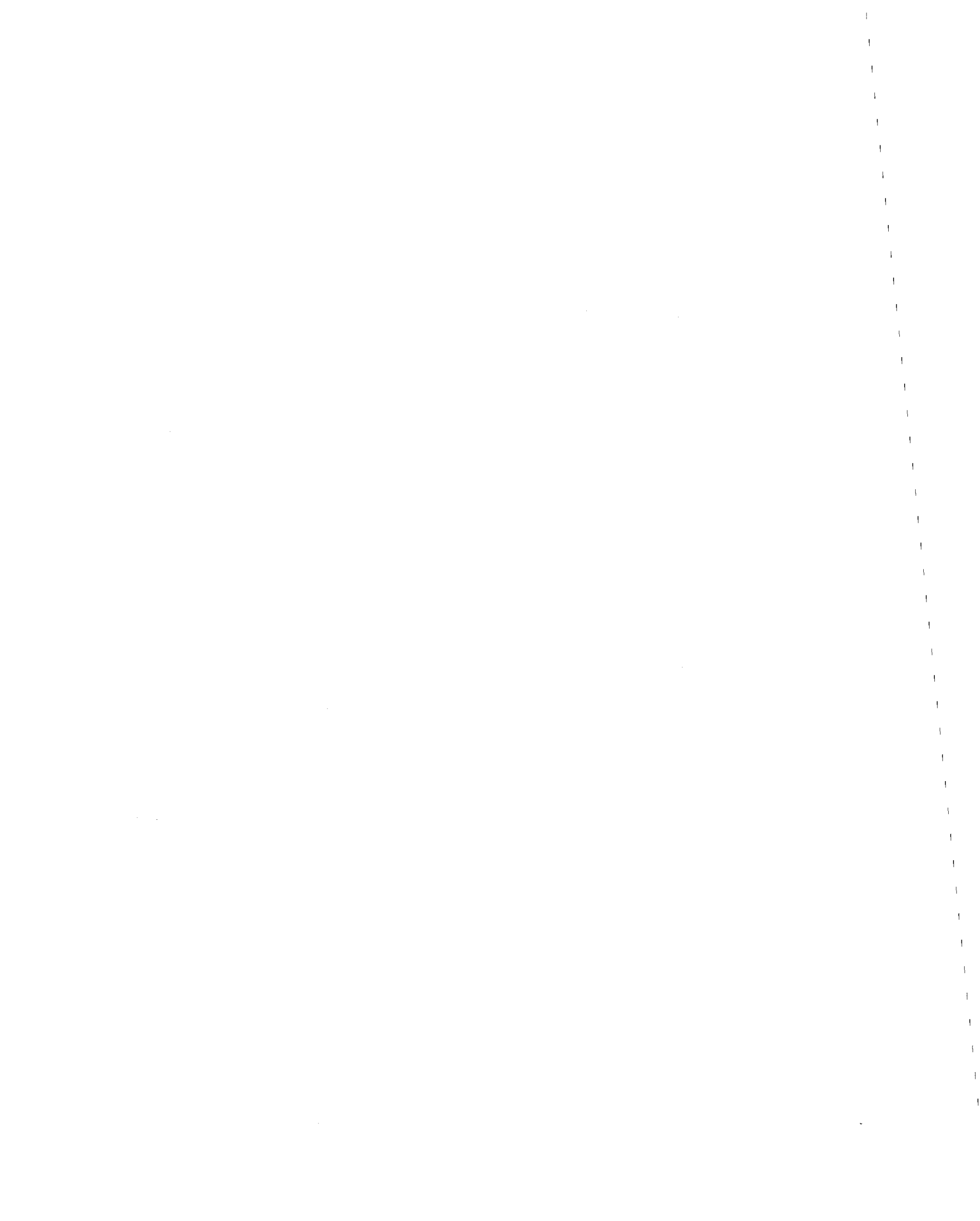
- [1] Park, R., and Paulay, T., Reinforced Concrete Structures, John Wiley and Sons, Inc., 1975.
- [2] Paulay, T., "Earthquake Resistant Structural Walls", Proceedings of a Workshop on Earthquake Resistant Reinforced Concrete Building Construction [ERCBC], Bertero, V. V., organizer, Vol. III, pp. 1339-1365, University of California, Berkeley, 1977.
- [3] Wang, T. Y., Bertero, V. V., and Popov, E. P. "Hysteretic Behavior of Reinforced Concrete Framed Walls", Report No. UCB/EERC-75/23, Earthquake Engineering Research Center, University of California, Berkeley, 1975.
- [4] Vallenias, J. M., Bertero, V. V., and Popov, E. P., "Hysteretic Behavior of Reinforced Concrete Structural Walls", Report No. UCB/EERC-79/20, Earthquake Engineering Research Center, University of California, Berkeley, 1979.
- [5] Iliya, R., and Bertero, V. V., "Effects of Amount of Arrangement of Wall-Panel Reinforcement on Hysteretic Behavior of Reinforced Concrete Walls", Report No. UCB/EERC-80/04, Earthquake Engineering Research Center, University of California, Berkeley, 1980.
- [6] Bertero, V. V., "Seismic Behavior of R C Wall Structural Systems", Proceedings, 7th World Conference on Earthquake Engineering, Vol. 6, Istanbul, Turkey, 1980.
- [7] Harris, H. G., Bertero, V. V., and Clough, R. W., "One-Fifth Scale Model of a Seven-Story Reinforced Concrete Frame-Wall Building Under Earthquake Loading", Proceedings, International Seminar on Dynamic Modelling of Structures, Building Research Station, Garston, England, 1981.
- [8] Aktan, A. E., and Bertero, V. V., "The Seismic Resistant Design of R C Coupled Structural Walls", Report No. UCB/EERC-81/07, Earthquake Engineering Research Center, University of California, Berkeley, 1981.
- [9] Aktan, A. E., and Bertero, V. V., "Analytical and Physical Modeling of R C Frame-Wall / Coupled Wall Structures", Proceedings, International Seminar on Dynamic Modelling of Structures, Building Research Station, Garston, England, 1981.
- [10] Aktan, A. E., and Bertero, V. V., "States of the Art and Practice in the Optimum Seismic Design and Analytical Response Prediction of R C Frame-Wall Structures", Report No. UCB/EERC-82/06, Earthquake Engineering Research Center, University of California, Berkeley, 1982.

- [11] Aktan, A. E., Bertero, V. V., and Piazza, M., "Prediction of the Seismic Responses of R C Frame-Coupled Wall Structures", Report No. UCB/EERC-82/12, Earthquake Engineering Research Center, University of California, Berkeley, 1982.
- [12] Aktan, A. E., and Bertero, V. V., "1/5 Scale Model of the 7-Story R C Frame-Wall Test Building: Design and Construction", Proceedings, 3rd Joint Technical Coordinating Committee, U.S.-Japan Joint Cooperative Earthquake Research Program, Building Research Institute, Tsukuba, Japan, 1982.
- [13] Bertero, V. V., "Implications of Recent Research Results on Present Methods for Seismic Resistant Design of R C Frame-Wall Building Structures", Proceedings, 51st Annual Convention of SEAOC, Sacramento, California, pp. 79-116, 1982.
- [14] Charney, F. A., and Bertero, V. V., "An Evaluation of the Design and Analytical Seismic Response of a Seven-Story Reinforced Concrete Frame-Wall Structure", Report No. UCB/EERC-82/08, Earthquake Engineering Research Center, University of California, Berkeley, 1982.
- [15] Wagner, M. T., and Bertero, V. V., "Mechanical Behavior of Shear Wall Vertical Boundary Members: An Experimental Investigation", Report No. UCB/EERC-82/18, Earthquake Engineering Research Center, University of California, Berkeley, 1982.
- [16] Aktan, A. E., Bertero, V. V., Chowdhury, A. A., and Nagashima, T., "Experimental and Analytical Predictions of the Mechanical Characteristics of a 7-Story 1/5 Scale Model R C Frame-Wall Building Structure", Report No. UCB/EERC-83/13, Earthquake Engineering Research Center, University of California, Berkeley, 1983.
- [17] Charney, F. A., and Bertero, V. V., "Correlation of Experimental and Analytical Response of a 1/5 Scale Reinforced Concrete Frame-Wall Structure", Proceedings, 4th Joint Technical Coordinating Committee, U.S.-Japan Joint Cooperative Earthquake Research Program, Building Research Institute, Tsukuba, Japan, 1983.
- [18] Aktan, A. E., and Bertero, V. V., "Seismic Response of R C Frame-Wall Structures", Journal of Structural Engineering, ASCE, Vol. 110, No. 8, August, 1984.
- [19] Bertero, V. V., "State of the Art and Practice in Seismic Resistant Design of R C Frame-Wall Structural Systems, Proceedings, 8th World Conference on Earthquake Engineering, Vol. 5, San Francisco, U.S.A., 1984.
- [20] Bertero, V. V., Aktan, A. E., Charney, F. A., and Sause, R., "U.S.-Japan Cooperative Earthquake Research Program: Earthquake Simulation Tests and Associate Studies of a 1/5th-Scale Model of a 7-Story Reinforced Concrete Test Structure", Report No. UCB/EERC-84/05, Earthquake Engineering Research Center, University of California, Berkeley, 1984.

- [21] Vulcano, A., and Bertero, V. V., "Nonlinear Analysis of R C Structural Walls", Proceedings, 8th European Conference on Earthquake Engineering, Vol. 3, Lisbon, Portugal, 1986.
- [22] Charney, F. A., "Correlation of the Analytical and Experimental Seismic Response of a 1/5th-Scale Seven-Story Reinforced Concrete Frame-Wall Structure", Ph. D. Dissertation, University of California, Berkeley, 1987.
- [23] Moazzami, S., and Bertero, V. V., "Three-Dimensional Inelastic Analysis of Reinforced Concrete Frame-Wall Structures", Report No. UCB/EERC-87/05, Earthquake Engineering Research Center, University of California, Berkeley, 1987.
- [24] Tomii, M., and Osaki, Y., "Shearing Resistance of Reinforced Concrete Bracing Walls", Transactions, Architectural Institute of Japan, No. 51, pp. 83-95, September, 1955.
- [25] Hirose, M., "Past Experimental Results on Reinforced Concrete Shear Walls and Analysis on Them" (in Japanese), Kenchiku Kenkyu Shiryo, No. 6, Building Research Institute, Ministry of Construction, 1975.
- [26] Otani, S., "Effectiveness of Structural Walls in Reinforced Concrete Buildings During Earthquake", Civil Engineering Studies, Structural Research Series, Report No. 492, University of Illinois, Urbana, 1981.
- [27] Kabeyasawa, H., Shioara, H., Otani, S., and Aoyama, H., "Analysis of the Full-Scale Seven-Story Reinforced Concrete Test Structure: Test PSD3", Proceedings, 3rd Joint Technical Coordinating Committee, U.S.-Japan Cooperative Earthquake Research Program, Building Research Institute, Tsukuba, Japan, 1982. See also: Kabeyasawa, T., Shioara, H., Otani, S., "U.S.-Japan Cooperative Research on R C Full-Scale Building Test - Part 5: Discussion on Dynamic Response System", Proceedings, 8th World Conference on Earthquake Engineering, Vol. 6, San Francisco, U.S.A., 1984.
- [28] Okamoto, S., et al., "A Progress Report on the Full-Scale Seismic Experiment of a Seven Story Reinforced Concrete Building - Part of the U.S.-Japan Cooperative Program", Proceedings, 3rd Joint Technical Coordinating Committee, U.S.-Japan Cooperative Earthquake Research Program, Building Research Institute, Tsukuba, Japan, 1982.
- [29] Hiraishi, H., "Evaluation of Shear and Flexural Deformations of Flexural Type Shear Walls", Proceedings, 4th Joint Technical Coordinating Committee, U.S.-Japan Cooperative Earthquake Research Program, Building Research Institute, Tsukuba, Japan, 1983.

- [30] U.S.-Japan Joint Technical Coordinating Committee, "Interim Summary Reports on Tests of 7-Story R C Building", *Journal of Structural Engineering*, ASCE, Vol. 110, No. 10, October, 1984.
- [31] Aristizabal-Ochoa, J. D., and Sozen, M. A., "Behaviour of 10-Story R C Walls Subjected to Earthquake Motions", *Civil Engineering Studies, Structural Research Series*, Report No. 431, University of Illinois, Urbana, 1976.
- [32] Barney, G. B., Shiu, K. N., Rabbat, B. G., Fiorato, A. E., Russel, H. G., and Corley, W. G., "Earthquake Resistant Structural Walls-Tests of Coupling Beams", report to National Science Foundation, submitted by Portland Cement Association, Skokie, Ill., Jan., 1978. Also available through National Technical Information Service, U.S. Dept. of Commerce, NTIS Accession No. PB281733, 5285 Port Royal Rd., Springfield, Va. 22161.
- [33] Oesterle, R. G., Aristizabal-Ochoa, J. D., Fiorato, A. E., Russel, H. G., and Corley, W. G., "Earthquake Resistant Structural Walls-Tests of Isolated Walls-Phase II", report to National Science Foundation, submitted by Portland Cement Association, Skokie, Ill., Oct., 1979. Also available through National Technical Information Service, U.S. Dept. of Commerce, NTIS Accession No. 271467/AS, 5285 Port Royal Rd., Springfield, Va. 22161.
- [34] Shiu, K. N., Aristizabal-Ochoa, J. D., Barney, G. B., Fiorato, A. E., and Corley, W. G., "Earthquake Resistant Structural Walls-Coupled Wall Tests", report to National Science Foundation, submitted by Portland Cement Association, Skokie, Ill., July, 1981. Also available through National Technical Service, U.S. Dept. of Commerce, NTIS Accession No. PB82-131954, 5285 Port Royal Rd., Springfield, Va. 22161.
- [35] Shiu, K. N., Daniel, J. I., Aristizabal-Ochoa, J. D., Fiorato, A. E., and Corley, W. G., "Earthquake Resistant Structural Walls-Tests of Walls With and Without Openings", report to National Science Foundation, submitted by Portland Cement Association, Skokie, Ill., July, 1981. Also available through National Technical Information Service, U.S. Dept. of Commerce, Accession No. PB82-131947, 5285 Port Royal Rd., Springfield, Va. 22161.
- [36] Takayanagi, T., and Schnobrich, W. C., "Nonlinear Analysis of Coupled Wall Systems", *Earthquake Engineering and Structural Dynamics*, Vol. 7, 1979.
- [37] Takayanagi, T., Derecho, A. T., and Corley, W. G., "Analysis of Inelastic Shear Deformation Effects in Reinforced Concrete Structural Wall Systems", *Nonlinear Design of Concrete Structures*, CSCE-ASCE-ACI-CEB International Symposium, University of Waterloo, Canada, 1979.
- [38] Keshavarzian, M., and Schnobrich, W. C., "Inelastic Analysis of R C Coupled Shear Walls", *Earthquake Engineering and Structural Dynamics*, Vol. 13, 1985.

- [39] Shiu, K. N., Takayanagi, T., and Corley, W. G., "Seismic Behaviour of Coupled Wall Systems", *Journal of Structural Engineering*, ASCE, Vol. 110, No. 5, May, 1984.
- [40] Finite Element Analysis of Reinforced Concrete , State of the Art Report published by ASCE, New York, 1982.
- [41] Kanaan, A. E., and Powell, G. H., "DRAIN-2D, A General Purpose Computer Program for Dynamic Analysis of Planar Structures", Report No. UCB/EERC-73/06, Earthquake Engineering Research Center, University of California, Berkeley, 1973.
- [42] Otani, S., "SAKE - A Computer Program for Inelastic Response of R C Frames to Earthquakes", *Civil Engineering Studies, Structural Research Series*, Report No. 413, University of Illinois ,Urbana, 1974.
- [43] Otani, S., "Inelastic Analysis of R C Frame Structures", *Journal of the Structural Division*, ASCE, Vol. 100, No. ST7, July, 1974.
- [44] Soleimani, D., Popov, E. P., and Bertero, V. V., "Nonlinear Beam Model for R C Frame Analysis", *Proceedings, 7th Conference on Electronic Computation*, St. Louis, U.S.A., 1979, published by ASCE, New York, 1979.
- [45] Meyer C., Roufaiel, M. S. L., and Arzoumanidis, S. G., "Analysis of Damaged Concrete Frames for Cyclic Loads", *Earthquake Engineering and Structural Dynamics*, Vol. 11, 1983.
- [46] Kaba, S., and Mahin, S., "Interactive Computer Analysis Methods for Predicting the Inelastic Cyclic Behavior of Sections", Report No. UCB/EERC-83/18, Earthquake Engineering Research Center, University of California, Berkeley, 1983.
- [47] Casciaro, R., "Time Evolutional Analysis of Nonlinear Structures", *Meccanica*, No. 3, Vol. X, 1975.



## APPENDIX A

### STIFFNESS PROPERTIES OF THE ELEMENTS CONSTITUTING THE MODEL OF SPECIMENS 3 AND 4

#### Outside Truss Elements

$$A_s (8\#6) = 8 \times 281 = 2248 \text{ mm}^2$$

$$A_c = 254 \times 254 - 2248 = 62268 \text{ mm}^2$$

$$F_y = 2248 \times 0.444 = 998.112 \text{ kN}$$

$$E_s A_s = 211.4 \times 2248 = 475227.2 \text{ kN}$$

$$E_c A_c = 22.5 \times 62268 = 1401030.0 \text{ kN}$$

By assuming  $K_t/K_c = 0.90$  and  $K_h/K_c = 0.001$ , as well as in Reference 27, the values of the bond-degradation parameter  $\lambda$  and the steel-hardening ratio  $r$  can be adjusted on the basis of Eqs. (3.7) :

$$\begin{aligned} \lambda &= (K_c/K_t - 1) E_s A_s / E_c A_c = \\ &= (1/0.90 - 1) 475227.2 / 1401030 = 0.0376 \end{aligned}$$

$$\begin{aligned} r &= (1 + E_c A_c / E_s A_s) / [1 + (K_c/K_h - 1) / \lambda] = \\ &= (1 + 1401030 / 475227.2) / (1 + 999 / 0.0376) = 0.000148 \end{aligned}$$

#### Central Element Springs

##### (a) Vertical Spring

$$A_s (\#2 \text{ at } 76 \text{ mm}) = 2 \times 25 \times 31.67 = 1584 \text{ mm}^2$$

$$A_c = 1880 \times 102 - 1584 = 190176 \text{ mm}^2$$

$$F_y = 1584 \times 0.507 = 803.088 \text{ kN}$$

$$E_s A_s = 211.0 \times 1584 = 334224 \text{ kN}$$

$$E_c A_c = 22.5 \times 190176 = 4278960 \text{ kN}$$

$$\lambda = (1 / 0.90 - 1) 334224 / 4278960 = 0.0087$$

$$r = (1 + 4278960 / 334224) / (1 + 999 / 0.0087) = 0.000120$$

(b) Horizontal Spring

$$A_w = (2388 - 254) \times 102 = 217668 \text{ mm}^2$$

$$G = E / [2(1+\nu)] = 22.5 / [2(1 + 0.2)] = 9.375 \text{ kN/mm}^2$$

$$u = 1880/2388 \quad ; \quad \nu = 102/254$$

The shape factor, according to Eq. (3.3b), is  $\chi = 1.191$ .

$$f'_c = 34.8 \text{ MPa}$$

$$f_{wh} = 507 \text{ MPa}$$

$$\rho_t = 100 \times 2248 / [134.335 \times (2388 - 254/2)] = 0.740127$$

$$\rho_{wh} = 2 \times 31.67 / (134.335 \times 76) = 0.00620405$$

$$\sigma_o = 2 \times 434000 / (254^2 + 1880 \times 102) = 2.7058 \text{ MPa}$$

$$b_e = (2 \times 254^2 + 1880 \times 102) / 2388 = 134.335 \text{ mm}$$

$$j = 7/8 (2388 - 254/2) = 1978.375 \text{ mm}$$

$$M / V L = (0.644 \times 2134 + 3009) / 2388 = 1.835 \text{ (first floor)}$$

$$M / V L = (0.644 \times 2134 + 1828) / 2388 = 1.341 \text{ (second floor)}$$

$$M / V L = (0.644 \times 2134 + 914) / 2388 = 0.958 \text{ (third floor)}$$

Therefore, the skeleton curve is defined by the following parameters:

$$K_s = 9.375 \times 217668 / (1.191 \times 1181) = 1450.79 \text{ kN / mm (first story)}$$

$$K_s = 9.375 \times 217668 / (1.191 \times 914) = 1874.60 \text{ kN / mm (second and third stories)}$$

$$\alpha_s = 0.14 + 0.46 \times 0.00621 \times 507 / 34.8 = 0.18$$

$$V_c = 0.438 \times 34.8^{1/2} \times 217668 = 562417 \text{ N} \cong 562 \text{ kN}$$

The yielding shear  $V_y$  is assumed practically equal to the ultimate shear  $V_u$ , which is calculated according to Eq. (3.5) \* :

$$V_y \equiv V_u \equiv 1101 \text{ kN (first story)}$$

$$V_y \equiv V_u \equiv 1200 \text{ kN (second story)}$$

$$V_y \equiv V_u \equiv 1320 \text{ kN (third story)}$$

(c) Rotational Spring

The stiffness properties of the rotational spring, based on displacement compatibility between the boundary columns and the central panel, are defined by referring to the following parameters, which have been determined in order to idealize as a softening trilinear curve the moment-curvature ( $M-\psi$ ) relationship determined for the central panel by the UNCOLA analysis [46] (Fig. 3.7):

$$M_c = 200000 \text{ kN mm} \quad ; \quad \psi_c = 1.5 \times 10^{-7} \text{ rad / mm}$$

$$M_y = 520000 \text{ kN mm} \quad ; \quad \psi_y = 1.5 \times 10^{-6} \text{ rad / mm}$$

$$p_\psi = - 0.03 \quad **$$

$$EI_o = M_c / \psi_c = 200000 / 1.5 \times 10^{-7} = 1.34 \times 10^{12} \text{ kN mm}^2$$

Therefore, based on the deformation of the wall member under a uniform distribution of flexural moment, as well as in Reference 27, the initial elastic stiffness of the rotational spring is in general for  $0 \leq c < 1$ :

$$K_\phi = 2 (1 - c) EI_o / h$$

In particular, for  $c = 0$  , as assumed in Reference 27 :

$$K_\phi = 2 \times 1.34 \times 10^{12} / 1181 = 2.27 \times 10^9 \text{ kN mm / rad (first story)}$$

$$K_\phi = 2 \times 1.34 \times 10^{12} / 914 = 2.93 \times 10^9 \text{ kN mm / rad (second and third stories)}$$

-----  
\* In Ref. [27] the same  $V_u$  value which was calculated with reference to the first story was assumed for all the stories. All the results presented in Section 5.4 are based on this assumption, just to check the reliability of the wall model.

\*\* In Ref. [27] the slope of the third branch was assumed as  $p_\psi = p_\phi = + 0.001$ . All the results presented in Section 5.4 are based on this assumption, just to check the reliability of the wall model.

The ratio of the stiffness of the second and third branches of the skeleton curve of the rotational spring to the initial elastic stiffness calculated above are, respectively,

$$\begin{aligned}\alpha_{\phi} = \alpha_{\psi} &= (M_y - M_c) / [(\psi_y - \psi_c) EI_0] = \\ &= (520000 - 200000) / [(1.5 - 0.15)10^{-6} \times 1.34 \times 10^{12}] = 0.17 \quad (\text{all stories})\end{aligned}$$

$$p_{\phi} = p_{\psi} = -0.03 \quad (p_{\phi} = +0.001, \text{ after Kabeyasawa et al. [27]})$$

## APPENDIX B

### STIFFNESS PROPERTIES OF THE ELEMENTS CONSTITUTING THE MODEL OF SPECIMENS 5 AND 6

#### Outside Truss Elements

$$A_s (9\#5) = 9 \times 198 = 1782 \text{ mm}^2$$

$$A_c = 279 \times 114 - 1782 = 30024 \text{ mm}^2$$

$$F_y = 1782 \times 0.482 = 858.924 \text{ kN}$$

$$E_s A_s = 216 \times 1782 = 384912 \text{ kN}$$

$$E_c A_c = 22.1 \times 30024 = 663530.4 \text{ kN}$$

$$\lambda = (1 / 0.90 - 1) 384912 / 663530.4 = 0.0645$$

$$r = (1 + 663530.4 / 384912) / (1 + 999 / 0.0645) = 0.000176$$

#### Central Element Springs

##### (a) Vertical Spring

$$A_s (\#2 \text{ at } 102 \text{ mm}) = 2 \times 19 \times 31.67 = 1203 \text{ mm}^2$$

$$A_c = 1854 \times 114 - 1203 = 210153 \text{ mm}^2$$

$$F_y = 1203 \times 0.507 = 609.921 \text{ kN}$$

$$E_s A_s = 211 \times 1203 = 253930 \text{ kN}$$

$$E_c A_c = 22.1 \times 210153 = 4644371 \text{ kN}$$

$$\lambda = (1 / 0.90 - 1) 253930 / 4644371 = 0.00607$$

$$r = (1 + 4644371 / 253930) / (1 + 999 / 0.00607) = 0.000117$$

(b) Horizontal Spring

$$A_w = (2412 - 279) \times 114 = 243162 \text{ mm}^2$$

$$G = 22.1 / [2 (1 + 0.2)] = 9.208 \text{ kN / mm}^2$$

$$u = 1854 / 2412 \quad ; \quad v = 114 / 114 = 1$$

The shape factor, according to Eq. 3.3b, is  $\chi = 1.326$

$$f'_c = 33.47 \text{ MPa}$$

$$f_{wh} = 507 \text{ MPa}$$

$$\rho_l = 100 \times 1782 / [114 \times (2412 - 279 / 2)] = 0.687858$$

$$\rho_{wh} = 2 \times 31.67 / (114 \times 102) = 0.0054472$$

$$\sigma_o = 2 \times 299000 / (2412 \times 114) = 2.1748 \text{ MPa}$$

$$b_c = 114 \text{ mm}$$

$$j = 7/8 (2412 - 279/2) = 1988.438 \text{ mm}$$

$$M / V L = (0.522 \times 2134 + 0.799 \times 3009 + 0.104 \times 2095 + 0.097 \times 1181) / 2412 = \\ = 1.595 \text{ (first floor)}$$

$$M / V L = (0.522 \times 2134 + 0.799 \times 1828 + 0.104 \times 914) / 2412 = 1.107 \text{ (second floor)}$$

$$M / V L = (0.522 \times 2134 + 0.799 \times 914) / 2412 = 0.764 \text{ (third floor)}$$

$$K_s = 9.208 \times 243162 / (1.326 \times 1181) = 1429.77 \text{ kN / mm (first story)}$$

$$K_s = 9.208 \times 243162 / (1.326 \times 914) = 1847.44 \text{ kN / mm (second and third stories)}$$

$$\alpha_s = 0.14 + 0.46 \times 0.0054472 \times 507 / 33.47 = 0.178$$

$$V_c = 0.438 \times 33.47^{1/2} \times 243162 = 616166 \text{ N} \cong 616 \text{ kN}$$

$$V_y \cong V_u \cong 918 \text{ kN (first story)}$$

$$V_y \cong V_u \cong 1018 \text{ kN (second story)}$$

$$V_y \cong V_u \cong 1134 \text{ kN (third story)}$$

(c) Rotational Spring

$$M_c = 127000 \text{ kN mm} \quad ; \quad \psi_c = 0.9 \times 10^{-7} \text{ rad / mm}$$

$$M_y = 590000 \text{ kN mm} \quad ; \quad \psi_y = 1.5 \times 10^{-6} \text{ rad / mm}$$

$$p_\psi = -0.03$$

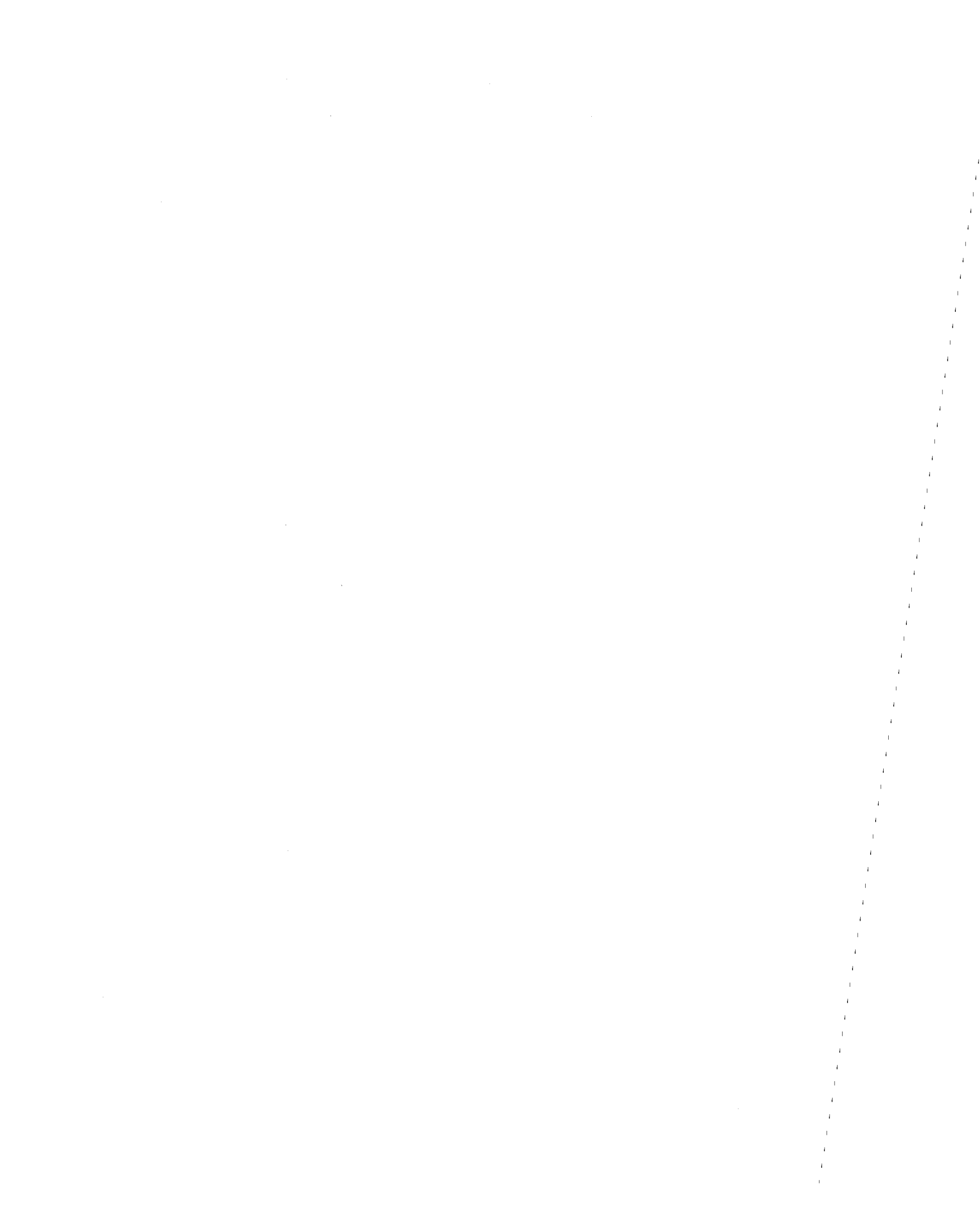
$$EI_0 = 127000 / 0.9 \times 10^{-7} = 1.41 \times 10^{12} \text{ kN mm}^2$$

$$K_\phi = 2 \times 1.41 \times 10^{12} / 1181 = 2.39 \times 10^9 \text{ kN mm / rad (first story)}$$

$$K_\phi = 2 \times 1.41 \times 10^{12} / 914 = 3.09 \times 10^9 \text{ kN mm / rad (second and third stories)}$$

$$\alpha_\phi = \alpha_\psi = (590000 - 127000) / [(1.5 - 0.09) \times 10^{-6} \times 1.41 \times 10^{12}] = 0.23 \text{ (all stories)}$$

$$p_\phi = p_\psi = -0.003 \quad (p_\phi = +0.001, \text{ after Kabeyasawa et al. [27]})$$



## TABLES



Table 5.1 - Mechanical Characteristics of Materials (Specimens 3 and 4 [4])

(a) STEEL PROPERTIES (See Fig. 5.6a)

Reinforcement		Bar Area (mm <sup>2</sup> )	E <sub>s</sub> (MPa)	f <sub>y</sub> (MPa)	f <sub>u</sub> (MPa)	ε <sub>SH</sub>	ε <sub>u</sub>
Boundary Columns	Longitudinal (#6)	281.00	211400	444	639	0.012	0.150
	Transverse (gage No. 7 wire)	16.28	190000	440	479	====	0.180
Central Panel	Horizontal and Vertical (#2)	31.67	211000	507	730	0.01	0.12

(b) CONCRETE PROPERTIES AT TIME OF TESTING (See Fig. 5.6b)

$$f'_c \text{ (average)} = (35.2 + 35.4 + 33.8) / 3 = 34.8 \text{ MPa} *$$

$$E_c \text{ (average)} = 46000 f'_c{}^{1/2} \text{ (psi)} = 3820 f'_c{}^{1/2} \text{ (MPa)} = 3820 \times 34.8^{1/2} \cong 22500 \text{ MPa}$$

Unconfined Concrete :

$$\epsilon_0' = 0.003$$

$$\epsilon_u' = 0.01$$

Confined Concrete :

$$k \cong 1.2$$

$$\epsilon_0 = 0.009$$

$$\epsilon_{.3k} = 0.053$$

$$\epsilon_u = 0.065$$

Units :

$$1 \text{ psi} = 6.895 \times 10^{-3} \text{ Mpa}$$

$$1 \text{ in} = 25.4 \text{ mm}$$

-----  
 \* This value has been calculated as an average of the values corresponding to the three stories of Specimen 3. The same value has been adopted also for Specimen 4, because the difference is practically negligible.

Table 5.2 - Mechanical Characteristics of Materials (Specimens 5 and 6 [4])

(a) STEEL PROPERTIES (See Fig. 5.6a)

Reinforcement		Bar Area (mm <sup>2</sup> )	E <sub>s</sub> (MPa)	f <sub>y</sub> (MPa)	f <sub>u</sub> (MPa)	ε <sub>SH</sub>	ε <sub>u</sub>
Boundary Columns	Longitudinal (#5)	198.00	216000	482	687	0.013	0.148
	Transverse (gage No. 7 wire)	16.28	190000	440	479	====	0.180
Central Panel	Horizontal and Vertical (#2)	31.67	211000	507	730	0.01	0.12

(b) CONCRETE PROPERTIES AT TIME OF TESTING (See Fig. 5.6b)

$$f'_c \text{ (average)} = (34.5 + 33.5 + 32.4) / 3 = 33.47 \text{ MPa} *$$

$$E_c \text{ (average)} = 46000 f'_c{}^{1/2} \text{ (psi)} = 3820 f'_c{}^{1/2} \text{ (MPa)} = 3820 \times 33.47^{1/2} \cong 22100 \text{ Mpa}$$

Unconfined Concrete :

$$\epsilon_0' = 0.003$$

$$\epsilon_u' = 0.01$$

Confined Concrete :

$$k \cong 1.2$$

$$\epsilon_0 = 0.009$$

$$\epsilon_{.3k} = 0.053$$

$$\epsilon_u = 0.065$$

Units :

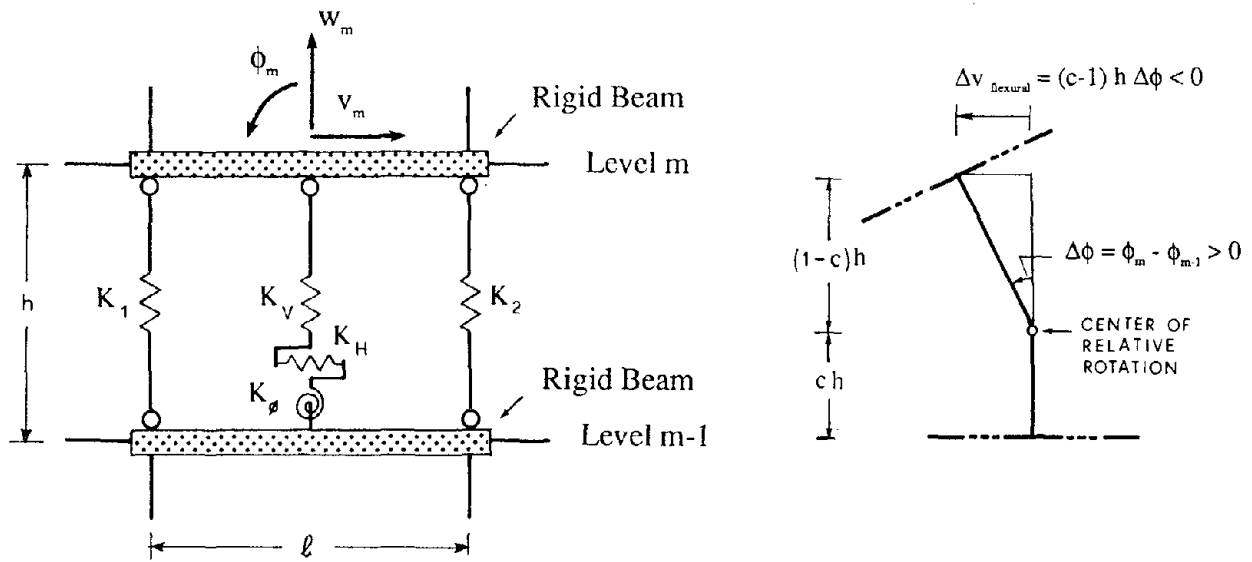
$$1 \text{ psi} = 6.895 \times 10^{-3} \text{ MPa}$$

$$1 \text{ in} = 25.4 \text{ mm}$$

\* This value has been calculated as an average of the values corresponding to the three stories of Specimen 5. The same value has been adopted also for Specimen 6, because the difference is practically negligible.



## FIGURES



(a) Wall Member Model

(b) Relationship Between Relative Flexural Displacement and Relative Rotation

Fig. 3.1 - RC Wall Model

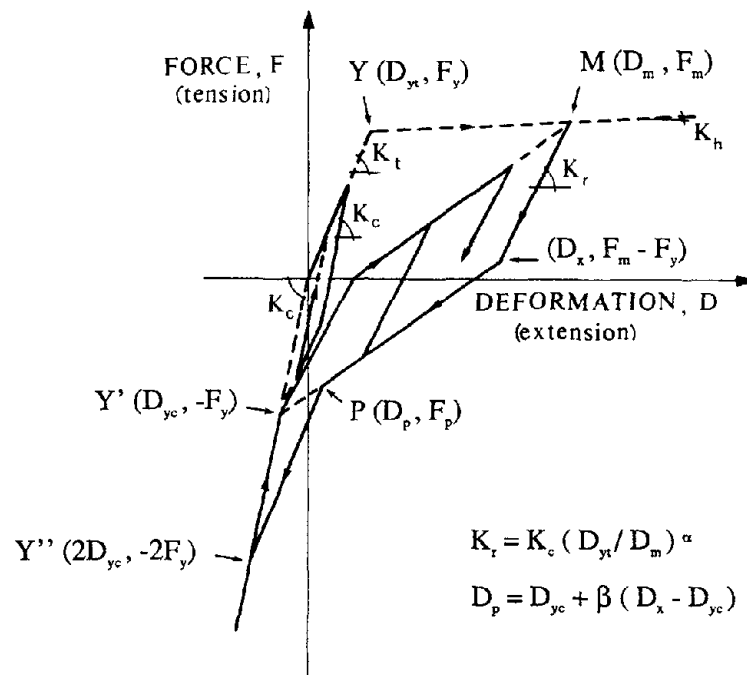
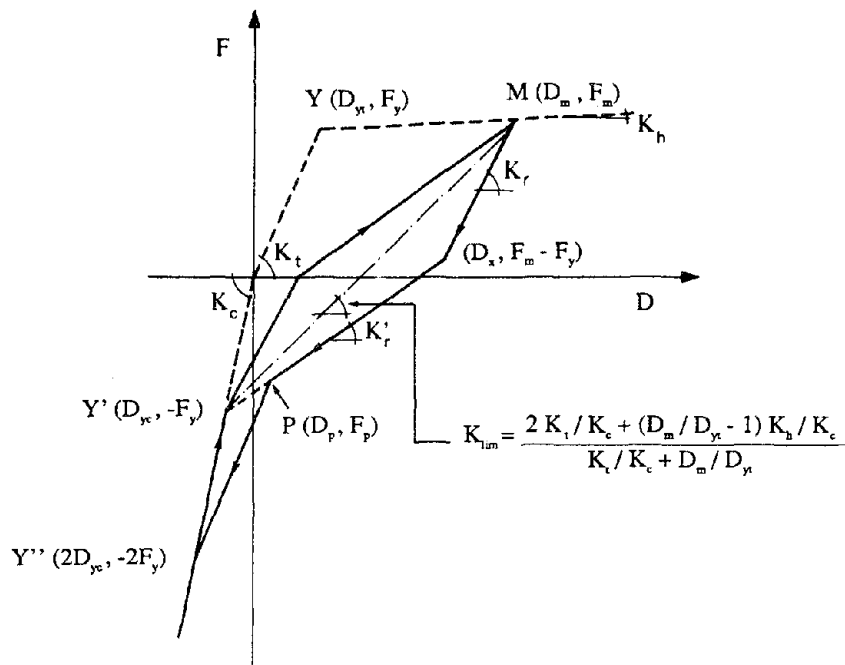
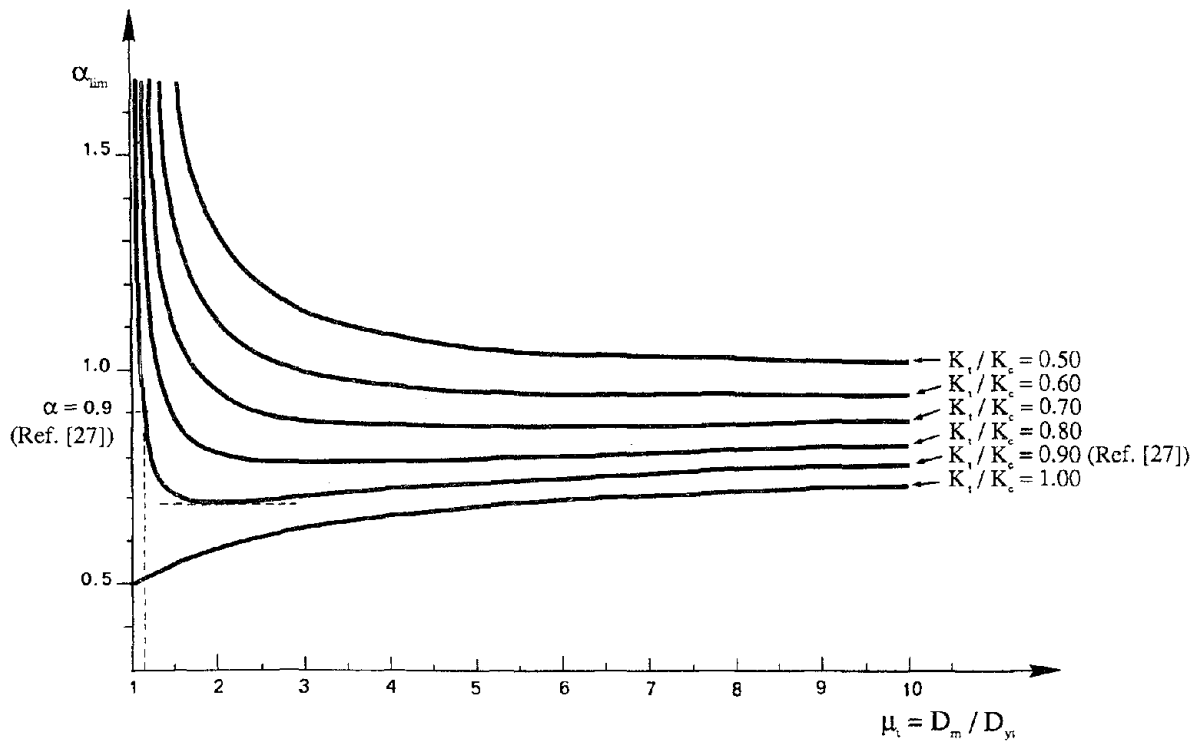


Fig. 3.2 - Axial-Stiffness Hysteresis Model Proposed by Kabeyasawa et al. [27]



(a) Limit Value ( $K_{lim}$ ) of the Unloading Stiffness  $K_r$



(b) Limit Value of the Unloading Degradation Parameter  $\alpha$  Versus Tensile Ductility Factor  $\mu_t$  ( $K_h/K_c = 0.001$ )

Fig. 3.3 - Limit Values of the Unloading Stiffness  $K_r$  and Degradation Parameter  $\alpha$  for the Axial-Stiffness Hysteresis Model in Fig. 3.2

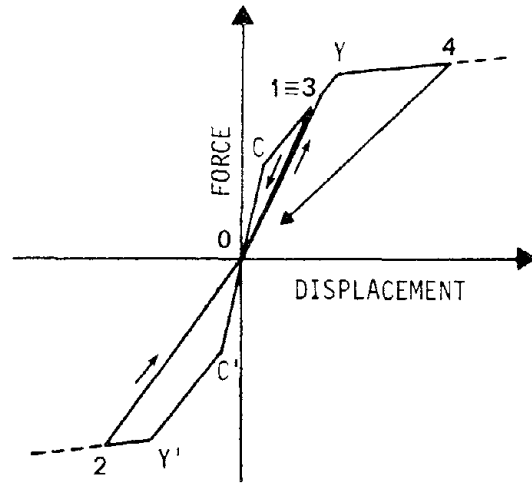


Fig. 3.4 - Origin-Oriented Hysteresis Model [27]

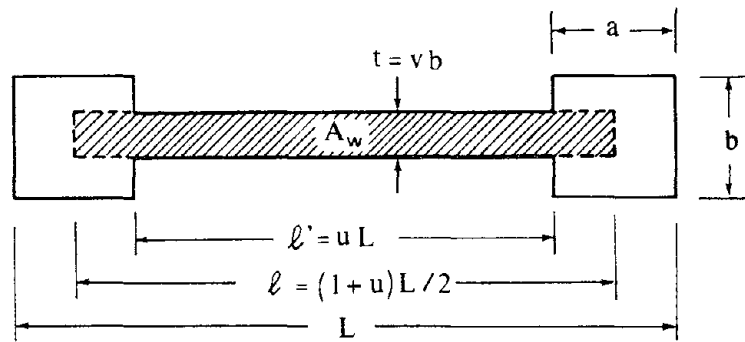
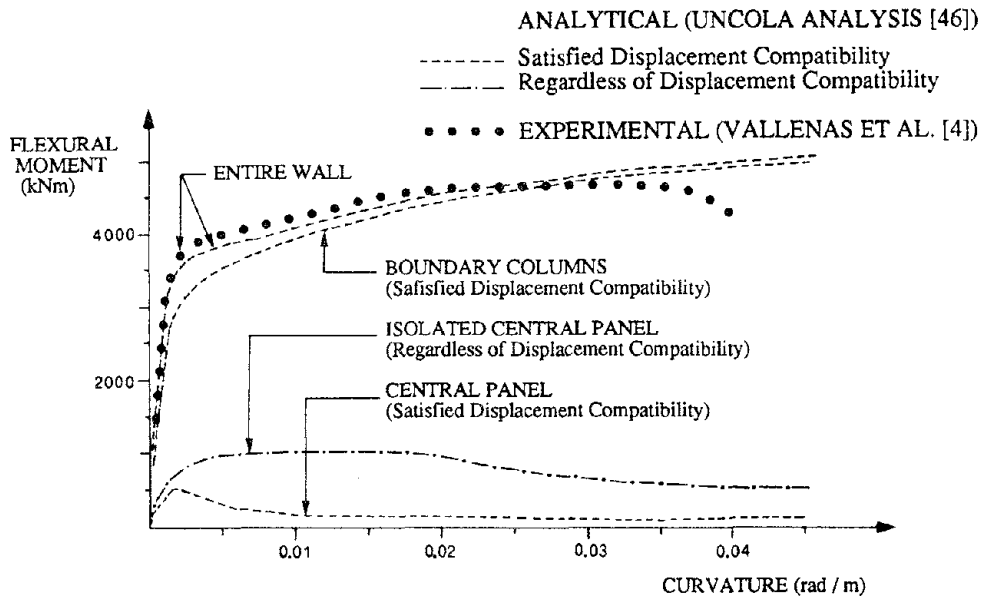
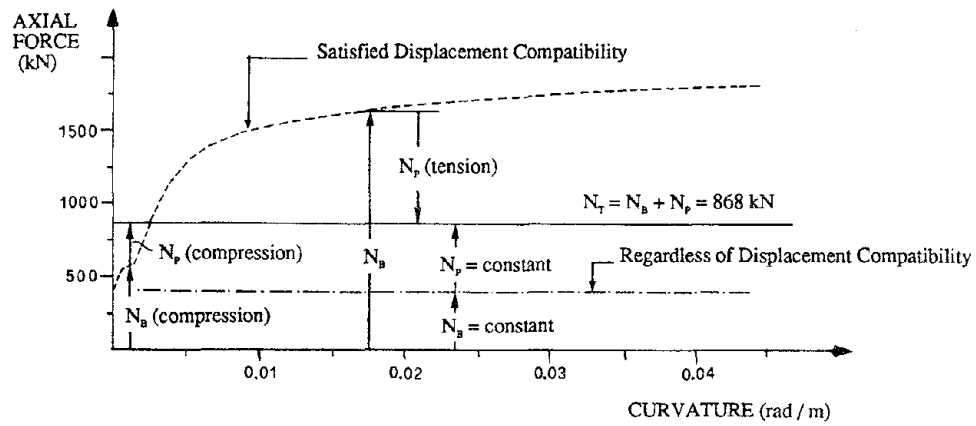


Fig. 3.5 - Geometrical Parameters



(a) Flexural Moment Versus Curvature



(b) Axial Force Versus Curvature

Fig. 3.6 - Experimental and Analytical Curves for the Cross-Section of Specimen 3 (Fig. 5.3a)

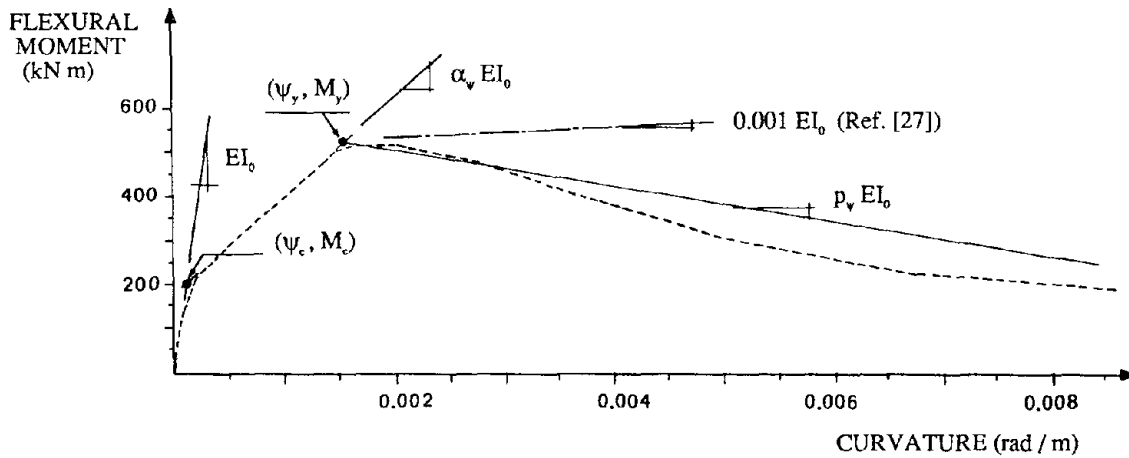
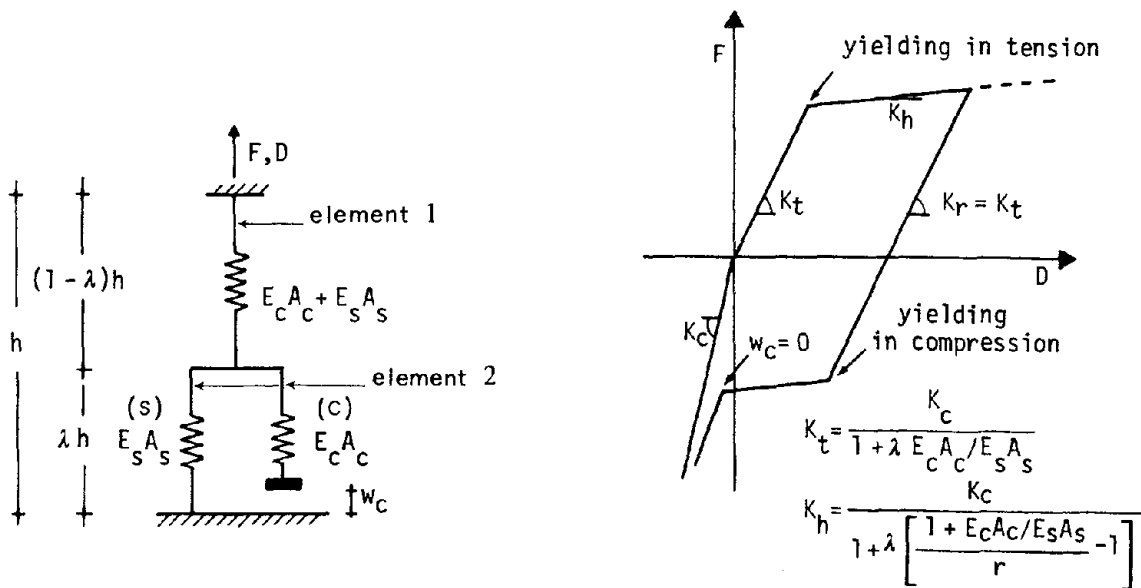


Fig. 3.7 - Idealization of the Moment-Curvature Relationship Obtained for the Central Panel by UNCOLA Analysis [46] under the Condition of Displacement Compatibility ( $\alpha_v = 0.17$  ;  $p_v = -0.003$ )



(a) Two-Element-in-Series Model

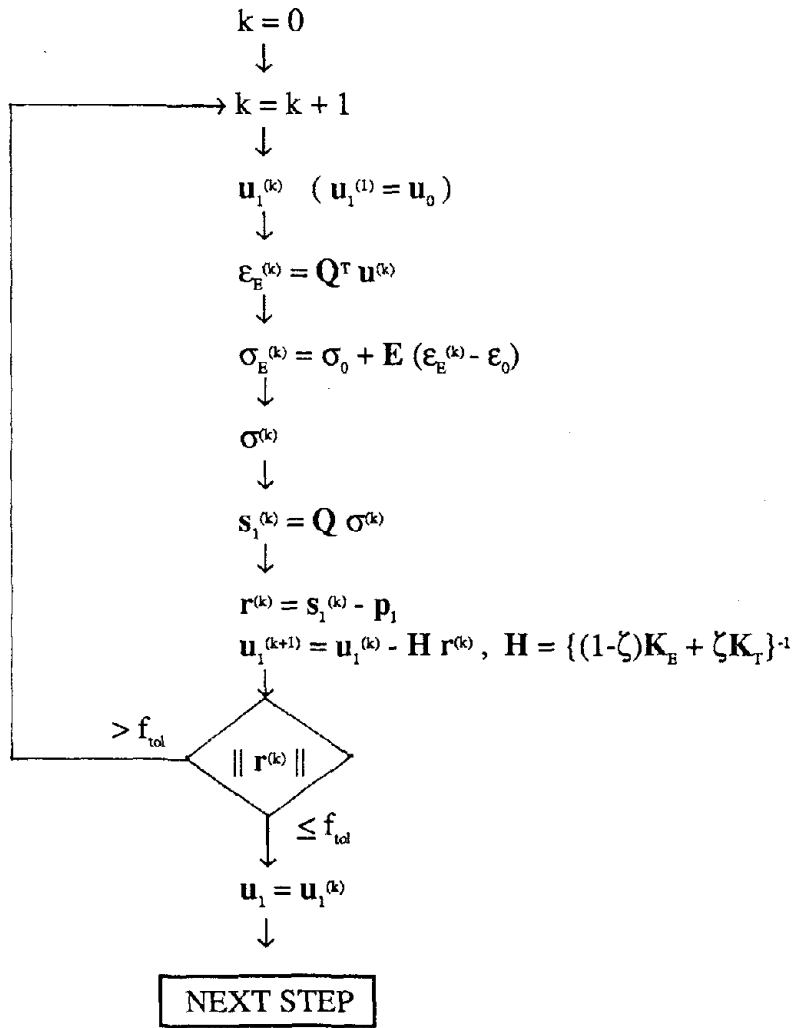
(b) Simplified Force-Deformation Relationship  
( $\lambda = \text{constant}$  ;  $r = \text{steel-hardening ratio}$ )

Fig. 3.8 - Proposed R C Column Model in Presence of Axial Load Reversals

$K_H$	0	$K_H(1-c)h$	$-K_H$	0	$K_H c h$
	$K_1+K_2+K_v$	$(K_2-K_1)l/2$	0	$-K_1-K_2-K_v$	$(K_1-K_2)l/2$
		$K_\phi +$ $+(K_1+K_2)l^2/4$ $+K_H(1-c)^2h^2$	$K_H(c-1)h$	$(K_1-K_2)l/2$	$-K_\phi +$ $-(K_1+K_2)l^2/4$ $+K_H c(1-c)h^2$
			$K_H$	0	$-K_H c h$
	SYMMETRIC			$K_1+K_2+K_v$	$(K_2-K_1)l/2$
					$K_\phi +$ $+(K_1+K_2)l^2/4$ $+K_H c^2h^2$

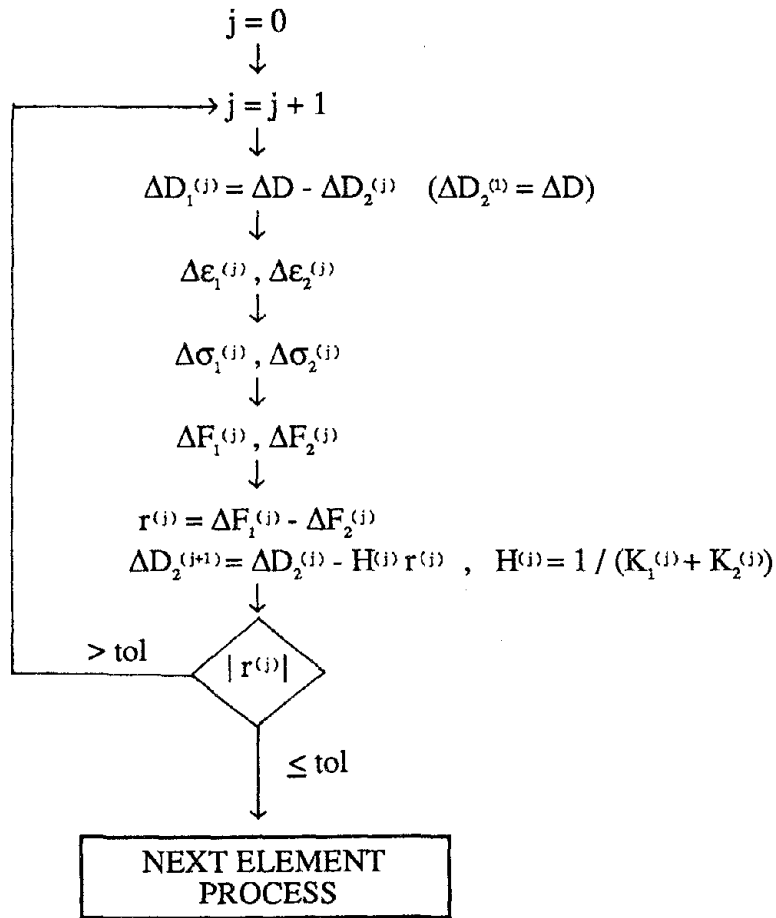
$K_c \equiv$

Fig. 4.1 - Elastic Stiffness Matrix of the Wall Member Model in Fig. 3.1



- $\mathbf{u}$  = Displacement Vector
- $\boldsymbol{\varepsilon}_E$  = Elastic Strain Vector
- $\boldsymbol{\sigma}_E$  = Incremental Elastic Stress Vector
- $\boldsymbol{\sigma}$  = Elastic-Plastic Stress Vector
- $\mathbf{s}$  = Structural Reaction Vector

Fig. 4.2 - Iterative Solution Process in the Generic Step of the Analysis



$\Delta D$  = Incremental Displacement of Overall Axial-Stiffness Element

$\Delta D_1, \Delta D_2$  = Incremental Displacement of the Two Elements in Series

$\Delta \epsilon_1, \Delta \epsilon_2$  = Increment of Strain of the Two Elements in Series

$\Delta \sigma_1, \Delta \sigma_2$  = Increment of Stress of the Two Elements in Series

$\Delta F_1, \Delta F_2$  = Increment of Strength of the Two Element in Series

$K_1, K_2$  = Stiffnesses of the two elements in series calculated as  $(i = 1, 2)$

$$K_i = (1 - \zeta_i) K_{ci} + \zeta_i K_{Ti}, \quad 0 \leq \zeta_i < 0.5$$

where  $K_{ci}$  and  $K_{Ti}$  are, respectively, the compressive stiffness and the generic tangent stiffness of the same two elements

Fig.4.3 - Iterative Solution Process Used to Calculate the State of Stress in the Truss Elements and Vertical Axial Spring of the Wall Member Model in Fig. 3.1a

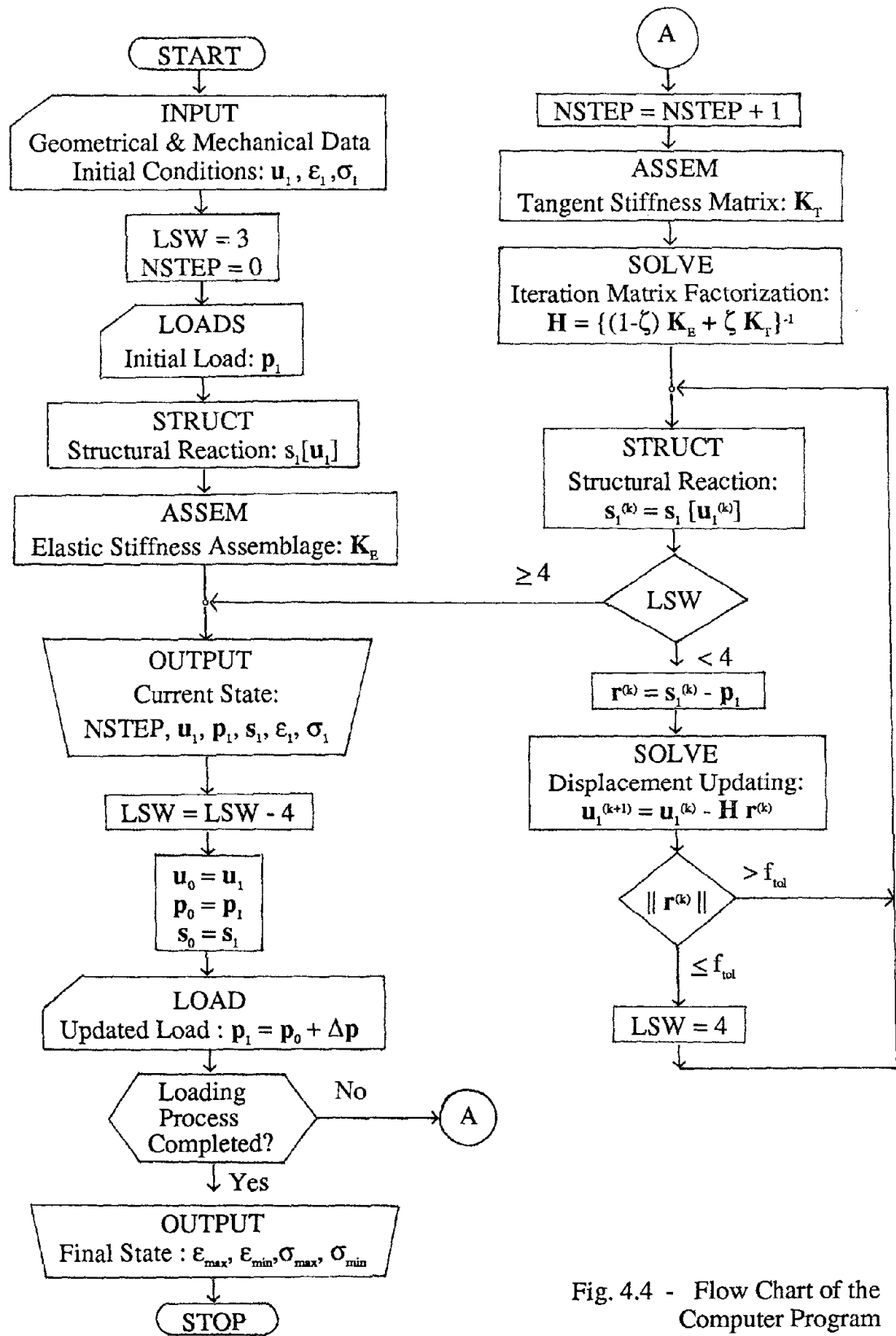
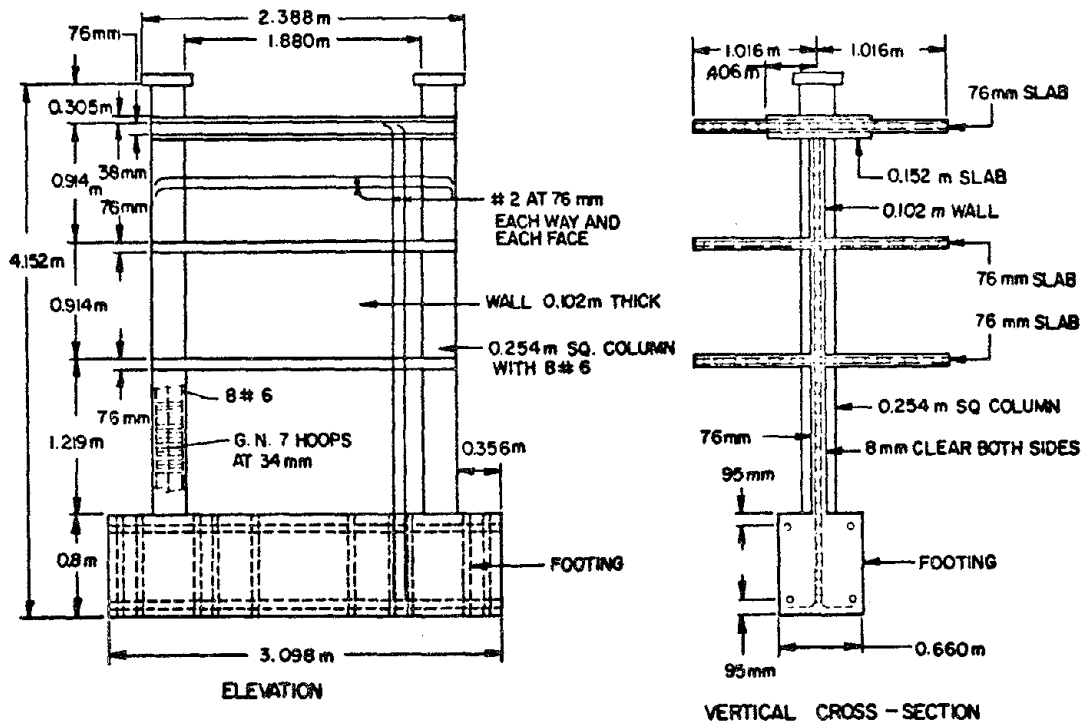
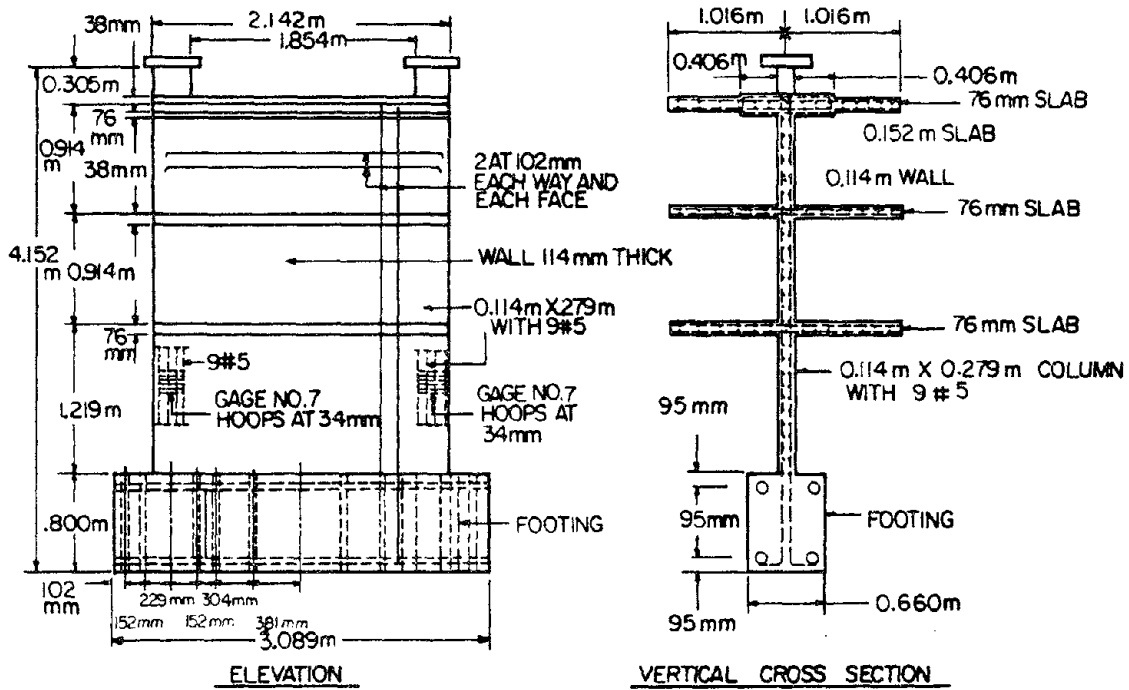


Fig. 4.4 - Flow Chart of the Computer Program

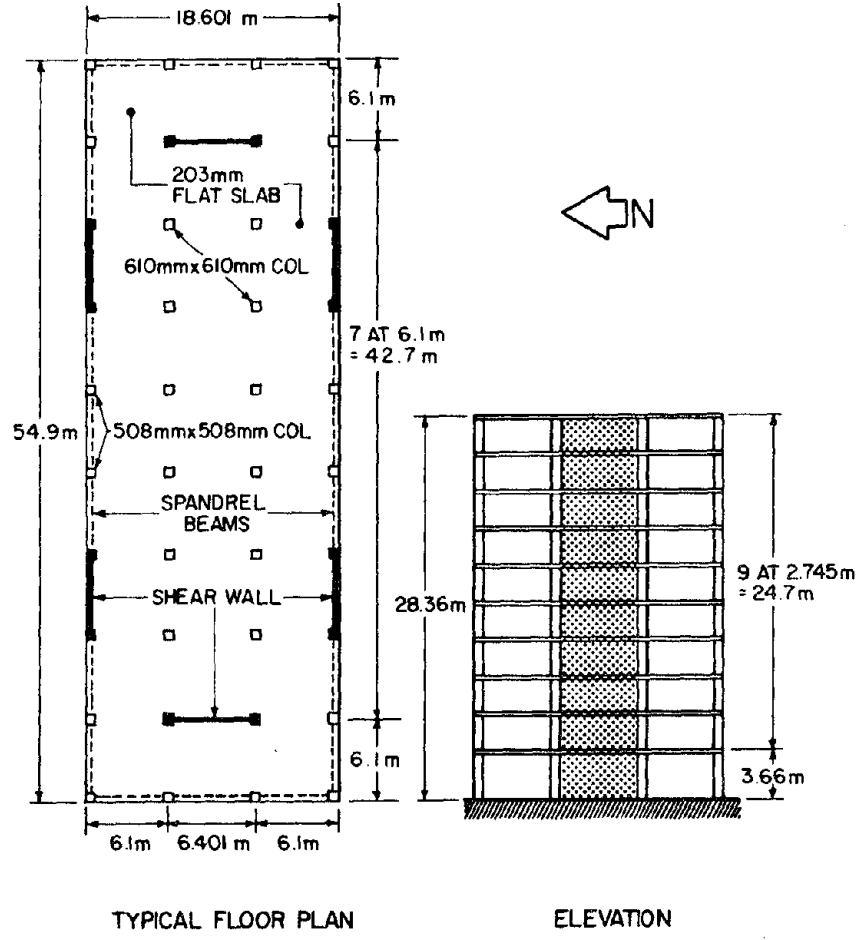


(a) Dimensions and Details of the Framed Wall (Specimens 3 and 4)

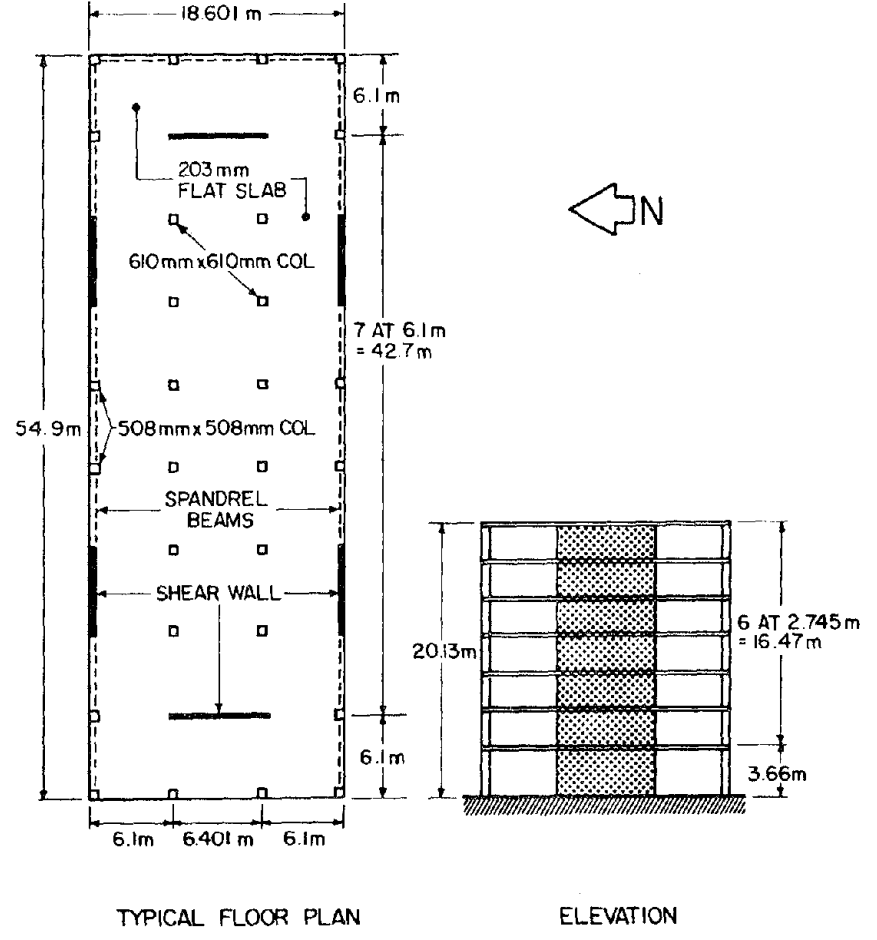


(b) Dimensions and Details of the Rectangular Wall (Specimens 5 and 6)

Fig. 5.1 - Test Walls (Reference 4)

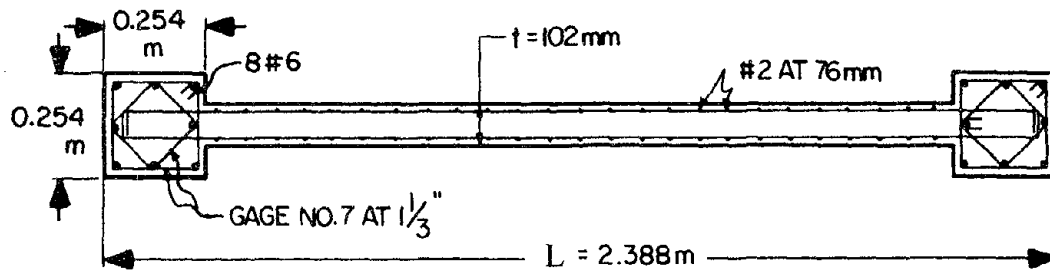


(a) Ten-Story Prototype Building

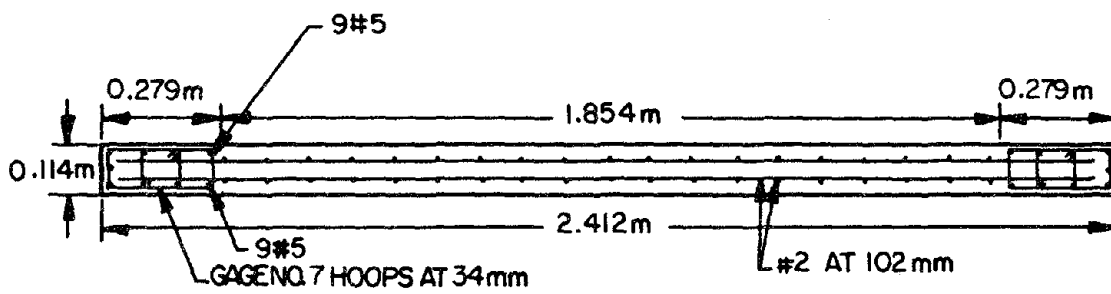


(b) Seven-Story Prototype Building

Fig. 5.2 - Prototype Buildings (Reference 4)

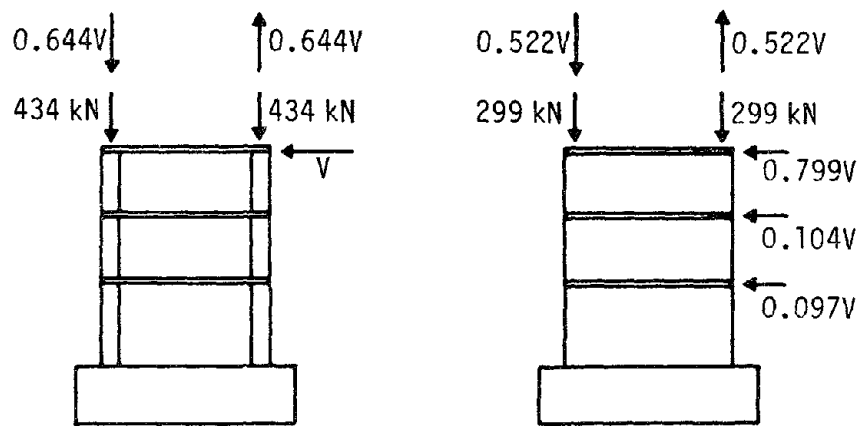


(a) Framed Wall (Specimens 3 and 4)



(b) Rectangular Wall (Specimens 5 and 6)

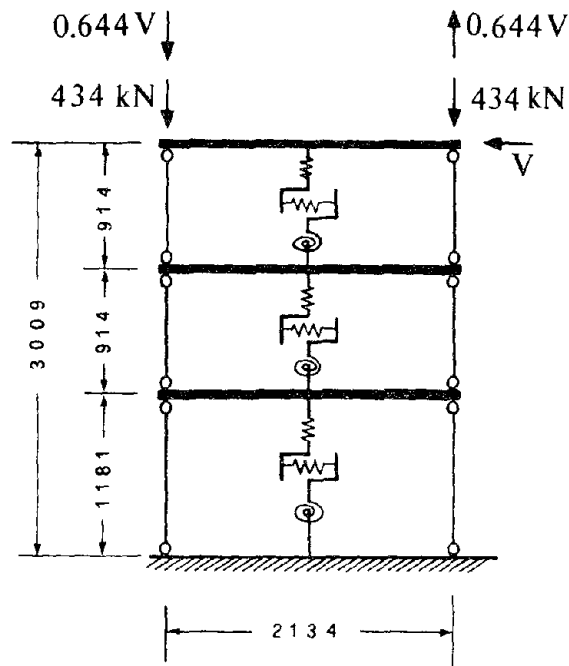
Fig. 5.3 - Detailed Cross-Sections



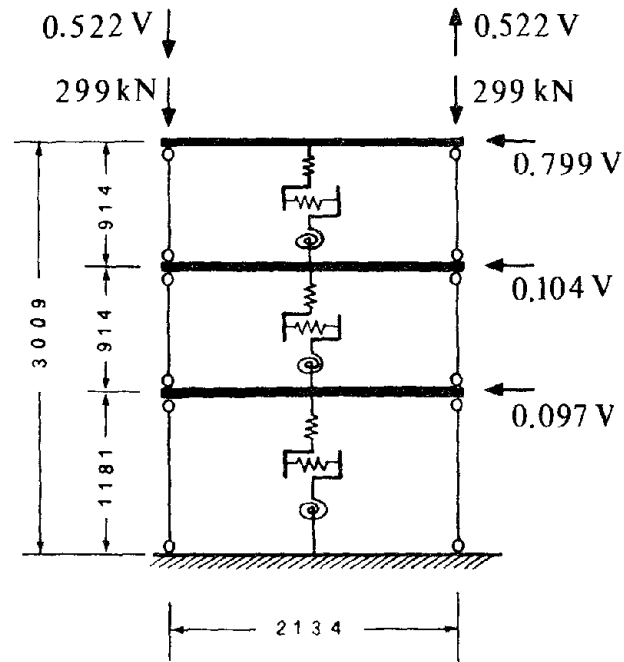
(a) Specimens 3 and 4

(b) Specimens 5 and 6

Fig. 5.4 - Loading Patterns of the Test Walls

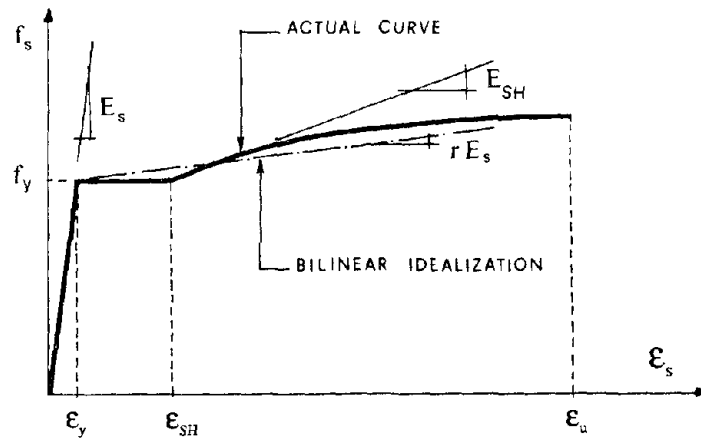


(a) Framed Wall (Specimens 3 and 4)

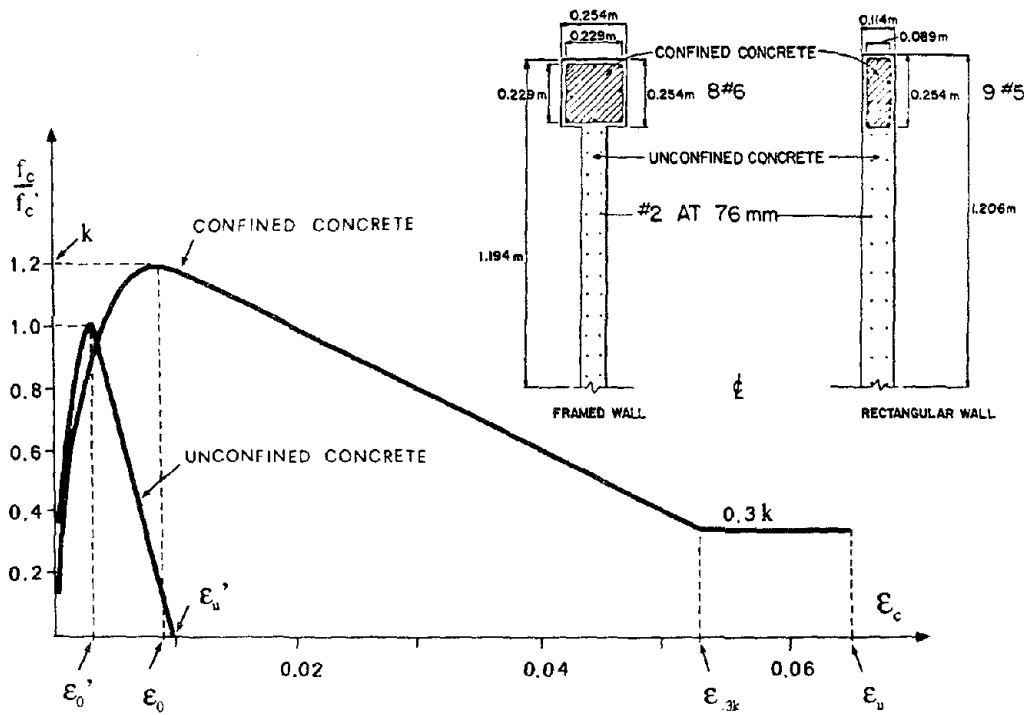


(b) Rectangular Wall (Specimens 5 and 6)

Fig. 5.5 - Modeling of the Test Walls in Fig. 5.1

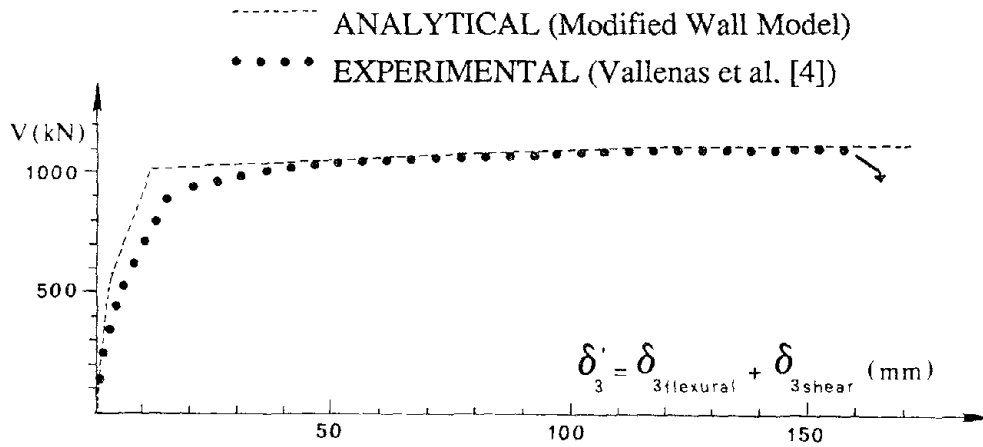


(a) Steel

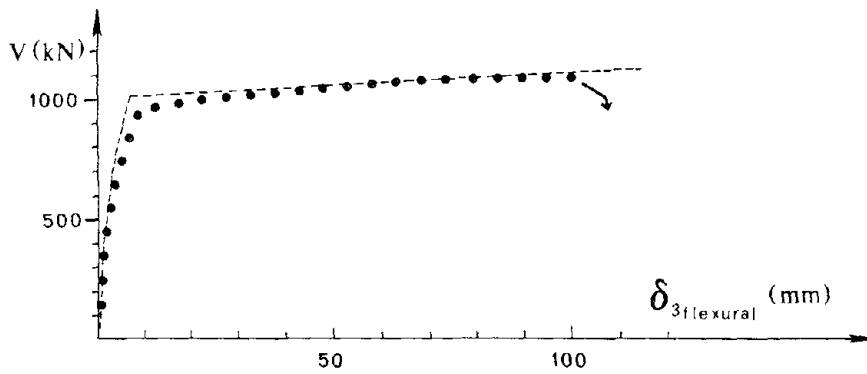


(b) Concrete

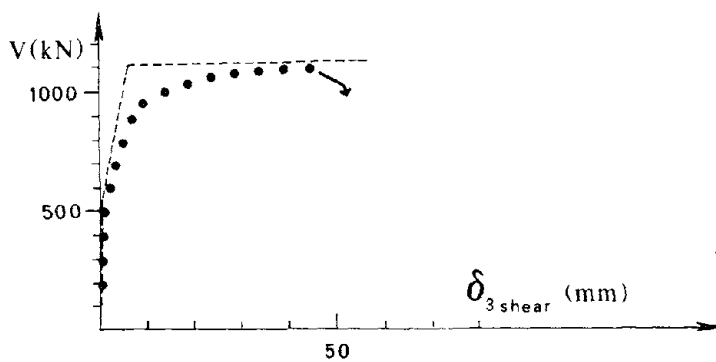
Fig. 5.6 - Constitutive Curves of the Materials



(a) Base Shear Versus Net Top Displacement at the Third Floor

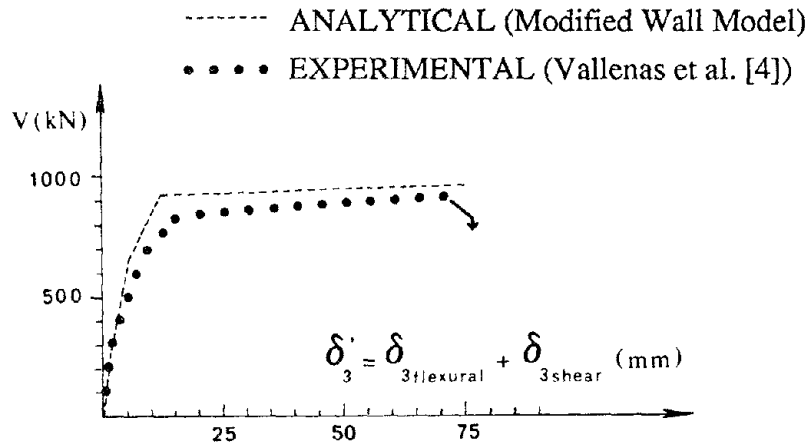


(b) Base Shear Versus Flexural Displacement at the Third Floor

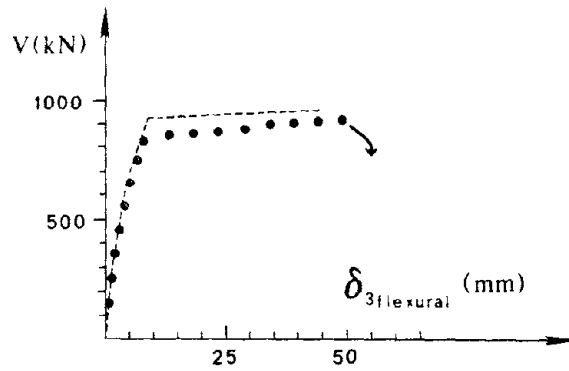


(c) Base Shear Versus Shear Displacement at the Third Floor

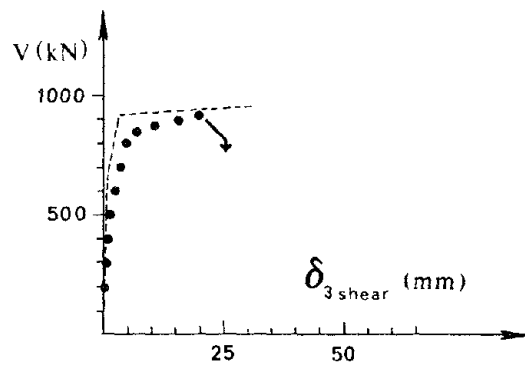
Fig. 5.7 - Analytical and Experimental Curves for the Framed Wall under Monotonic Loading (Specimen 3)



(a) Base Shear Versus Net Top Displacement at the Third Floor

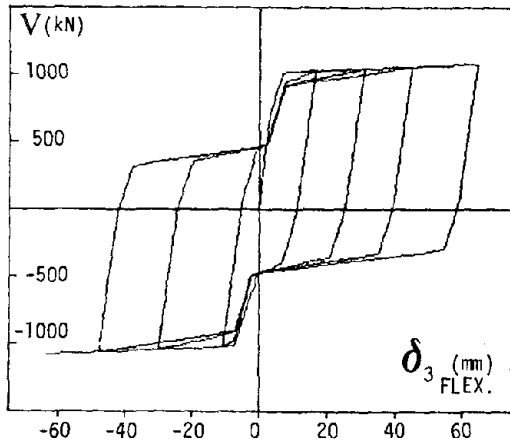


(b) Base Shear Versus Flexural Displacement at the Third Floor

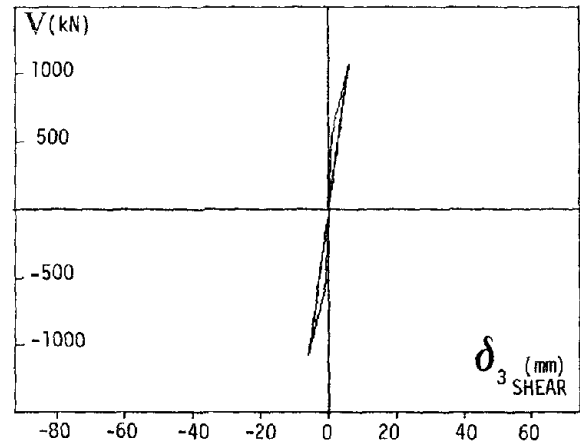


(c) Base Shear Versus Shear Displacement at the Third Floor

Fig. 5.8 - Analytical and Experimental Curves for the Rectangular Wall under Monotonic Loading (Specimen 5)

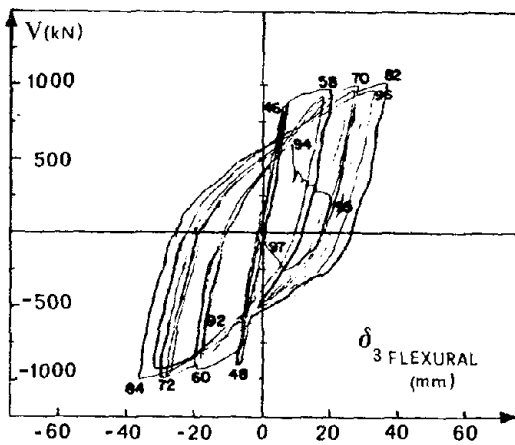


(a) Base Shear Versus Flexural Displacement at the Third Floor

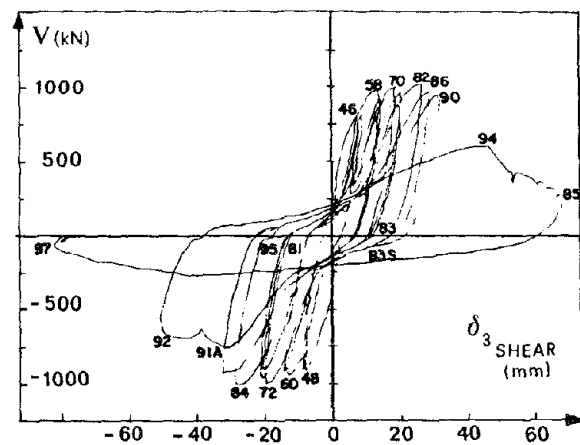


(b) Base Shear Versus Shear Displacement at the Third Floor

ANALYTICAL



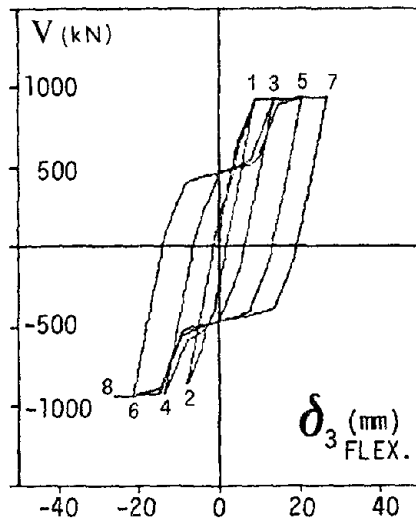
(c) Base Shear Versus Flexural Displacement at the Third Floor



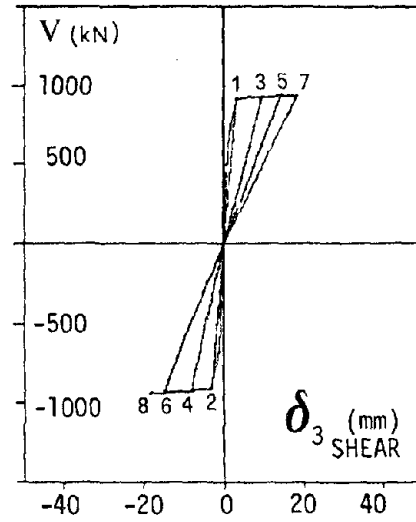
(d) Base Shear Versus Shear Displacement at the Third Floor

EXPERIMENTAL

Fig. 5.9 - Analytical and Experimental Curves for the Framed Wall under Cyclic Loading (Specimen 4)

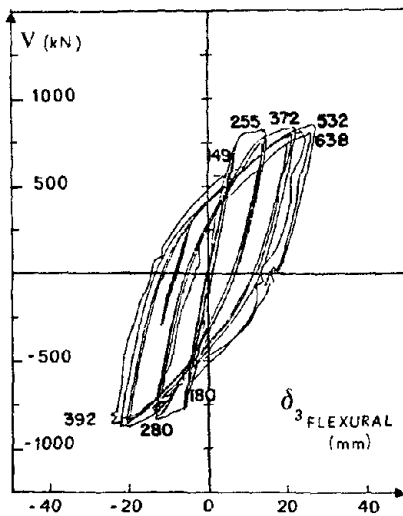


(a) Base Shear Versus Flexural Displacement at the Third Floor

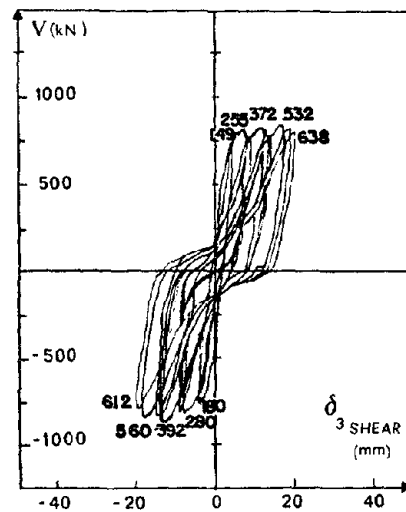


(b) Base Shear Versus Shear Displacement at the Third Floor

ANALYTICAL



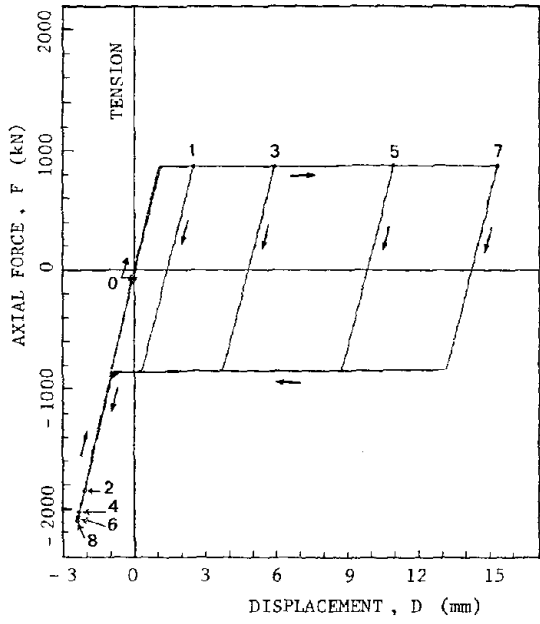
(c) Base Shear Versus Flexural Displacement at the Third Floor



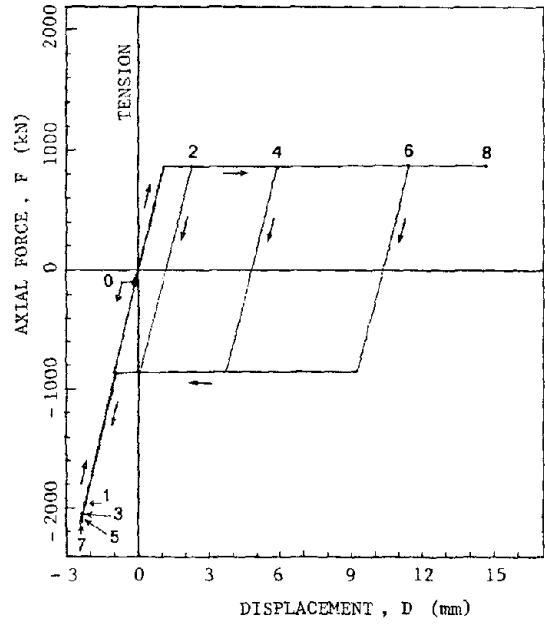
(d) Base Shear Versus Shear Displacement at the Third Floor

EXPERIMENTAL

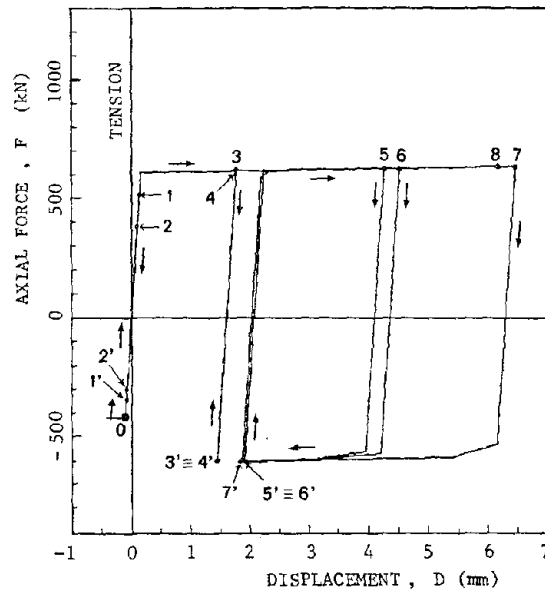
Fig. 5.10 - Analytical and Experimental Curves for the Rectangular Wall under Cyclic Loading (Specimen 6)



(a) South Truss-Element Response



(b) North Truss-Element Response



(c) Central-Vertical-Spring Response (Loading Process: 0, 1, 1', 2, 2', ..., 7, 7', 8)

Fig. 5.11 - Analytical Response of the First Story Axial-Stiffness Elements of the Wall Model in Fig. 5.5b (Specimen 6)

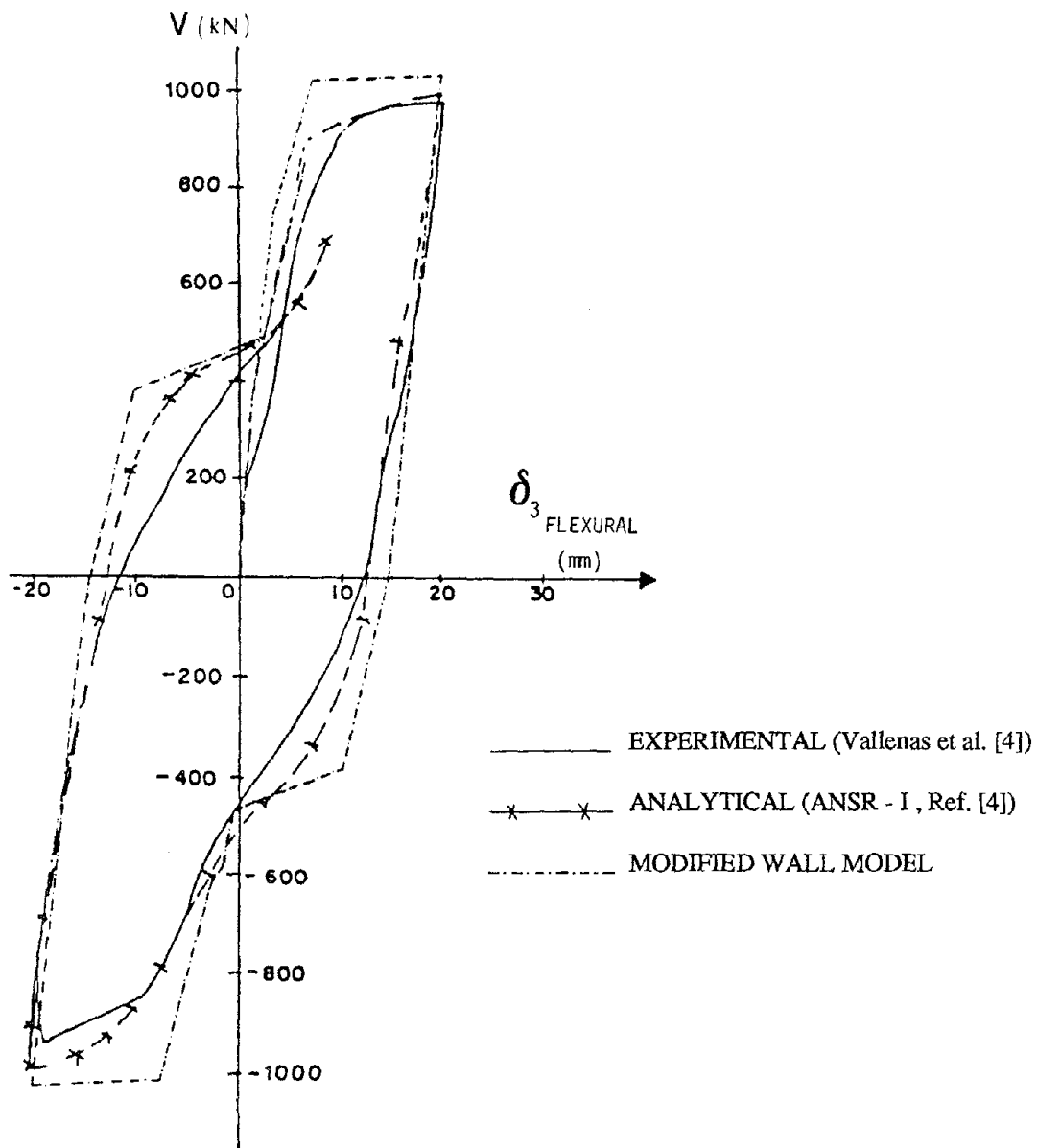


Fig. 5.12 - Analytical and Experimental Curves Representing the Flexural Response of the Framed Wall (Specimen 4)

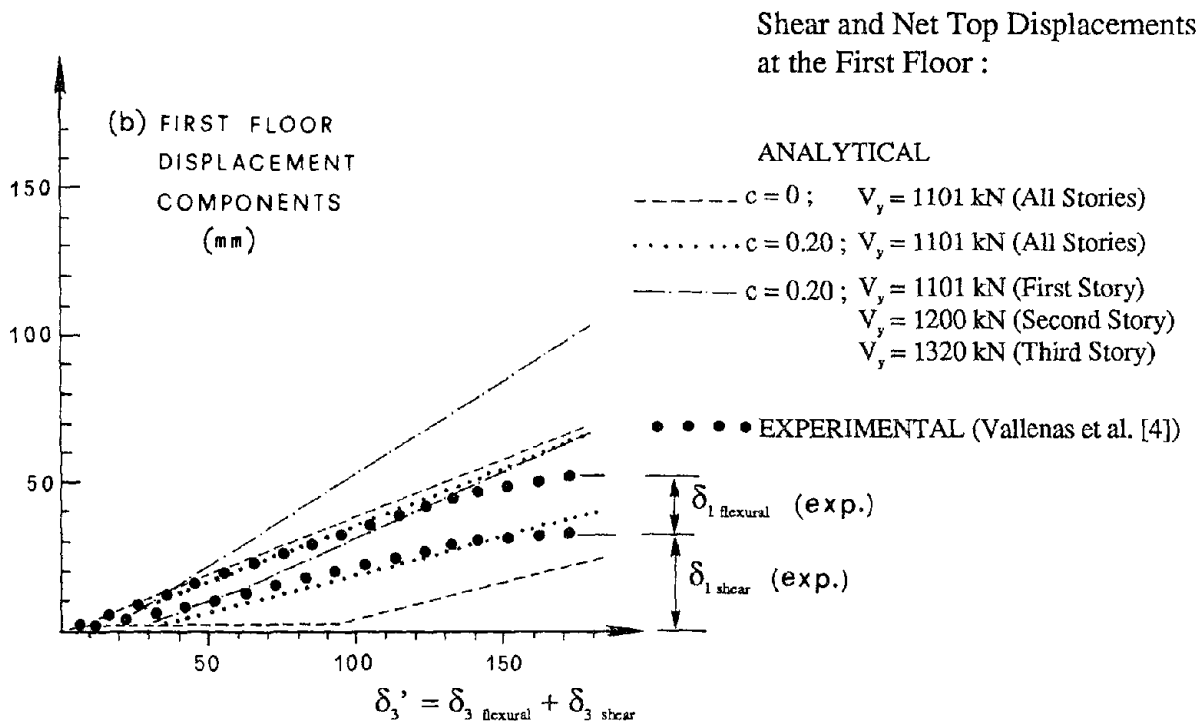
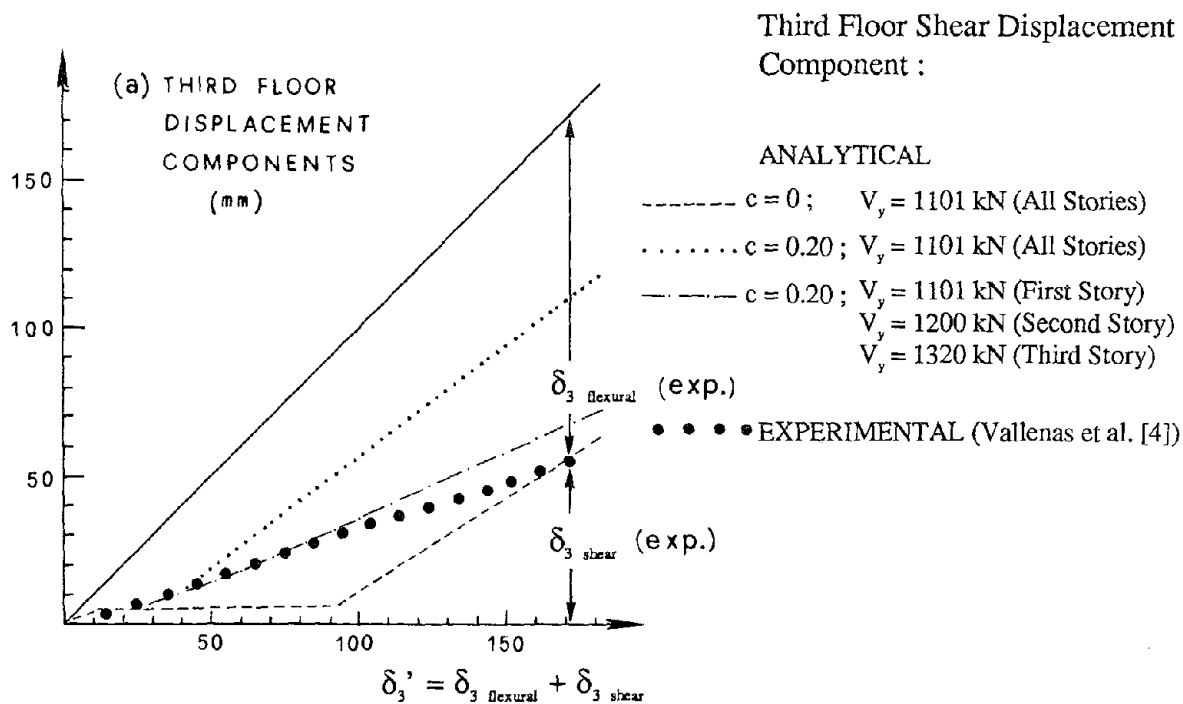


Fig. 5.13 - Comparison of Shear and Flexural Displacement Components Obtained for Specimen 3 Experimentally (Ref. [4]) and Analytically, by Assuming for the Modified Wall Model Different Values of the Parameters  $c$  and  $V_y$  (Other Data as in APPENDIX A)

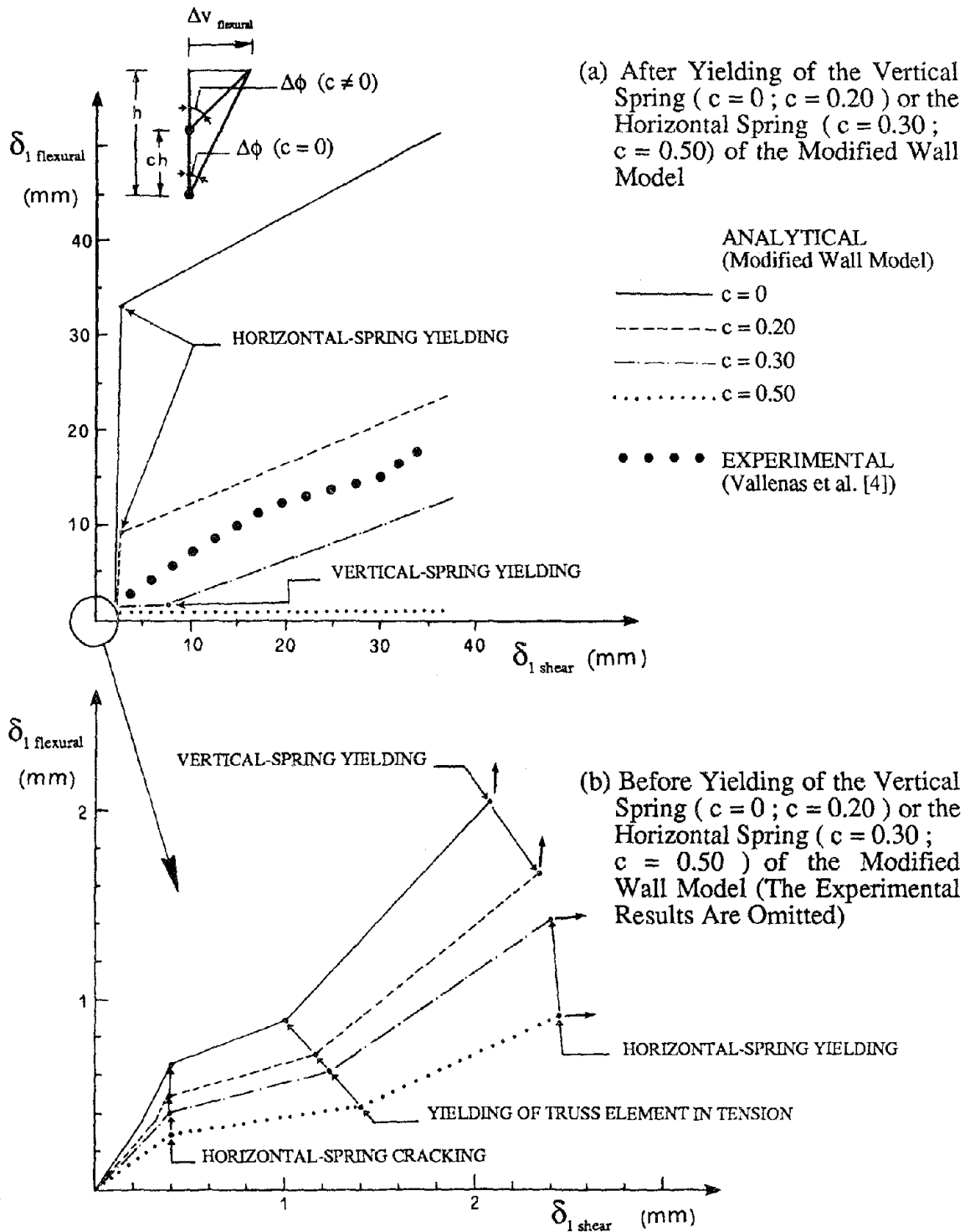


Fig. 5.14 - First Floor Shear and Flexural Displacement Components for Specimen 3 Obtained Experimentally (Ref. [4]) and Analytically, by Assuming for the Modified Wall Model Different Values of the Parameter  $c$  ( $V_y = 1101$  kN for All the Stories; Other Data as in APPENDIX A)

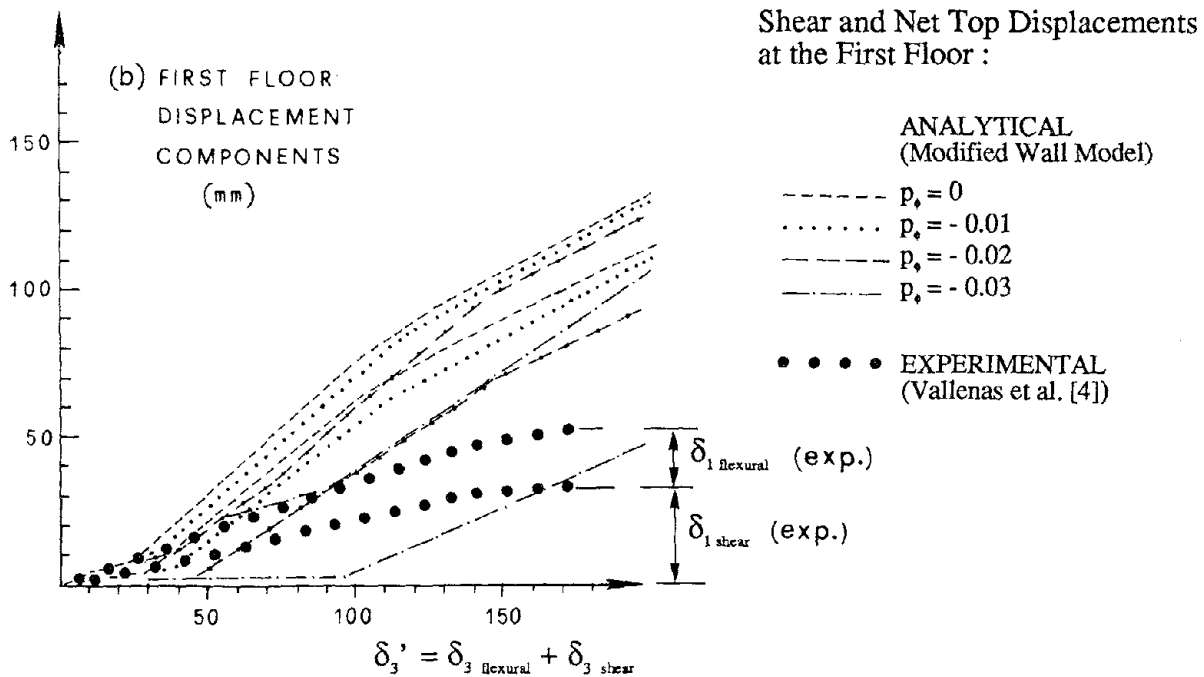
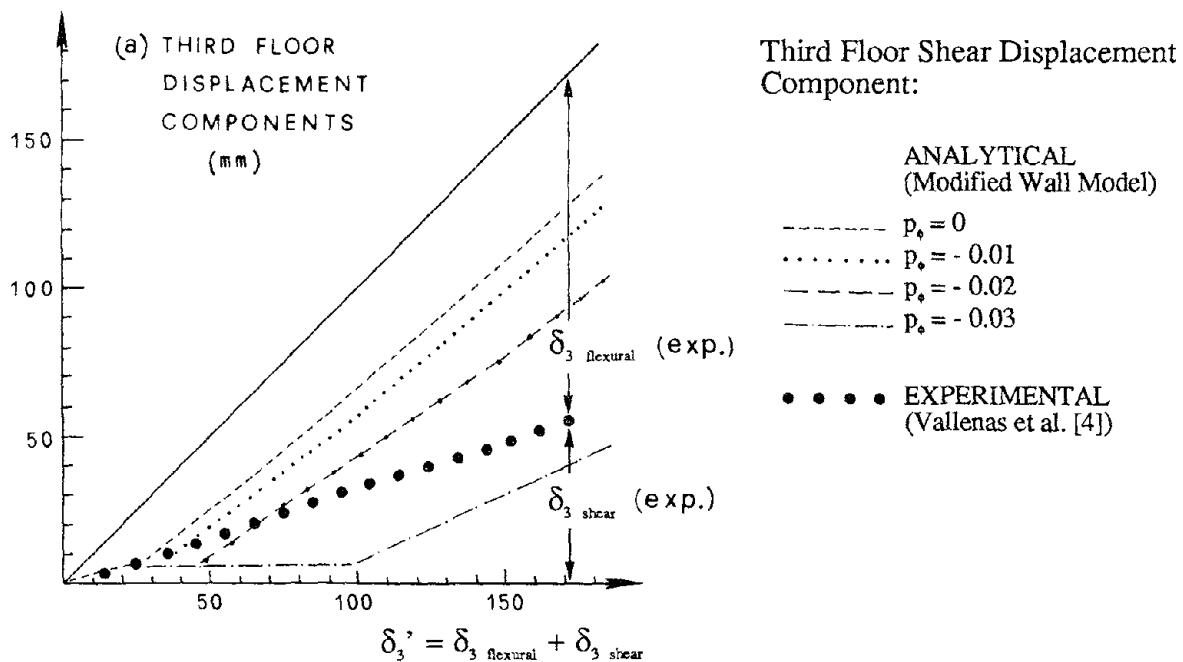


Fig. 5.15 - Comparison of Shear and Flexural Displacement Components Obtained for Specimen 3 Experimentally (Ref. [4]) and Analytically, by Assuming Different Values of the Softening Ratio  $p_s$  for the Rotational Spring of the Modified Wall Model (Other Data as in APPENDIX A, Except  $r = 0.001$ )

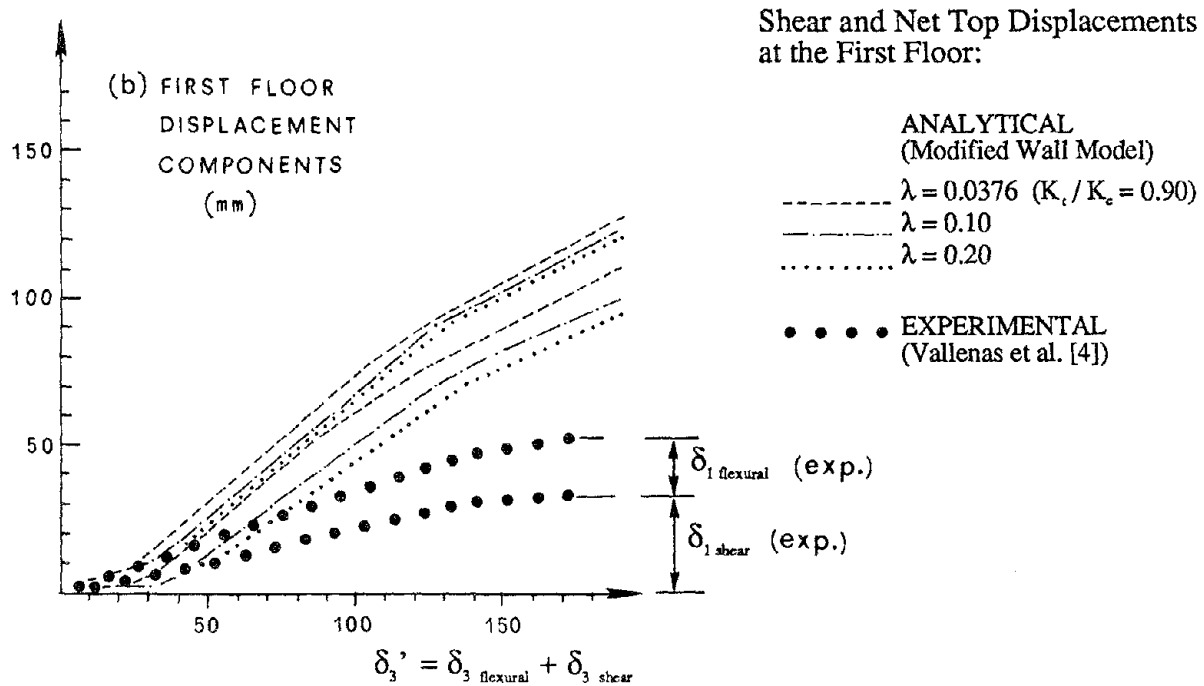
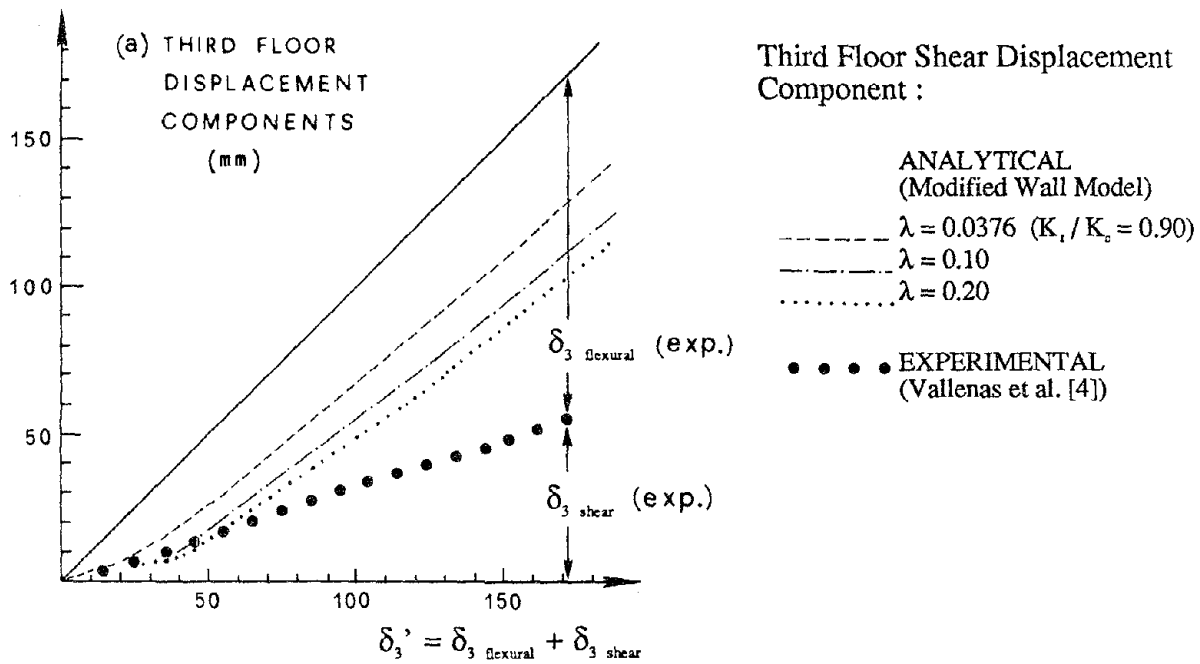


Fig. 5.16 - Comparison of Shear and Flexural Displacement Components Obtained for Specimen 3 Experimentally (Ref. [4]) and Analytically, by Assuming Different Values of the Parameter  $\lambda$  for the Outside Truss Elements of the Modified Wall Model (Other Data as in APPENDIX A, Except  $p_\phi = 0$  and  $r = 0.001$ )

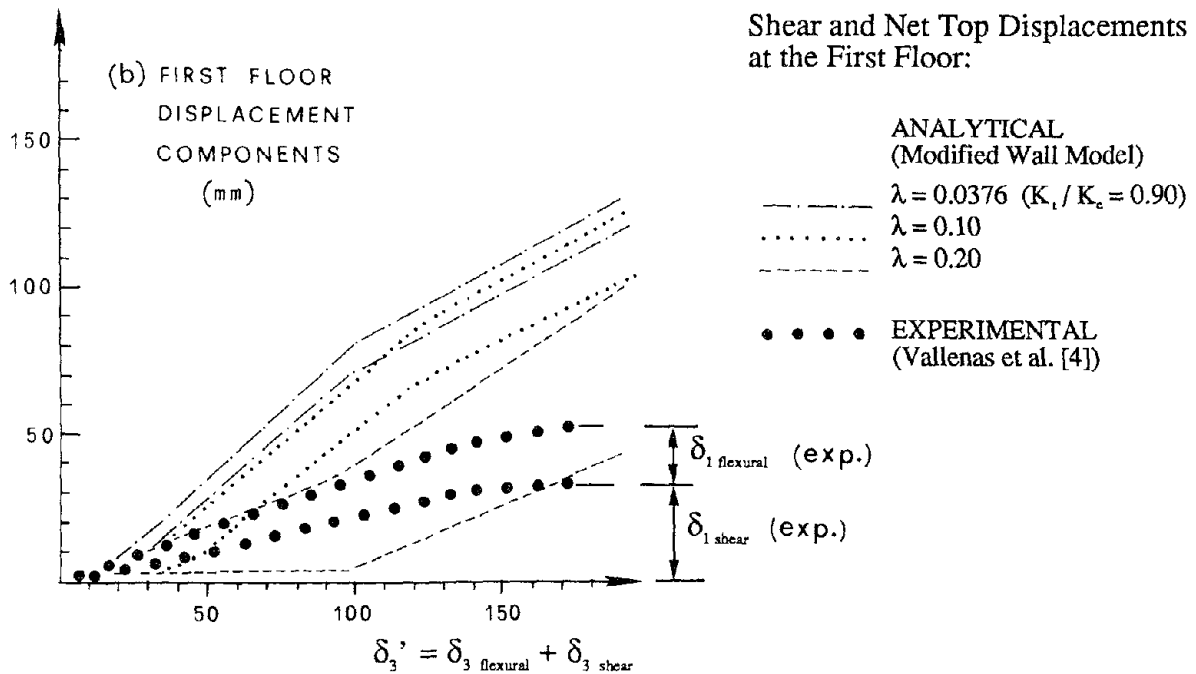
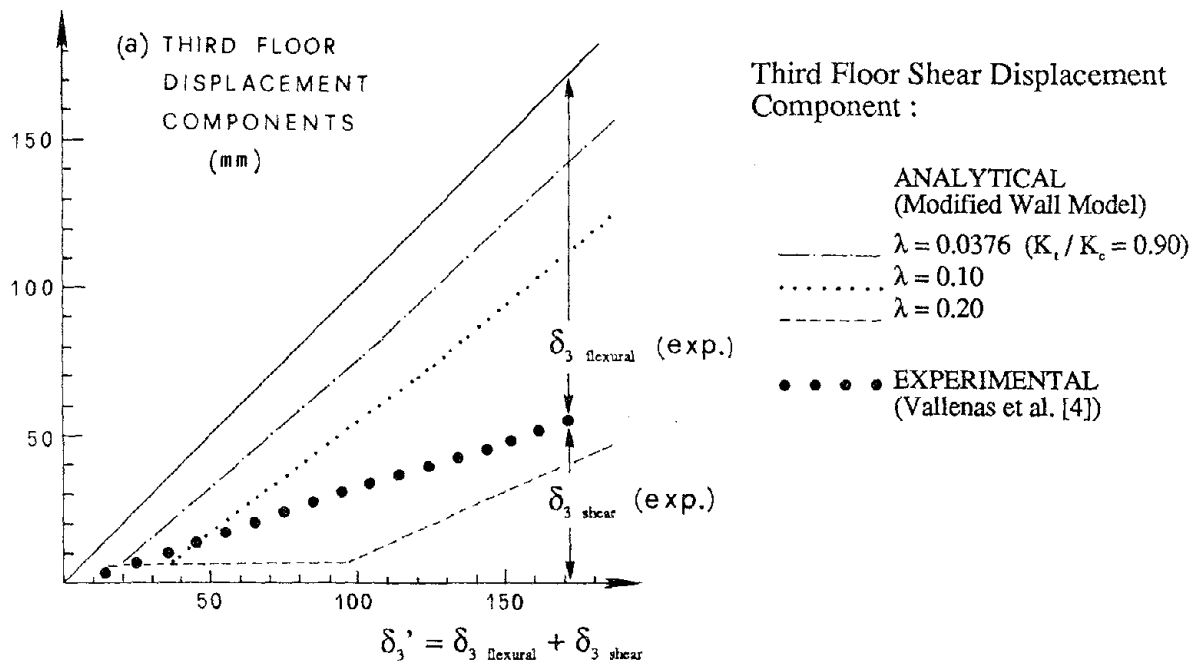


Fig. 5.17 - Comparison of Shear and Flexural Displacement Components Obtained for Specimen 3 Experimentally (Ref. [4]) and Analytically, by Assuming Different Values of the Parameter  $\lambda$  for the Outside Truss Elements of the Modified Wall Model (Other Data as in APPENDIX A, Except  $p_s = -0.03$  and  $r = 0.001$ )

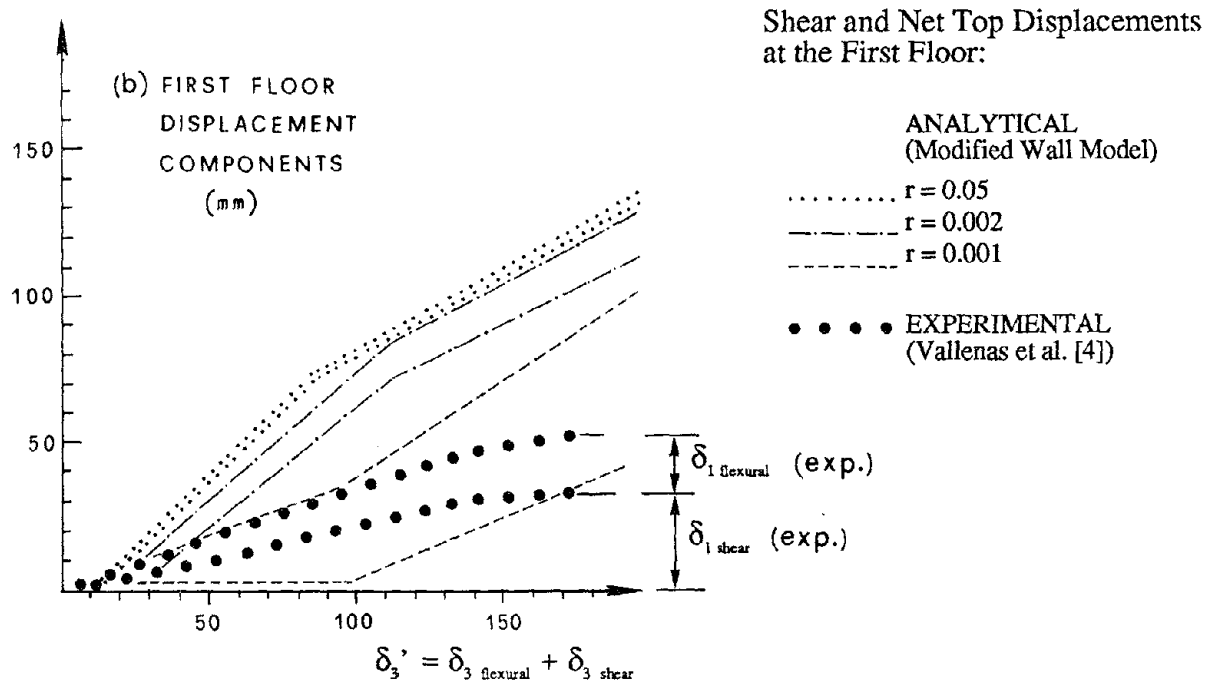
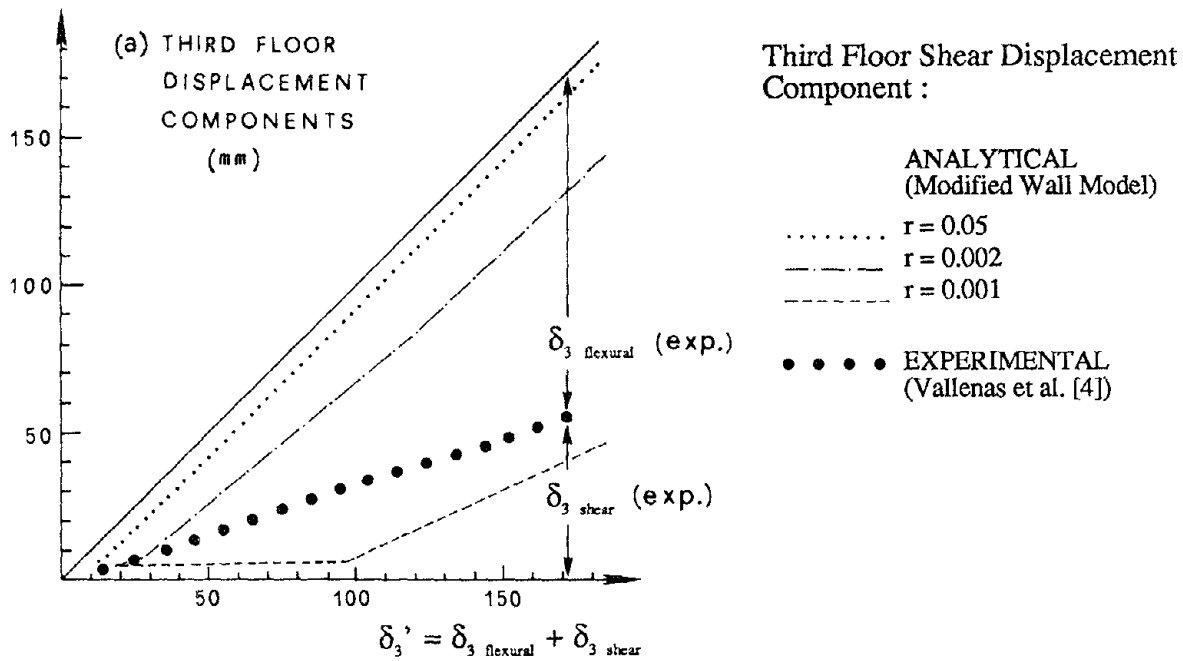
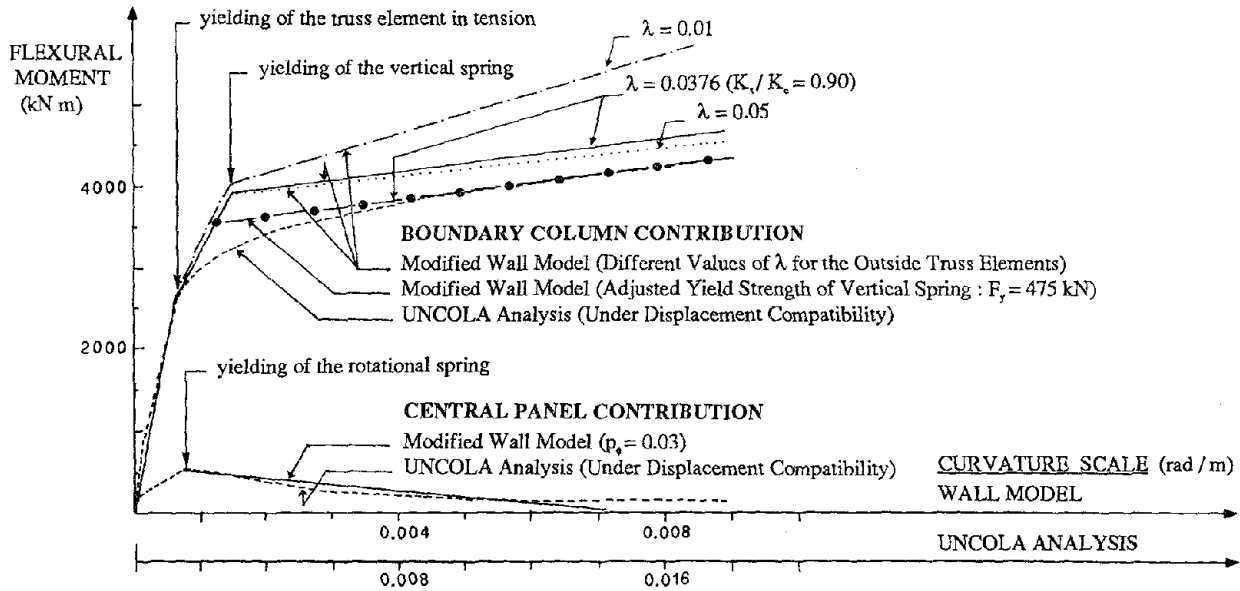
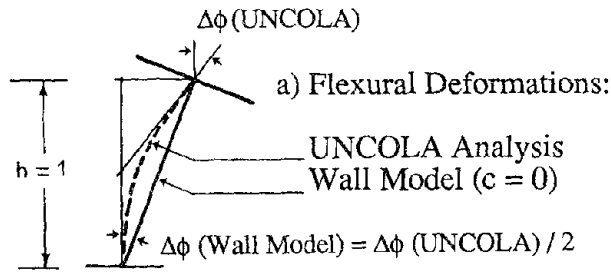
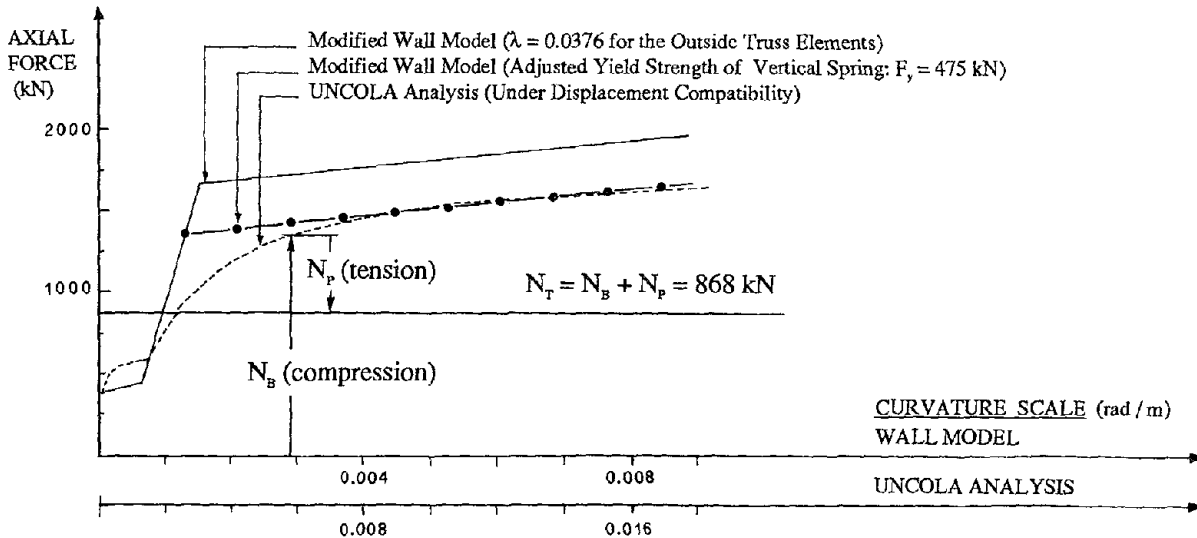


Fig. 5.18 - Comparison of Shear and Flexural Displacement Components Obtained for Specimen 3 Experimentally (Ref. [4]) and Analytically by Assuming Different Values of the Parameter  $r$  for All the Axial-Stiffness Elements of the Modified Wall Model (Other Data as in APPENDIX A, Except  $p_s = -0.03$ )



(b) Flexural Moment Versus Curvature



(c) Axial Force Versus Curvature

Fig. 5.19 - Flexural Deformations and Analytical Curves for a Wall Member of Unit Height under Uniform Flexural Moment (Cross-Section and Mechanical Properties of Specimen 3)



## EARTHQUAKE ENGINEERING RESEARCH CENTER REPORT SERIES

EERC reports are available from the National Information Service for Earthquake Engineering(NISEE) and from the National Technical Information Service(NTIS). Numbers in parentheses are Accession Numbers assigned by the National Technical Information Service; these are followed by a price code. Contact NTIS, 5285 Port Royal Road, Springfield Virginia, 22161 for more information. Reports without Accession Numbers were not available from NTIS at the time of printing. For a current complete list of EERC reports (from EERC 67-1) and availability information, please contact University of California, EERC, NISEE, 1301 South 46th Street, Richmond, California 94804.

- UCB/EERC-80/01 "Earthquake Response of Concrete Gravity Dams Including Hydrodynamic and Foundation Interaction Effects," by Chopra, A.K., Chakrabarti, P. and Gupta, S., January 1980, (AD-A087297)A10.
- UCB/EERC-80/02 "Rocking Response of Rigid Blocks to Earthquakes," by Yim, C.S., Chopra, A.K. and Penzien, J., January 1980, (PB80 166 002)A04.
- UCB/EERC-80/03 "Optimum Inelastic Design of Seismic-Resistant Reinforced Concrete Frame Structures," by Zagajski, S.W. and Bertero, V.V., January 1980, (PB80 164 635)A06.
- UCB/EERC-80/04 "Effects of Amount and Arrangement of Wall-Panel Reinforcement on Hysteretic Behavior of Reinforced Concrete Walls," by Iliya, R. and Bertero, V.V., February 1980, (PB81 122 525)A09.
- UCB/EERC-80/05 "Shaking Table Research on Concrete Dam Models," by Niwa, A. and Clough, R.W., September 1980, (PB81 122 368)A06.
- UCB/EERC-80/06 "The Design of Steel Energy-Absorbing Restrainers and their Incorporation into Nuclear Power Plants for Enhanced Safety (Vol 1a): Piping with Energy Absorbing Restrainers: Parameter Study on Small Systems," by Powell, G.H., Oughourlian, C. and Simons, J., June 1980.
- UCB/EERC-80/07 "Inelastic Torsional Response of Structures Subjected to Earthquake Ground Motions," by Yamazaki, Y., April 1980, (PB81 122 327)A08.
- UCB/EERC-80/08 "Study of X-Braced Steel Frame Structures under Earthquake Simulation," by Ghanaat, Y., April 1980, (PB81 122 335)A11.
- UCB/EERC-80/09 "Hybrid Modelling of Soil-Structure Interaction," by Gupta, S., Lin, T.W. and Penzien, J., May 1980, (PB81 122 319)A07.
- UCB/EERC-80/10 "General Applicability of a Nonlinear Model of a One Story Steel Frame," by Sveinsson, B.I. and McNiven, H.D., May 1980, (PB81 124 877)A06.
- UCB/EERC-80/11 "A Green-Function Method for Wave Interaction with a Submerged Body," by Kioka, W., April 1980, (PB81 122 269)A07.
- UCB/EERC-80/12 "Hydrodynamic Pressure and Added Mass for Axisymmetric Bodies," by Nilrat, F., May 1980, (PB81 122 343)A08.
- UCB/EERC-80/13 "Treatment of Non-Linear Drag Forces Acting on Offshore Platforms," by Dao, B.V. and Penzien, J., May 1980, (PB81 153 413)A07.
- UCB/EERC-80/14 "2D Plane/Axisymmetric Solid Element (Type 3-Elastic or Elastic-Perfectly Plastic) for the ANSR-II Program," by Mondkar, D.P. and Powell, G.H., July 1980, (PB81 122 350)A03.
- UCB/EERC-80/15 "A Response Spectrum Method for Random Vibrations," by Der Kiureghian, A., June 1981, (PB81 122 301)A03.
- UCB/EERC-80/16 "Cyclic Inelastic Buckling of Tubular Steel Braces," by Zayas, V.A., Popov, E.P. and Martin, S.A., June 1981, (PB81 124 885)A10.
- UCB/EERC-80/17 "Dynamic Response of Simple Arch Dams Including Hydrodynamic Interaction," by Porter, C.S. and Chopra, A.K., July 1981, (PB81 124 000)A13.
- UCB/EERC-80/18 "Experimental Testing of a Friction Damped Aseismic Base Isolation System with Fail-Safe Characteristics," by Kelly, J.M., Beucke, K.E. and Skinner, M.S., July 1980, (PB81 148 595)A04.
- UCB/EERC-80/19 "The Design of Steel Energy-Absorbing Restrainers and their Incorporation into Nuclear Power Plants for Enhanced Safety (Vol.1B): Stochastic Seismic Analyses of Nuclear Power Plant Structures and Piping Systems Subjected to Multiple Supported Excitations," by Lee, M.C. and Penzien, J., June 1980, (PB82 201 872)A08.
- UCB/EERC-80/20 "The Design of Steel Energy-Absorbing Restrainers and their Incorporation into Nuclear Power Plants for Enhanced Safety (Vol 1C): Numerical Method for Dynamic Substructure Analysis," by Dickens, J.M. and Wilson, E.L., June 1980.
- UCB/EERC-80/21 "The Design of Steel Energy-Absorbing Restrainers and their Incorporation into Nuclear Power Plants for Enhanced Safety (Vol 2): Development and Testing of Restraints for Nuclear Piping Systems," by Kelly, J.M. and Skinner, M.S., June 1980.
- UCB/EERC-80/22 "3D Solid Element (Type 4-Elastic or Elastic-Perfectly-Plastic) for the ANSR-II Program," by Mondkar, D.P. and Powell, G.H., July 1980, (PB81 123 242)A03.
- UCB/EERC-80/23 "Gap-Friction Element (Type 5) for the Ansr-II Program," by Mondkar, D.P. and Powell, G.H., July 1980, (PB81 122 285)A03.
- UCB/EERC-80/24 "U-Bar Restraint Element (Type 11) for the ANSR-II Program," by Oughourlian, C. and Powell, G.H., July 1980, (PB81 122 293)A03.
- UCB/EERC-80/25 "Testing of a Natural Rubber Base Isolation System by an Explosively Simulated Earthquake," by Kelly, J.M., August 1980, (PB81 201 360)A04.
- UCB/EERC-80/26 "Input Identification from Structural Vibrational Response," by Hu, Y., August 1980, (PB81 152 308)A05.
- UCB/EERC-80/27 "Cyclic Inelastic Behavior of Steel Offshore Structures," by Zayas, V.A., Mahin, S.A. and Popov, E.P., August 1980, (PB81 196 180)A15.
- UCB/EERC-80/28 "Shaking Table Testing of a Reinforced Concrete Frame with Biaxial Response," by Oliva, M.G., October 1980, (PB81 154 304)A10.
- UCB/EERC-80/29 "Dynamic Properties of a Twelve-Story Prefabricated Panel Building," by Bouwkamp, J.G., Kollegger, J.P. and Stephen, R.M., October 1980, (PB82 138 777)A07.
- UCB/EERC-80/30 "Dynamic Properties of an Eight-Story Prefabricated Panel Building," by Bouwkamp, J.G., Kollegger, J.P. and Stephen, R.M., October 1980, (PB81 200 313)A05.
- UCB/EERC-80/31 "Predictive Dynamic Response of Panel Type Structures under Earthquakes," by Kollegger, J.P. and Bouwkamp, J.G., October 1980, (PB81 152 316)A04.
- UCB/EERC-80/32 "The Design of Steel Energy-Absorbing Restrainers and their Incorporation into Nuclear Power Plants for Enhanced Safety (Vol 3): Testing of Commercial Steels in Low-Cycle Torsional Fatigue," by Spanner, P., Parker, E.R., Jongewaard, E. and Dory, M., 1980.

- UCB/EERC-80/33 "The Design of Steel Energy-Absorbing Restrainers and their Incorporation into Nuclear Power Plants for Enhanced Safety (Vol 4): Shaking Table Tests of Piping Systems with Energy-Absorbing Restrainers." by Stiemer, S.F. and Godden, W.G., September 1980, (PB82 201 880)A05.
- UCB/EERC-80/34 "The Design of Steel Energy-Absorbing Restrainers and their Incorporation into Nuclear Power Plants for Enhanced Safety (Vol 5): Summary Report," by Spencer, P., 1980.
- UCB/EERC-80/35 "Experimental Testing of an Energy-Absorbing Base Isolation System," by Kelly, J.M., Skinner, M.S. and Beucke, K.E., October 1980, (PB81 154 072)A04.
- UCB/EERC-80/36 "Simulating and Analyzing Artificial Non-Stationary Earth Ground Motions," by Nau, R.F., Oliver, R.M. and Pister, K.S., October 1980, (PB81 153 397)A04.
- UCB/EERC-80/37 "Earthquake Engineering at Berkeley - 1980," by , September 1980, (PB81 205 674)A09.
- UCB/EERC-80/38 "Inelastic Seismic Analysis of Large Panel Buildings," by Schricker, V. and Powell, G.H., September 1980, (PB81 154 338)A13.
- UCB/EERC-80/39 "Dynamic Response of Embankment, Concrete-Gavity and Arch Dams Including Hydrodynamic Interaction," by Hall, J.F. and Chopra, A.K., October 1980, (PB81 152 324)A11.
- UCB/EERC-80/40 "Inelastic Buckling of Steel Struts under Cyclic Load Reversal," by Black, R.G., Wenger, W.A. and Popov, E.P., October 1980, (PB81 154 312)A08.
- UCB/EERC-80/41 "Influence of Site Characteristics on Buildings Damage during the October 3,1974 Lima Earthquake," by Repetto, P., Arango, I. and Seed, H.B., September 1980, (PB81 161 739)A05.
- UCB/EERC-80/42 "Evaluation of a Shaking Table Test Program on Response Behavior of a Two Story Reinforced Concrete Frame," by Blondet, J.M., Clough, R.W. and Mahin, S.A., December 1980, (PB82 196 544)A11.
- UCB/EERC-80/43 "Modelling of Soil-Structure Interaction by Finite and Infinite Elements," by Medina, F., December 1980, (PB81 229 270)A04.
- UCB/EERC-81/01 "Control of Seismic Response of Piping Systems and Other Structures by Base Isolation," by Kelly, J.M., January 1981, (PB81 200 735)A05.
- UCB/EERC-81/02 "OPTNSR- An Interactive Software System for Optimal Design of Statically and Dynamically Loaded Structures with Nonlinear Response," by Bhatti, M.A., Ciampi, V. and Pister, K.S., January 1981, (PB81 218 851)A09.
- UCB/EERC-81/03 "Analysis of Local Variations in Free Field Seismic Ground Motions," by Chen, J.-C., Lysmer, J. and Seed, H.B., January 1981, (AD-A099508)A13.
- UCB/EERC-81/04 "Inelastic Structural Modeling of Braced Offshore Platforms for Seismic Loading," by Zayas, V.A., Shing, P.-S.B., Mahin, S.A. and Popov, E.P., January 1981, (PB82 138 777)A07.
- UCB/EERC-81/05 "Dynamic Response of Light Equipment in Structures," by Der Kiureghian, A., Sackman, J.L. and Nour-Omid, B., April 1981, (PB81 218 497)A04.
- UCB/EERC-81/06 "Preliminary Experimental Investigation of a Broad Base Liquid Storage Tank," by Bouwkamp, J.G., Kollegger, J.P. and Stephen, R.M., May 1981, (PB82 140 385)A03.
- UCB/EERC-81/07 "The Seismic Resistant Design of Reinforced Concrete Coupled Structural Walls," by Aktan, A.E. and Bertero, V.V., June 1981, (PB82 113 358)A11.
- UCB/EERC-81/08 "Unassigned," by Unassigned, 1981.
- UCB/EERC-81/09 "Experimental Behavior of a Spatial Piping System with Steel Energy Absorbers Subjected to a Simulated Differential Seismic Input," by Stiemer, S.F., Godden, W.G. and Kelly, J.M., July 1981, (PB82 201 898)A04.
- UCB/EERC-81/10 "Evaluation of Seismic Design Provisions for Masonry in the United States," by Sveinsson, B.I., Mayes, R.L. and McNiven, H.D., August 1981, (PB82 166 075)A08.
- UCB/EERC-81/11 "Two-Dimensional Hybrid Modelling of Soil-Structure Interaction," by Tzong, T.-J., Gupta, S. and Penzien, J., August 1981, (PB82 142 118)A04.
- UCB/EERC-81/12 "Studies on Effects of Infills in Seismic Resistant R/C Construction," by Brokken, S. and Bertero, V.V., October 1981, (PB82 166 190)A09.
- UCB/EERC-81/13 "Linear Models to Predict the Nonlinear Seismic Behavior of a One-Story Steel Frame," by Valdimarsson, H., Shah, A.H. and McNiven, H.D., September 1981, (PB82 138 793)A07.
- UCB/EERC-81/14 "TLUSH: A Computer Program for the Three-Dimensional Dynamic Analysis of Earth Dams," by Kagawa, T., Mejia, L.H., Seed, H.E. and Lysmer, J., September 1981, (PB82 139 940)A06.
- UCB/EERC-81/15 "Three Dimensional Dynamic Response Analysis of Earth Dams," by Mejia, L.H. and Seed, H.B., September 1981, (PB82 137 274)A12.
- UCB/EERC-81/16 "Experimental Study of Lead and Elastomeric Dampers for Base Isolation Systems," by Kelly, J.M. and Hodder, S.B., October 1981, (PB82 166 182)A05.
- UCB/EERC-81/17 "The Influence of Base Isolation on the Seismic Response of Light Secondary Equipment," by Kelly, J.M., April 1981, (PB82 255 266)A04.
- UCB/EERC-81/18 "Studies on Evaluation of Shaking Table Response Analysis Procedures," by Blondet, J. M., November 1981, (PB82 197 278)A10.
- UCB/EERC-81/19 "DELIGHT.STRUCT: A Computer-Aided Design Environment for Structural Engineering," by Balling, R.J., Pister, K.S. and Polak, E., December 1981, (PB82 218 496)A07.
- UCB/EERC-81/20 "Optimal Design of Seismic-Resistant Planar Steel Frames," by Balling, R.J., Ciampi, V. and Pister, K.S., December 1981, (PB82 220 179)A07.
- UCB/EERC-82/01 "Dynamic Behavior of Ground for Seismic Analysis of Lifeline Systems," by Sato, T. and Der Kiureghian, A., January 1982, (PB82 218 926)A05.
- UCB/EERC-82/02 "Shaking Table Tests of a Tubular Steel Frame Model," by Ghanaat, Y. and Clough, R.W., January 1982, (PB82 220 161)A07.

- UCB/EERC-82/03 "Behavior of a Piping System under Seismic Excitation: Experimental Investigations of a Spatial Piping System supported by Mechanical Shock Arrestors." by Schneider, S., Lee, H.-M. and Godden, W. G., May 1982, (PB83 172 544)A09.
- UCB/EERC-82/04 "New Approaches for the Dynamic Analysis of Large Structural Systems." by Wilson, E.L., June 1982, (PB83 148 080)A05.
- UCB/EERC-82/05 "Model Study of Effects of Damage on the Vibration Properties of Steel Offshore Platforms." by Shahrivar, F. and Bouwkamp, J.G., June 1982, (PB83 148 742)A10.
- UCB/EERC-82/06 "States of the Art and Practice in the Optimum Seismic Design and Analytical Response Prediction of R/C Frame Wall Structures." by Aktan, A.E. and Bertero, V.V., July 1982, (PB83 147 736)A05.
- UCB/EERC-82/07 "Further Study of the Earthquake Response of a Broad Cylindrical Liquid-Storage Tank Model," by Manos, G.C. and Clough, R.W., July 1982, (PB83 147 744)A11.
- UCB/EERC-82/08 "An Evaluation of the Design and Analytical Seismic Response of a Seven Story Reinforced Concrete Frame." by Charney, F.A. and Bertero, V.V., July 1982, (PB83 157 628)A09.
- UCB/EERC-82/09 "Fluid-Structure Interactions: Added Mass Computations for Incompressible Fluid." by Kuo, J.S.-H., August 1982, (PB83 156 281)A07.
- UCB/EERC-82/10 "Joint-Opening Nonlinear Mechanism: Interface Smeared Crack Model," by Kuo, J.S.-H., August 1982, (PB83 149 195)A05.
- UCB/EERC-82/11 "Dynamic Response Analysis of Techí Dam." by Clough, R.W., Stephen, R.M. and Kuo, J.S.-H., August 1982, (PB83 147 496)A06.
- UCB/EERC-82/12 "Prediction of the Seismic Response of R/C Frame-Coupled Wall Structures," by Aktan, A.E., Bertero, V.V. and Piazza, M., August 1982, (PB83 149 203)A09.
- UCB/EERC-82/13 "Preliminary Report on the Smart 1 Strong Motion Array in Taiwan," by Bölt, B.A., Loh, C.H., Penzien, J. and Tsai, Y.B., August 1982, (PB83 159 400)A10.
- UCB/EERC-82/14 "Shaking-Table Studies of an Eccentrically X-Braced Steel Structure," by Yang, M.S., September 1982, (PB83 260 778)A12.
- UCB/EERC-82/15 "The Performance of Stairways in Earthquakes," by Roha, C., Axley, J.W. and Bertero, V.V., September 1982, (PB83 157 693)A07.
- UCB/EERC-82/16 "The Behavior of Submerged Multiple Bodies in Earthquakes." by Liao, W.-G., September 1982, (PB83 158 709)A07.
- UCB/EERC-82/17 "Effects of Concrete Types and Loading Conditions on Local Bond-Slip Relationships," by Cowell, A.D., Popov, E.P. and Bertero, V.V., September 1982, (PB83 153 577)A04.
- UCB/EERC-82/18 "Mechanical Behavior of Shear Wall Vertical Boundary Members: An Experimental Investigation," by Wagner, M.T. and Bertero, V.V., October 1982, (PB83 159 764)A05.
- UCB/EERC-82/19 "Experimental Studies of Multi-support Seismic Loading on Piping Systems," by Kelly, J.M. and Cowell, A.D., November 1982.
- UCB/EERC-82/20 "Generalized Plastic Hinge Concepts for 3D Beam-Column Elements," by Chen, P. F.-S. and Powell, G.H., November 1982, (PB83 247 981)A13.
- UCB/EERC-82/21 "ANSR-II: General Computer Program for Nonlinear Structural Analysis," by Oughourlian, C.V. and Powell, G.H., November 1982, (PB83 251 330)A12.
- UCB/EERC-82/22 "Solution Strategies for Statically Loaded Nonlinear Structures," by Simons, J.W. and Powell, G.H., November 1982, (PB83 197 970)A06.
- UCB/EERC-82/23 "Analytical Model of Deformed Bar Anchorages under Generalized Excitations," by Ciampi, V., Eligehausen, R., Bertero, V.V. and Popov, E.P., November 1982, (PB83 169 532)A06.
- UCB/EERC-82/24 "A Mathematical Model for the Response of Masonry Walls to Dynamic Excitations," by Sucuoglu, H., Mengi, Y. and McNiven, H.D., November 1982, (PB83 169 011)A07.
- UCB/EERC-82/25 "Earthquake Response Considerations of Broad Liquid Storage Tanks," by Cambra, F.J., November 1982, (PB83 251 215)A09.
- UCB/EERC-82/26 "Computational Models for Cyclic Plasticity, Rate Dependence and Creep," by Mosaddad, B. and Powell, G.H., November 1982, (PB83 245 829)A08.
- UCB/EERC-82/27 "Inelastic Analysis of Piping and Tubular Structures," by Mahasuverachai, M. and Powell, G.H., November 1982, (PB83 249 987)A07.
- UCB/EERC-83/01 "The Economic Feasibility of Seismic Rehabilitation of Buildings by Base Isolation," by Kelly, J.M., January 1983, (PB83 197 988)A05.
- UCB/EERC-83/02 "Seismic Moment Connections for Moment-Resisting Steel Frames," by Popov, E.P., January 1983, (PB83 195 412)A04.
- UCB/EERC-83/03 "Design of Links and Beam-to-Column Connections for Eccentrically Braced Steel Frames," by Popov, E.P. and Malley, J.O., January 1983, (PB83 194 811)A04.
- UCB/EERC-83/04 "Numerical Techniques for the Evaluation of Soil-Structure Interaction Effects in the Time Domain," by Bayo, E. and Wilson, E.L., February 1983, (PB83 245 605)A09.
- UCB/EERC-83/05 "A Transducer for Measuring the Internal Forces in the Columns of a Frame-Wall Reinforced Concrete Structure," by Sause, R. and Bertero, V.V., May 1983, (PB84 119 494)A06.
- UCB/EERC-83/06 "Dynamic Interactions Between Floating Ice and Offshore Structures," by Croteau, P., May 1983, (PB84 119 486)A16.
- UCB/EERC-83/07 "Dynamic Analysis of Multiply Tuned and Arbitrarily Supported Secondary Systems," by Igusa, T. and Der Kiureghian, A., July 1983, (PB84 118 272)A11.
- UCB/EERC-83/08 "A Laboratory Study of Submerged Multi-body Systems in Earthquakes," by Ansari, G.R., June 1983, (PB83 261 842)A17.
- UCB/EERC-83/09 "Effects of Transient Foundation Uplift on Earthquake Response of Structures," by Yim, C.-S. and Chopra, A.K., June 1983, (PB83 261 396)A07.
- UCB/EERC-83/10 "Optimal Design of Friction-Braced Frames under Seismic Loading," by Austin, M.A. and Pister, K.S., June 1983, (PB84 119 288)A06.
- UCB/EERC-83/11 "Shaking Table Study of Single-Story Masonry Houses: Dynamic Performance under Three Component Seismic Input and Recommendations," by Manos, G.C., Clough, R.W. and Mayes, R.L., July 1983, (UCB/EERC-83/11)A08.
- UCB/EERC-83/12 "Experimental Error Propagation in Pseudodynamic Testing," by Shiing, P.B. and Mahin, S.A., June 1983, (PB84 119 270)A09.
- UCB/EERC-83/13 "Experimental and Analytical Predictions of the Mechanical Characteristics of a 1/5-scale Model of a 7-story R/C Frame-Wall Building Structure." by Aktan, A.E., Bertero, V.V., Chowdhury, A.A. and Nagashima, T., June 1983, (PB84 119 213)A07.

- UCB/EERC-83/14 "Shaking Table Tests of Large-Panel Precast Concrete Building System Assemblages," by Oliva, M.G. and Clough, R.W., June 1983, (PB86 110 210/AS)A11.
- UCB/EERC-83/15 "Seismic Behavior of Active Beam Links in Eccentrically Braced Frames," by Hjelmstad, K.D. and Popov, E.P., July 1983, (PB84 119 676)A09.
- UCB/EERC-83/16 "System Identification of Structures with Joint Rotation," by Dimsdale, J.S., July 1983, (PB84 192 210)A06.
- UCB/EERC-83/17 "Construction of Inelastic Response Spectra for Single-Degree-of-Freedom Systems," by Mahin, S. and Lin, J., June 1983, (PB84 208 834)A05.
- UCB/EERC-83/18 "Interactive Computer Analysis Methods for Predicting the Inelastic Cyclic Behaviour of Structural Sections," by Kaba, S. and Mahin, S., July 1983, (PB84 192 012)A06.
- UCB/EERC-83/19 "Effects of Bond Deterioration on Hysteretic Behavior of Reinforced Concrete Joints," by Filippou, F.C., Popov, E.P. and Bertero, V.V., August 1983, (PB84 192 020)A10.
- UCB/EERC-83/20 "Analytical and Experimental Correlation of Large-Panel Precast Building System Performance," by Oliva, M.G., Clough, R.W., Velkov, M. and Gavrilovic, P., November 1983.
- UCB/EERC-83/21 "Mechanical Characteristics of Materials Used in a 1/5 Scale Model of a 7-Story Reinforced Concrete Test Structure," by Bertero, V.V., Aktan, A.E., Harris, H.G. and Chowdhury, A.A., October 1983, (PB84 193 697)A05.
- UCB/EERC-83/22 "Hybrid Modelling of Soil-Structure Interaction in Layered Media," by Tzong, T.-J. and Penzien, J., October 1983, (PB84 192 178)A08.
- UCB/EERC-83/23 "Local Bond Stress-Slip Relationships of Deformed Bars under Generalized Excitations," by Eligehausen, R., Popov, E.P. and Bertero, V.V., October 1983, (PB84 192 848)A09.
- UCB/EERC-83/24 "Design Considerations for Shear Links in Eccentrically Braced Frames," by Malley, J.O. and Popov, E.P., November 1983, (PB84 192 186)A07.
- UCB/EERC-84/01 "Pseudodynamic Test Method for Seismic Performance Evaluation: Theory and Implementation," by Shing, P.-S.B. and Mahin, S.A., January 1984, (PB84 190 644)A08.
- UCB/EERC-84/02 "Dynamic Response Behavior of Kiang Hong Dian Dam," by Clough, R.W., Chang, K.-T., Chen, H.-Q. and Stephen, R.M., April 1984, (PB84 209 402)A08.
- UCB/EERC-84/03 "Refined Modelling of Reinforced Concrete Columns for Seismic Analysis," by Kaba, S.A. and Mahin, S.A., April 1984, (PB84 234 384)A06.
- UCB/EERC-84/04 "A New Floor Response Spectrum Method for Seismic Analysis of Multiply Supported Secondary Systems," by Asfura, A. and Der Kiureghian, A., June 1984, (PB84 239 417)A06.
- UCB/EERC-84/05 "Earthquake Simulation Tests and Associated Studies of a 1/5th-scale Model of a 7-Story R/C Frame-Wall Test Structure," by Bertero, V.V., Aktan, A.E., Charney, F.A. and Sause, R., June 1984, (PB84 239 409)A09.
- UCB/EERC-84/06 "R/C Structural Walls: Seismic Design for Shear," by Aktan, A.E. and Bertero, V.V., 1984.
- UCB/EERC-84/07 "Behavior of Interior and Exterior Flat-Plate Connections subjected to Inelastic Load Reversals," by Zee, H.L. and Moehle, J.P., August 1984, (PB86 117 629/AS)A07.
- UCB/EERC-84/08 "Experimental Study of the Seismic Behavior of a Two-Story Flat-Plate Structure," by Moehle, J.P. and Diebold, J.W., August 1984, (PB86 122 553/AS)A12.
- UCB/EERC-84/09 "Phenomenological Modeling of Steel Braces under Cyclic Loading," by Ikeda, K., Mahin, S.A. and Dermitzakis, S.N., May 1984, (PB86 132 198/AS)A08.
- UCB/EERC-84/10 "Earthquake Analysis and Response of Concrete Gravity Dams," by Fenves, G. and Chopra, A.K., August 1984, (PB85 193 902/AS)A11.
- UCB/EERC-84/11 "EAGD-84: A Computer Program for Earthquake Analysis of Concrete Gravity Dams," by Fenves, G. and Chopra, A.K., August 1984, (PB85 193 613/AS)A05.
- UCB/EERC-84/12 "A Refined Physical Theory Model for Predicting the Seismic Behavior of Braced Steel Frames," by Ikeda, K. and Mahin, S.A., July 1984, (PB85 191 450/AS)A09.
- UCB/EERC-84/13 "Earthquake Engineering Research at Berkeley - 1984," by , August 1984, (PB85 197 341/AS)A10.
- UCB/EERC-84/14 "Moduli and Damping Factors for Dynamic Analyses of Cohesionless Soils," by Seed, H.B., Wong, R.T., Idriss, I.M. and Tokimatsu, K., September 1984, (PB85 191 468/AS)A04.
- UCB/EERC-84/15 "The Influence of SPT Procedures in Soil Liquefaction Resistance Evaluations," by Seed, H.B., Tokimatsu, K., Harder, L.F. and Chung, R.M., October 1984, (PB85 191 732/AS)A04.
- UCB/EERC-84/16 "Simplified Procedures for the Evaluation of Settlements in Sands Due to Earthquake Shaking," by Tokimatsu, K. and Seed, H.B., October 1984, (PB85 197 887/AS)A03.
- UCB/EERC-84/17 "Evaluation of Energy Absorption Characteristics of Bridges under Seismic Conditions," by Imbsen, R.A. and Penzien, J., November 1984.
- UCB/EERC-84/18 "Structure-Foundation Interactions under Dynamic Loads," by Liu, W.D. and Penzien, J., November 1984, (PB87 124 889/AS)A11.
- UCB/EERC-84/19 "Seismic Modelling of Deep Foundations," by Chen, C.-H. and Penzien, J., November 1984, (PB87 124 798/AS)A07.
- UCB/EERC-84/20 "Dynamic Response Behavior of Quan Shui Dam," by Clough, R.W., Chang, K.-T., Chen, H.-Q., Stephen, R.M., Ghanaat, Y. and Qi, J.-H., November 1984, (PB86 115177/AS)A07.
- UCB/EERC-85/01 "Simplified Methods of Analysis for Earthquake Resistant Design of Buildings," by Cruz, E.F. and Chopra, A.K., February 1985, (PB86 112299/AS)A12.
- UCB/EERC-85/02 "Estimation of Seismic Wave Coherency and Rupture Velocity using the SMART 1 Strong-Motion Array Recordings," by Abrahamson, N.A., March 1985, (PB86 214 343)A07.

- UCB/EERC-85/03 "Dynamic Properties of a Thirty Story Condominium Tower Building," by Stephen, R.M., Wilson, E.L. and Stander, N., April 1985, (PB86 118965/AS)A06.
- UCB/EERC-85/04 "Development of Substructuring Techniques for On-Line Computer Controlled Seismic Performance Testing," by Dermitzakis, S. and Mahin, S., February 1985, (PB86 132941/AS)A08.
- UCB/EERC-85/05 "A Simple Model for Reinforcing Bar Anchorages under Cyclic Excitations," by Filippou, F.C., March 1985, (PB86 112 919/AS)A05.
- UCB/EERC-85/06 "Racking Behavior of Wood-framed Gypsum Panels under Dynamic Load," by Oliva, M.G., June 1985.
- UCB/EERC-85/07 "Earthquake Analysis and Response of Concrete Arch Dams," by Fok, K.-L. and Chopra, A.K., June 1985, (PB86 139672/AS)A10.
- UCB/EERC-85/08 "Effect of Inelastic Behavior on the Analysis and Design of Earthquake Resistant Structures," by Lin, J.P. and Mahin, S.A., June 1985, (PB86 135340/AS)A08.
- UCB/EERC-85/09 "Earthquake Simulator Testing of a Base-Isolated Bridge Deck," by Kelly, J.M., Buckle, I.G. and Tsai, H.-C., January 1986, (PB87 124 152/AS)A06.
- UCB/EERC-85/10 "Simplified Analysis for Earthquake Resistant Design of Concrete Gravity Dams," by Fennes, G. and Chopra, A.K., June 1986, (PB87 124 160/AS)A08.
- UCB/EERC-85/11 "Dynamic Interaction Effects in Arch Dams," by Clough, R.W., Chang, K.-T., Chen, H.-Q. and Ghanaat, Y., October 1985, (PB86 135027/AS)A05.
- UCB/EERC-85/12 "Dynamic Response of Long Valley Dam in the Mammoth Lake Earthquake Series of May 25-27, 1980," by Lai, S. and Seed, H.B., November 1985, (PB86 142304/AS)A05.
- UCB/EERC-85/13 "A Methodology for Computer-Aided Design of Earthquake-Resistant Steel Structures," by Austin, M.A., Pister, K.S. and Mahin, S.A., December 1985, (PB86 159480/AS)A10.
- UCB/EERC-85/14 "Response of Tension-Leg Platforms to Vertical Seismic Excitations," by Liou, G.-S., Penzien, J. and Yeung, R.W., December 1985, (PB87 124 871/AS)A08.
- UCB/EERC-85/15 "Cyclic Loading Tests of Masonry Single Piers: Volume 4 - Additional Tests with Height to Width Ratio of 1," by Sveinsson, B., McNiven, H.D. and Sucuoglu, H., December 1985.
- UCB/EERC-85/16 "An Experimental Program for Studying the Dynamic Response of a Steel Frame with a Variety of Infill Partitions," by Yanev, B. and McNiven, H.D., December 1985.
- UCB/EERC-86/01 "A Study of Seismically Resistant Eccentrically Braced Steel Frame Systems," by Kasai, K. and Popov, E.P., January 1986, (PB87 124 178/AS)A14.
- UCB/EERC-86/02 "Design Problems in Soil Liquefaction," by Seed, H.B., February 1986, (PB87 124 186/AS)A03.
- UCB/EERC-86/03 "Implications of Recent Earthquakes and Research on Earthquake-Resistant Design and Construction of Buildings," by Bertero, V.V., March 1986, (PB87 124 194/AS)A05.
- UCB/EERC-86/04 "The Use of Load Dependent Vectors for Dynamic and Earthquake Analyses," by Leger, P., Wilson, E.L. and Clough, R.W., March 1986, (PB87 124 202/AS)A12.
- UCB/EERC-86/05 "Two Beam-To-Column Web Connections," by Tsai, K.-C. and Popov, E.P., April 1986, (PB87 124 301/AS)A04.
- UCB/EERC-86/06 "Determination of Penetration Resistance for Coarse-Grained Soils using the Becker Hammer Drill," by Harder, L.F. and Seed, H.B., May 1986, (PB87 124 210/AS)A07.
- UCB/EERC-86/07 "A Mathematical Model for Predicting the Nonlinear Response of Unreinforced Masonry Walls to In-Plane Earthquake Excitations," by Mengi, Y. and McNiven, H.D., May 1986, (PB87 124 780/AS)A06.
- UCB/EERC-86/08 "The 19 September 1985 Mexico Earthquake: Building Behavior," by Bertero, V.V., July 1986.
- UCB/EERC-86/09 "EACD-3D: A Computer Program for Three-Dimensional Earthquake Analysis of Concrete Dams," by Fok, K.-L., Hall, J.F. and Chopra, A.K., July 1986, (PB87 124 228/AS)A08.
- UCB/EERC-86/10 "Earthquake Simulation Tests and Associated Studies of a 0.3-Scale Model of a Six-Story Concentrically Braced Steel Structure," by Uang, C.-M. and Bertero, V.V., December 1986, (PB87 163 564/AS)A17.
- UCB/EERC-86/11 "Mechanical Characteristics of Base Isolation Bearings for a Bridge Deck Model Test," by Kelly, J.M., Buckle, I.G. and Koh, C.-G., 1987.
- UCB/EERC-86/12 "Effects of Axial Load on Elastomeric Isolation Bearings," by Koh, C.-G. and Kelly, J.M., 1987.
- UCB/EERC-87/01 "The FPS Earthquake Resisting System: Experimental Report," by Zayas, V.A., Low, S.S. and Mahin, S.A., June 1987.
- UCB/EERC-87/02 "Earthquake Simulator Tests and Associated Studies of a 0.3-Scale Model of a Six-Story Eccentrically Braced Steel Structure," by Whitaker, A., Uang, C.-M. and Bertero, V.V., July 1987.
- UCB/EERC-87/03 "A Displacement Control and Uplift Restraint Device for Base-Isolated Structures," by Kelly, J.M., Griffith, M.C. and Aiken, I.G., April 1987.
- UCB/EERC-87/04 "Earthquake Simulator Testing of a Combined Sliding Bearing and Rubber Bearing Isolation System," by Kelly, J.M. and Chalhoub, M.S., 1987.
- UCB/EERC-87/05 "Three-Dimensional Inelastic Analysis of Reinforced Concrete Frame-Wall Structures," by Moazzami, S. and Bertero, V.V., May 1987.
- UCB/EERC-87/06 "Experiments on Eccentrically Braced Frames with Composite Floors," by Ricles, J. and Popov, E., June 1987.
- UCB/EERC-87/07 "Dynamic Analysis of Seismically Resistant Eccentrically Braced Frames," by Ricles, J. and Popov, E., June 1987.
- UCB/EERC-87/08 "Undrained Cyclic Triaxial Testing of Gravels-The Effect of Membrane Compliance," by Evans, M.D. and Seed, H.B., July 1987.
- UCB/EERC-87/09 "Hybrid Solution Techniques for Generalized Pseudo-Dynamic Testing," by Thewalt, C. and Mahin, S.A., July 1987.
- UCB/EERC-87/10 "Investigation of Ultimate Behavior of AISC Group 4 and 5 Heavy Steel Rolled-Section Splices with Full and Partial Penetration Butt Welds," by Bruneau, M. and Mahin, S.A., July 1987.

- UCB/EERC-87/11 "Residual Strength of Sand from Dam Failures in the Chilean Earthquake of March 3, 1985," by De Alba, P., Seed, H.B., Retamal, E. and Seed, R.B., September 1987.
- UCB/EERC-87/12 "Inelastic Seismic Response of Structures with Mass or Stiffness Eccentricities in Plan," by Bruneau, M. and Mahin, S.A., September 1987.
- UCB/EERC-87/13 "CSTRUCT: An Interactive Computer Environment for the Design and Analysis of Earthquake Resistant Steel Structures," by Austin, M.A., Mahin, S.A. and Pister, K.S., September 1987.
- UCB/EERC-87/14 "Experimental Study of Reinforced Concrete Columns Subjected to Multi-Axial Loading," by Low, S.S. and Moehle, J.P., September 1987.
- UCB/EERC-87/15 "Relationships between Soil Conditions and Earthquake Ground Motions in Mexico City in the Earthquake of Sept. 19, 1985," by Seed, H.B., Romo, M.P., Sun, J., Jaime, A. and Lysmer, J., October 1987.
- UCB/EERC-87/16 "Experimental Study of Seismic Response of R. C. Setback Buildings," by Shahrooz, B.M. and Moehle, J.P., October 1987.
- UCB/EERC-87/17 "Three Dimensional Aspects of the Behavior of R. C. Structures Subjected to Earthquakes," by Pantazopoulou, S.J. and Moehle, J.P., October 1987.
- UCB/EERC-87/18 "Design Procedures for R-FBI Bearings," by Mostaghel, N. and Kelly, J.M., November 1987.
- UCB/EERC-87/19 "Analytical Models for Predicting the Lateral Response of R C Shear Walls: Evaluation of their Reliability," by Vulcano, A. and Bertero, V.V., November 1987.